

## Predicting and preventing in-plane shear induced fiber angle deviations during automated handling of non-crimp fabrics

de Zeeuw, C.M.

**DOI**

[10.4233/uuid:ad7c33be-979f-4e27-8edd-c2eb193389ae](https://doi.org/10.4233/uuid:ad7c33be-979f-4e27-8edd-c2eb193389ae)

**Publication date**

2023

**Document Version**

Final published version

**Citation (APA)**

de Zeeuw, C. M. (2023). *Predicting and preventing in-plane shear induced fiber angle deviations during automated handling of non-crimp fabrics*. [Dissertation (TU Delft), Delft University of Technology]. <https://doi.org/10.4233/uuid:ad7c33be-979f-4e27-8edd-c2eb193389ae>

**Important note**

To cite this publication, please use the final published version (if applicable). Please check the document version above.

**Copyright**

Other than for strictly personal use, it is not permitted to download, forward or distribute the text or part of it, without the consent of the author(s) and/or copyright holder(s), unless the work is under an open content license such as Creative Commons.

**Takedown policy**

Please contact us and provide details if you believe this document breaches copyrights. We will remove access to the work immediately and investigate your claim.

**PREDICTING AND PREVENTING IN-PLANE SHEAR  
INDUCED FIBER ANGLE DEVIATIONS DURING  
AUTOMATED HANDLING OF NON-CRIMP FABRICS**



# **PREDICTING AND PREVENTING IN-PLANE SHEAR INDUCED FIBER ANGLE DEVIATIONS DURING AUTOMATED HANDLING OF NON-CRIMP FABRICS**

## **Dissertation**

for the purpose of obtaining the degree of doctor

at Delft University of Technology

by the authority of the Rector Magnificus, Prof. dr.ir. T.H.J. van der Hagen,

chair of the Board for Doctorates,

to be defended publicly on 18 October 2023 at 10:00 o'clock

by

**Chantal Marina DE ZEEUW**

Ingenieur Lucht- en Ruimtevaart,  
Delft University of Technology, Delft, Nederland,

born in Purmerend, Nederland.

This dissertation has been approved by the promotors.

Composition of the doctoral committee:

Rector Magnificus,	chairperson
prof. dr. ir. R. Benedictus,	Delft University of Technology, promotor
dr. ir. D.M.J. Peeters,	Delft University of Technology, copromotor
dr. ir. O.K. Bergsma,	Delft University of Technology, copromotor

*Independent members:*

prof. dr. ir. K.M.B. Jansen,	Delft University of Technology
prof. dr. M. Åkermo,	KTH Royal Institute of Technology, Sweden
prof. dr hab. Eng. W. Świąszkowski,	Warsaw University of Technology, Poland
prof. dr. ir. A.W. van Vuure,	KU Leuven, Belgium
prof. dr. ir. C. Simão Ferreira,	Delft University of Technology, reserve member

*This research is supported by Delft University of Technology, SAMXL, and by the Aeronautics roadmap of TKI-HTSM, under Grant TKI-HTSM/17.1187*



**Holland High Tech**  
Global Challenges, Smart Solutions

Copyright © 2023 by C.M. de Zeeuw

An electronic version of this dissertation is available at  
<http://repository.tudelft.nl/>.

# CONTENTS

<b>Summary</b>	<b>vii</b>
<b>Samenvatting</b>	<b>xi</b>
<b>1 Introduction</b>	<b>1</b>
1.1 Background and Motivation . . . . .	1
1.2 Objective, Approach and Outline . . . . .	3
<b>2 Review of the state of the art</b>	<b>7</b>
2.1 Introduction . . . . .	7
2.2 Challenges . . . . .	8
2.3 Strategies in literature. . . . .	11
2.3.1 Ply handling techniques . . . . .	11
2.3.2 Gripping point strategies. . . . .	14
2.3.3 Accuracy in pick-and-place processes . . . . .	19
2.4 Discussion . . . . .	20
2.4.1 Ply handling strategies . . . . .	20
2.4.2 Gripping strategies. . . . .	21
2.5 Conclusions. . . . .	24
2.6 Research goal and research questions. . . . .	25
<b>3 Setting bounds for in-plane shear induced fiber angle deviations in bi-axial non-crimp fabrics</b>	<b>33</b>
3.1 Introduction . . . . .	33
3.2 Fiber angle deviations and in-plane shear in an NCF . . . . .	35
3.3 Setting limits for in-plane shear and fiber angle deviations based on picture frame tests . . . . .	40
3.4 Discussion . . . . .	42
3.5 Conclusions. . . . .	45
<b>4 Mesoscopic modeling of non-crimp fabrics for the determination of homogenised elastic properties</b>	<b>49</b>
4.1 Introduction . . . . .	49
4.2 Setting up the representative volume element . . . . .	51
4.3 Obtaining tow properties for RVE input . . . . .	54
4.4 Determination of homogenised material properties using RVE . . . . .	57
4.5 Validation of the RVE . . . . .	58
4.5.1 Flexural rigidity test using wide fabric specimens . . . . .	58
4.5.2 Picture frame tests of fabric specimens . . . . .	59
4.6 Discussion . . . . .	62

4.7	Conclusions. . . . .	64
<b>5</b>	<b>Using unit cell pick-up point patterns to evaluate in-plane shear strains</b>	<b>67</b>
5.1	Introduction . . . . .	67
5.2	Experimental work with gravity loaded reinforcements . . . . .	69
5.2.1	Set-up for experimental work . . . . .	69
5.2.2	Results for experimental work . . . . .	70
5.3	Numerical work with gravity loaded reinforcements . . . . .	71
5.3.1	Basic model set-up and validation . . . . .	71
5.3.2	Additional model set-up for simulations . . . . .	78
5.3.3	Results for numerical work. . . . .	82
5.4	Discussion . . . . .	87
5.4.1	Experimental work with gravity loaded reinforcements . . . . .	87
5.4.2	Numerical work with gravity loaded reinforcements . . . . .	88
5.5	Conclusions. . . . .	90
<b>6</b>	<b>Guidelines for moving towards industrial implementation</b>	<b>95</b>
6.1	Setting tolerances for in-plane shear strain induced fiber angle deviations .	95
6.2	Mesoscopic modeling for the determination of homogenised elastic prop- erties . . . . .	97
6.2.1	Elastic properties for bi-axial NCFs . . . . .	97
6.2.2	Multi-axial NCFs . . . . .	100
6.2.3	Stabilizing yarns . . . . .	101
6.3	Using unit cell pick-up point patterns to evaluate in-plane shear strains. . . . .	102
6.3.1	Unexpected deformations due to sliding of bottom layers . . . . .	102
6.3.2	Local in-plane shear strains . . . . .	103
6.3.3	Pick-up point placement. . . . .	103
6.3.4	Vertical and horizontal accelerations. . . . .	104
6.3.5	Pre-tension strategy . . . . .	107
<b>7</b>	<b>Conclusions</b>	<b>111</b>
	<b>Acknowledgements</b>	<b>113</b>
<b>A</b>	<b>Appendix A</b>	<b>115</b>
<b>B</b>	<b>Appendix B</b>	<b>117</b>
<b>C</b>	<b>Appendix C</b>	<b>123</b>
	<b>Curriculum Vitæ</b>	<b>127</b>
	<b>List of Publications</b>	<b>129</b>

# SUMMARY

Over the years the use of composites as an aircraft structural material has significantly increased. Currently, the industry still relies largely on manually manufactured components. Automated manufacturing can however bring advantages such as reduced manufacturing costs and a more consistent and higher quality end product. An attractive automated option for the handling of reinforcements is the pick and place process, which involves the picking up, moving and placing down of objects. The pick and place process makes it possible to place layers of reinforcement as a whole and brings opportunities for the handling of multiple layers and/or large layers of reinforcement. Literature shows countless different strategies to execute a pick-and-place operation, with research typically focusing on developing more highly specialized concepts. This generally involves demonstrating the feasibility of the concept but does not include reporting on the accuracy. Not taking the accuracy of the pick-and-place process and the quality of the reinforcement during handling into account might result in inconsistent or substandard final products.

For the aerospace industry to widely implement pick-and-place operations the quality of products manufactured using this process will need to be guaranteed. One important quality criterion when working with composites is the orientation of the fibers. The fiber orientations of the final product should match the orientations as intended in the design. To achieve this, the fiber angles, defined as the angle between two adjacent filament directions in a reinforcement, should be taken into account when studying and designing pick-and-place processes. One factor that directly influences the fiber angles is the in-plane shear that occurs in the reinforcement during the pick-and-place process. The fiber angles and in-plane shear are typically studied in the scenario of draping reinforcements. However, the possible changes that occur during the handling of reinforcements prior to draping are typically not taken into account. The behaviour of the reinforcement during handling is influenced by a variety of design choices, including the positioning of the pick-up points. The pick-up points used to grip the reinforcements during handling need to be positioned in such a way that the in-plane shear strains and resulting fiber angles stay within predefined tolerances.

The research goal is the development of a framework for the prediction and prevention of fiber angle deviations due to in-plane shear during handling of large-sized bi-axial non-crimp fabrics [NCFs]. The first step towards reaching this goal is to set tolerances for in-plane shear induced fiber angle deviations in NCFs. This has been done using experimental research in which bi-axial NCFs are loaded under shear using a picture frame. Specimens are loaded at increasing loads and unloaded in between incremental load levels. These experiments showed that even low shear angles will result in permanent fiber angle deviations in bi-axial NCFs. It was observed that the permanent changes

build upon each other as the experiments continued and the fabric is further sheared. Upon reloading after unloading the fabric shows an initial region with a reduced shear resistance. This region of reduced shear resistance gets larger with the application of higher loads. Tolerances are set based on the load level that will, upon reloading, result in a reduced shear resistance extending beyond an angle of  $1^\circ$ . Based on the experimental work and this criterion the tolerance has been set for  $1.4^\circ$ . The presented strategy for determining tolerances for in-plane shear induced fiber angle deviations opens opportunities for implementation in a smart factory setting. Reinforcements could for example be monitored in real time, with pick-up point placement and/or orientation being adapted when tolerances are approached.

Periodic representative volume homogenisation is used to determine homogenised elastic properties for a bi-axial NCF based on its dimensions and stitching pattern. Elastic properties for the tows are based on a flexural rigidity test and further calibrated using a finite element model. This is required to ensure the bending behaviour of the tows is correctly represented. This behaviour cannot be predicted based on the standard axial stiffness. The results for the homogenised properties have been validated using flexural rigidity tests and small displacement picture frame tests. For the current work a representative volume element [RVE] is used, this also gives the opportunity to observe the effect of changes in tow/stitch geometry, stitching pattern and/or tow and stitch elastic properties on the homogenised elastic properties. This RVE can be expanded to include additional sublayers, tows or stitches to represent different NCF configurations or multi-axial NCFs. For scenarios where the choice of reinforcement is already fixed it might be more appropriate to determine elastic properties at the macroscale. An additional reason for the determination of elastic properties on the macroscale instead of the meso-scale is that the RVE was found to be unable to capture all mesoscopic fabric deformation mechanisms and couplings. When experimentally determining properties on the macroscale more of these mechanisms and couplings will automatically be included in the results. For the current work the stabilizing yarns that are present in the NCF are not taken into account, resulting in a conservative estimate. For implementation in industry these will have to be taken into account.

The homogenised elastic properties are used in a finite element model for the evaluation of in-plane shear strains during handling. This model shows that it is possible to predict the suitability of a repeating pick-up point pattern for the handling of a specific reinforcement in terms of in-plane shear strains using a single quick simulation. For the current work the focus has been on the global in-plane shear strains, the in-plane shear strains that are not affected by the shape of the pick-up point. Experimental work has been carried out with different sized bi-axial NCF specimens loaded under gravity. These results show that bi-axial NCFs preferably need to be treated as multiple layers when choosing a gripping strategy to handle them. If the bottom layer(s) are not supported the NCF will exhibit atypical deformation patterns due to sliding of the bottom layers. Needle grippers are considered to be the most appropriate currently available gripping mechanisms for handling multiple layers, they can however not fully prevent this from happening.

---

For industrial implementation the local in-plane shear strains will need to be taken into account. Additionally, it will need to be taken into account that pick-up points might be required to be in (or avoid) specific locations. Tolerances will be required for the positioning of the pick-up points. The current work only looked at the case of reinforcements loaded under gravity. For implementation in industry vertical and horizontal accelerations will also need to be studied. Finally, further research is needed on the development of a gripping strategy with predictable accuracies that will be able to support all the layers and prevent sliding.



# SAMENVATTING

In de loop der jaren is het gebruik van composieten als constructiemateriaal voor vliegtuigen aanzienlijk toegenomen. Momenteel is de industrie nog grotendeels afhankelijk van handmatig vervaardigde onderdelen. Geautomatiseerde productie kan echter voordelen bieden, zoals lagere productiekosten en een consistentere en hogere kwaliteit van het eindproduct. Een aantrekkelijke geautomatiseerde optie voor het hanteren van vezelversterkingen is het "pick and place" proces. Binnen dit proces worden objecten opgepakt, verplaatst en neergelegd. Het "pick and place" proces maakt het mogelijk om gehele lagen vezelversterking te plaatsen en biedt mogelijkheden voor het hanteren van meerdere lagen en/of grote lagen vezelversterking. De literatuur toont talloze verschillende strategieën voor het uitvoeren van een "pick-and-place" operatie, waarbij het onderzoek meestal gericht is op het ontwikkelen van meer gespecialiseerde concepten. Dit onderzoek omvat doorgaans het aantonen van de haalbaarheid van het concept, maar doorgaans niet het rapporteren van de nauwkeurigheid. Het niet meenemen van de nauwkeurigheid van het "pick-and-place" proces en de kwaliteit van de vezelversterking tijdens het hanteren kan resulteren in inconsistente of ondermaatse eindproducten.

Voordat de luchtvaartindustrie "pick-and-place" operaties breed zal implementeren, zal de kwaliteit van producten die met dit proces zijn vervaardigd moeten kunnen worden gegarandeerd. Een belangrijk kwaliteitscriterium bij het werken met composieten is de oriëntatie van de vezels. De vezeloriëntaties van het eindproduct moeten overeenkomen met de oriëntaties zoals bedoeld in het ontwerp. Om dit te bereiken, moeten de vezelhoeken, gedefinieerd als de hoek tussen twee aangrenzende filamentrichtingen in een vezelversterking, worden meegenomen bij het bestuderen en ontwerpen van "pick-and-place" processen. Een factor die de vezelhoeken direct beïnvloedt, is de afschuiving die in het vlak optreedt in de vezelversterking tijdens het "pick-and-place" proces. De vezelhoeken en afschuiving in het vlak worden meestal bestudeerd in de context van het draperen van vezelversterkingen. Er wordt echter doorgaans geen rekening gehouden met de mogelijke veranderingen die optreden tijdens de verwerking van vezelversterkingen vóór het draperen. Het gedrag van de vezelversterking tijdens het verplaatsen wordt beïnvloed door verschillende ontwerpkeuzes, waaronder de positionering van de oppakpunten. De oppakpunten die worden gebruikt om de vezelversterkingen vast te pakken, moeten zo worden gepositioneerd dat de schuifspanningen in het vlak en resulterende vezelhoeken binnen vooraf gedefinieerde toleranties blijven.

Het doel van dit onderzoek is de ontwikkeling van een raamwerk voor het voorspellen en voorkomen van vezelhoekafwijkingen als gevolg van afschuivingen in het vlak tijdens de verwerking van grootformaat bi-axiale non-crimp stoffen [NCF's]. De eerste stap om dit doel te bereiken is het vaststellen van toleranties voor afwijkingen in de vezelhoeken ver-

oorzaakt door afschuiving in het vlak. Dit is gedaan met behulp van experimenteel onderzoek waarin bi-axiale NCF's onder schuifbelasting worden getest met behulp van een zogenaamd "picture frame". Proefstukken worden getest bij toenemende belastingen en tussendoor ontlast. Deze experimenten toonden aan dat zelfs lage afschuifhoeken resulteren in permanente vezelhoekafwijkingen in bi-axiale NCF's. Er werd waargenomen dat de permanente veranderingen zich opstapelen naarmate de experimenten doorgaan en het weefsel verder wordt afgeschoven. Bij het opnieuw belasten na het ontlasten vertoont de stof een initiële regio met een verminderde schuifweerstand. Deze regio van verminderde schuifweerstand wordt groter na toepassing van hogere belastingen. Toleranties zijn ingesteld op basis van het belastingsniveau dat, bij herbelasting, resulteert in een verminderde schuifweerstand die zich uitstrekt tot een hoek van  $1^\circ$ . Op basis van het experimentele werk en dit criterium is de tolerantie ingesteld op  $1.4^\circ$ . De gepresenteerde strategie voor het bepalen van toleranties voor vezelhoekafwijkingen geïnduceerd door afschuivingen in het vlak opent mogelijkheden voor implementatie in een slimme fabrieksomgeving. Versterkingen kunnen bijvoorbeeld in realtime worden gecontroleerd, waarbij de plaatsing en/of oriëntatie van de oppakpunten kan worden aangepast wanneer de toleranties worden benaderd.

Periodieke representatieve volumehomogenisatie wordt gebruikt om gehomogeniseerde elastische eigenschappen te bepalen voor een bi-axiale NCF op basis van de afmetingen en het stikselpatroon. Elastische eigenschappen voor de vezelbundels zijn gebaseerd op een buigstijfheidstest en verder gekalibreerd met behulp van een eindige elementen model. Dit is nodig om ervoor te zorgen dat het buiggedrag van de vezelbundels correct wordt weergegeven. Dit gedrag kan niet worden voorspeld op basis van de standaard axiale stijfheid. De resultaten voor de gehomogeniseerde eigenschappen zijn gevalideerd met behulp van buigstijfheidstesten en kleine verplaatsings "picture frame" testen. Voor het huidige werk wordt een representatief volume element [RVE] gebruikt. Een dergelijke RVE biedt ook de mogelijkheid om het effect van veranderingen in de vezelbundel/stiksels geometrie, stikselpatroon en/of elastische eigenschappen van de vezelbundels/stiksels op de gehomogeniseerde elastische eigenschappen te observeren. Deze RVE kan worden uitgebreid om aanvullende sublagen, vezelbundels of stiksels op te nemen om verschillende NCF-configuraties of multi-axiale NCFs weer te geven. Voor scenario's waarin de keuze van de vezelversterking al is vastgelegd, kan het meer geschikt zijn om elastische eigenschappen op macroschaal te bepalen. Een aanvullende reden voor het bepalen van elastische eigenschappen op macroschaal in plaats van mesoschaal is dat is gebleken dat de RVE niet in staat is om alle mesoscopische weefselvormingsmechanismen en koppelingen vast te leggen. Bij experimentele bepaling van eigenschappen op macroschaal zullen automatisch meer van deze mechanismen en koppelingen in de resultaten worden opgenomen. Voor het huidige werk zijn de stabiliserende vezels die aanwezig zijn in de NCF niet in aanmerking genomen, wat resulteert in een conservatieve schatting. Voor implementatie in de industrie moeten deze echter worden meegenomen.

De gehomogeniseerde elastische eigenschappen worden gebruikt in een eindige elementen model voor de evaluatie van schuifspanningen in het vlak tijdens het verplaatsen. Dit model toont aan dat het mogelijk is om de geschiktheid van een herhalend

oppakpuntenpatroon voor de verwerking van een specifieke vezelversterking in termen van schuifspanningen in het vlak te voorspellen met behulp van een enkele simulatie. Voor het huidige werk lag de focus op de globale schuifspanningen in het vlak, de schuifspanningen die niet worden beïnvloed door de vorm van het oppakpunt. Experimenteel onderzoek is uitgevoerd met bi-axiale NCF-proefstukken van verschillende grootte die door zwaartekracht werden belast. Deze resultaten tonen aan dat bij het kiezen van een oppakstrategie om bi-axiale NCF's te hanteren deze bij voorkeur als meerdere lagen moet worden behandeld. Als de onderste l(a)ag(en) niet worden ondersteund, vertoont de NCF atypische vervormingspatronen door het schuiven van de onderste lagen. Naaldgrijpers worden beschouwd als het meest geschikte momenteel beschikbare grijpmechanisme voor het hanteren van meerdere lagen. Ook naaldgrijpers kunnen dit schuiven echter niet volledig voorkomen.

Voor industriële implementatie van het “pick and place” proces moeten ook de lokale schuifspanningen in het vlak worden meegenomen. Bovendien moet rekening worden gehouden met het feit dat oppakpunten mogelijk op specifieke locaties moeten worden geplaatst of dat locaties moeten worden vermeden. Toleranties zullen vastgesteld moeten worden voor de positionering van de oppakpunten. Het huidige onderzoek heeft alleen gekeken naar het geval van versterkingen die onder invloed van zwaartekracht worden belast. Voor implementatie in de industrie moeten ook verticale en horizontale versnellingen worden bestudeerd. Ten slotte is verder onderzoek nodig naar de ontwikkeling van een oppakstrategie met voorspelbare nauwkeurigheden die in staat zal zijn om alle lagen te ondersteunen en schuiven te voorkomen.



# 1

## INTRODUCTION

### 1.1. BACKGROUND AND MOTIVATION

OVER the past decades the use of composites as an aircraft structural material has significantly increased: from a mere 1% composites by weight in the 1969 Boeing 747 to 52% composites by weight in the 2015 wide body version of the Airbus A350 [1]. When composites were first implemented their application was limited to secondary structures. As more experience and understanding was gained, composites started to be used in smaller aircraft, with some of these small aircraft being all-composite. In recent years efficiency has become an important criteria for environmental reasons and to reduce operation costs. These criteria, combined with a wide body of research on composites, has resulted in fiber reinforced plastics being used on a large scale in larger aircraft [2].

With the increased use of composite materials comes an increased interest in making the manufacturing process more repeatable and/or more cost-effective. Additionally, the manufacturing process needs to be such that the advantages and opportunities composites can bring come through in the final product. Due to high customization and relatively low volume production the aerospace industry still relies heavily on manually manufactured components. Automating the manufacturing process can however bring advantages such as a reduction in the manufacturing cost [3] and a more consistent and higher quality end product [4].

Not all automated solutions will always be a suitable alternative for manual lay-up. Techniques such as Automated Tape Laying [ATL] and Automated Fiber Placement [AFP] are for example limited to unidirectional [UD] materials and to the handling of strips of material. Figure 1.1 illustrates an alternative to these strategies: the pick-and-place process. The pick-and-place process involves the picking up, moving and placing down of objects.



Figure 1.1: Grip, transfer and drop phases of the pick-and-place process. Adapted with permission from: Schuster *et al.* [5].

The pick-and-place principle is used and researched for use in a wide variety of applications. Manufacturing processes where pick-and-place systems are typically seen include part sorting, bin picking, assembly, packing and inspection [6]. Examples of recent research on pick-and-place systems include Dewi *et al.* [7] who present an automatic vision guided system for a fruit picking and placing robot and Zeng *et al.* [8] who developed a pick-and-place system that can handle and recognise novel objects in a cluttered environment.

An application of pick-and-place that is close to the handling of reinforcements is the handling of fabrics and garments. Recent research include Avigal *et al.* [9] whose robotic system uses two arms to efficiently smooth and fold garments that are presented in arbitrary initial (crumpled) configurations and Zhang & Demiris [10] who propose a method for robot-assisted dressing that can dress a mannequin in a hospital gown with an over 90% success rate.

In the case of handling reinforcements using the pick-and-place process, the process involves picking up, moving, and placing of a layer of reinforcement as a whole, instead of building it up on a mould using strips of material as seen with ATL and AFP. With the right end-effectors a wide range of different shapes and sizes of reinforcements can be handled. Additionally, the pick-and-place process could provide opportunities for the swift handling of multiple layers of reinforcement and/or large layers of reinforcements. Compared to ATL or AFP, pick-and-place processes require relatively straightforward and available equipment, tooling and programming. This can make the process competitive even for smaller parts and lower volume productions [3].

Literature shows that there are countless different strategies to execute a pick-and-place operation and that research tends to focus on highly specialized end-effectors, resulting in inflexible single-purpose solutions [11]. The state of the art mainly presents demonstrators of different pick-and-place concepts. The accuracy that has been achieved with these concepts in placing reinforcements is typically not reported. However, for the implementation of the pick-and-place processes in the manufacturing of composite structures the product quality is of most importance for certification.

One of the quality criteria that is used when working with composites is the orientation of the fibers. This fiber orientation is part of the design when designing the product and it is important that the fibers in the final product match the intended directions. To ensure

the desired orientation can be achieved in the final product the fiber angles, defined as the angle between two adjacent filament directions in a reinforcement, should be taken into account when studying and designing pick-and-place processes.

Fiber angles are directly influenced by in-plane shear that occurs during the pick-and-place process. Handling reinforcements will result in deformations due to gravity loads and forces resulting from accelerations, decelerations, etc. The main deformation mode during forming processes is in-plane shear [12]. This will also be the main deformation mode during handling. The behaviour of the reinforcement during handling will be influenced by several factors. One important factor is the positioning of pick-up points. The positioning of these pick-up points need to be done in a way that the in-plane shear and resulting fiber angles deviations stay within an acceptable range. To be able to evaluate the positioning of these points, tolerances need to be set for the in-plane shear and fiber angle deviations first.

## 1.2. OBJECTIVE, APPROACH AND OUTLINE

The main focus of the current work is fiber angle deviations in reinforcements handled using pick-and-place processes. The positioning of pick-up points is studied as a factor influencing these fiber angle deviations. Experiments and numerical methods have been used to set tolerances for deviations in the fiber angles. Additionally, a mesoscopic representative volume element [RVE] model, to be used for the determination of homogenized elastic properties for non-crimp fabrics [NCFs], has been created and validated. Finally, reinforcements have been subjected to gravity loading in an experimental and numerical study of their behaviour.

The outcome of the thesis will be a framework that can be used to predict and prevent fiber angle deviations in non-crimp fabrics using different pick-and-place strategies. The results can be used both in the design phase and in the manufacturing phase of a pick-and-place process.

The state of the art has been studied and discussed on the suitability of the presented solutions for the accurate and swift handling of multiple and/or large layers or reinforcement to determine the exact gaps in research to be studied in this research.

The outline of the thesis is as follows: first, chapter 2 presents the current state of the art and discusses the suitability of these techniques for the accurate and swift handling of multiple large-sized layers of reinforcements. Special attention is given to section 2.6 where the topic and goal of this thesis is derived from this review. Chapter 3 outlines the approach that has been taken to set tolerances for the fiber angle deviations. Next, chapter 4 presents the set-up and validation for the mesoscale RVE model used to determine homogenized elastic properties for the NCF used in the current work. Chapter 5 discusses the set-up and validation for simulations where reinforcements are subjected to gravity loading while picked up in four corners. Results will be presented showing the influence of pick-up point distribution on the fiber angle deviations. Chapter 6 presents a discussion on the current work and gives guidelines for implementation in industry. Finally, chapter 7 will give the conclusions and recommendations.



# BIBLIOGRAPHY

- [1] S Pantelakis. “Historical development of aeronautical materials”. In: *Revolutionizing aircraft materials and processes*. Springer, 2020, pp. 1–19.
- [2] C Kassapoglou. “Applications of Advanced Composites in Aircraft Structures”. In: *Design and Analysis of Composite Structures: With Applications to Aerospace Structures*; John Wiley & Sons, Ltd.: Hoboken, NJ, USA (2013), pp. 1–7.
- [3] JC de Kruijk. *Automated composite manufacturing using robotics lowers cost, lead-time and scrap rate*. Tech. rep. NLR-TP-2018-143. Netherlands Aerospace Centre NLR, 2018.
- [4] GC Newell, RO Buckingham and K Khodabandehloo. “The automated manufacture of prepreg broadgoods components—a review of literature”. In: *Composites Part A: Applied Science and Manufacturing* 27.3 (1996), pp. 211–217.
- [5] Alfons Schuster, Michael Kupke and Lars Larsen. “Autonomous Manufacturing of Composite Parts by a Multi-Robot System”. In: *Procedia Manufacturing* 11 (2017), pp. 249–255.
- [6] Aztek Marketing - SDC. *Applications for pick and Place Robots*. Mar. 2022. URL: <https://sdcautomation.com/applications-for-pick-and-place-robots/>.
- [7] Tresna Dewi et al. “BLOB analysis of an automatic vision guided system for a fruit picking and placing robot”. In: *International Journal of Computational Vision and Robotics* 11.3 (2021), pp. 315–327.
- [8] Andy Zeng et al. “Robotic pick-and-place of novel objects in clutter with multi-affordance grasping and cross-domain image matching”. In: *The International Journal of Robotics Research* 41.7 (2022), pp. 690–705.
- [9] Yahav Avigal et al. “Speedfolding: Learning efficient bimanual folding of garments”. In: *arXiv preprint arXiv:2208.10552* (2022).
- [10] Fan Zhang and Yiannis Demiris. “Learning garment manipulation policies toward robot-assisted dressing”. In: *Science robotics* 7.65 (2022), eabm6010.
- [11] Stefan Flixeder, Tobias Glück and Andreas Kugi. “Force-based cooperative handling and lay-up of deformable materials: Mechatronic design, modeling, and control of a demonstrator”. In: *Mechatronics* 47 (2017), pp. 246–261.
- [12] Eduardo Guzman-Maldonado et al. “Experimental and numerical analyses of the mechanical behavior during draping of non-orthogonal bi-axial non-crimp fabric composite reinforcements”. In: *Materials & Design* 218 (2022).



# 2

## REVIEW OF THE STATE OF THE ART

### 2.1. INTRODUCTION

OVER the years, the manufacturing processes for traditional materials have been improved and streamlined, resulting in reductions in manufacturing time/cost and an increase in the mechanical properties of the final part. For the application of composite materials to become more widespread and replace traditional materials their manufacturing processes and final products will need to be competitive and for example be lighter, stronger, stiffer or quicker/easier to produce than traditional materials. Pick-and-place processes can potentially make a step towards this by being able to accurately handle more and larger layers at higher speeds.

Despite a large variety of published research on pick and place systems there is not yet a widespread implementation in industry. This can partly be explained by existing technologies being unable to match the ability of skilled laminators when draping fabrics on double curved surfaces or complex moulds [1, 2]. The inability to drape on complex surfaces can be overcome by decoupling of lay-up and forming in a two step process [2, 3]. An additional advantage of full stack forming is the potentially major reduction in overall draping time and associated manufacturing cost [4]. The state of the art focuses on the handling of single layers of reinforcement. For full stack forming processes it is desirable to handle multiple layers simultaneously. Laminates could first be stacked on a flat surface, then picked up as a whole and finally formed. In scenario's with single curvature moulds the pick-and-place process could drape the stack of reinforcements in or on the mould. This does however require pick-and-place strategies and techniques that are suitable for the handling of multiple layers.

---

Parts of this chapter have previously been published in:

Chantal M. de Zeeuw, Daniël M. J. Peeters, Otto K. Bergsma & Rinze Benedictus (2020) Strategies for swift automated pick-and-place operations of multiple large-sized layers of reinforcement - a critical review, *Advanced Manufacturing: Polymer & Composites Science*, 6:2, 57-71, DOI: 10.1080/20550340.2020.1750329

Another reason for the limited implementation in industry is the size of the fabrics that are handled in literature. The ability to handle large-sized reinforcements is a great potential advantage of pick-and place operations. Despite this potential, published research generally focuses on lab-sized demonstrators. The maximum ply size reported in literature is  $4300 \times 1315 \text{ mm}^2$  by Deden *et al.* [5], with Gerngross *et al.* [6] showcasing dimensions up to  $6000 \times 1220 \text{ mm}^2$  can also be handled using a similar set-up. These are however not typical dimensions and most demonstrators are designed to handle plies with dimensions smaller than 1000 mm. Real life applications of composites will however often be much larger than this. The Boeing 787 does for example have a 60 m wingspan [7] while the current largest carbon/glass hybrid composite wind turbine rotor blade is 107 m long [8]. For these large-scale applications of FRPs it can be advantageous to handle larger layers. This is also reflected in larger lay-up systems being developed in industry. Kuka Robotics together with Bombardier Aerospace have for example created a system with dimensions of  $12 \times 1.2 \text{ m}^2$  for wing manufacture [9].

The speed of pick-and-place operations is typically not disclosed in literature. Operating at higher speeds can bring advantages in terms of the lead time required to produce a part. The state of the art research focuses on the development of demonstrators. The highly specialized end-effectors that are developed generally result in inflexible single purpose solutions [10]. Additionally, often the main focus is with the demonstration of a concept. The quality of the reinforcement and placements is typically not reported. For the final product and for certification it is however crucial that a consistent high quality product can be delivered. This chapter focuses on evaluating the current pick and place strategies on their suitability for the accurate and swift simultaneous handling of multiple layers and on the handling of large-sized layers.

Section 2.2 starts by establishing challenges that are associated with pick-and-place handling of reinforcements. First, general challenges will be presented followed by challenges associated with handling large-sized layers or multiple layers. The section will then formulate criteria that need to be fulfilled for a pick and place operation to be considered successful. In section 2.3 the different strategies for handling composite plies used in literature will be presented. Hereafter, the strategies are discussed in section 2.4 using the criteria that have been formulated. A conclusion is given in section 2.5. Finally, section 2.6 presents the research goal and research questions of the research project.

## 2.2. CHALLENGES

The end-goal of a pick-and-place operation is to successfully place a reinforcement in or on a mould. Setting requirements for the pick-and-place process and/or the final product will influence how plies are transported from the cutting table to the mould. Different requirements will result in different challenges during automated handling. The interest of the current work lays in challenges associated with the plies. These challenges partly come from the properties of the reinforcement material but also from the ply size and the number of layers that is being handled. Additionally, the quality of the final product is to be in line with the requirements of the industry. Quality requirements can for example include positional accuracy, accuracy of the fiber directions and requirements for contamination free handling.

Some handling related challenges associated with dry reinforcements are e.g. their low and even anisotropic bending stiffness, sensitivity regarding shear forces, high permeability and structural instability [10–13]. Despite pre-preg having a higher stiffness, shear and bending behaviour are still important factors to consider when designing the manufacturing process. Pre-preg provides additional challenges through their tack and the backing paper that is present on either one side or both sides of the plies [14].

The non-rigidity of composite plies can result in several problems during the pick-and-place process [15]:

**Pick** When a reinforcement is picked up the forces can result in deformation of the ply. This can damage the ply and/or result in inaccuracies in the process through e.g. fiber angle variations.

**Move** The low stiffness of a composite ply can cause high deformations - possibly resulting in unexpected collisions. Additionally, depending on the number and location of pick up points a picked up reinforcement can experience high (local) stresses and strains.

**Place** The deformation of the reinforcement during handling can make it difficult to achieve an accurate placement. Problems such as edge folding can also occur during the placement operation.

The placement phase of the pick-and-place process typically works by draping the plies in or on a mould. Draping is more straight forward for single curved moulds than for double curved moulds. For these complex moulds draping will typically have to be sophisticated to conform the reinforcement to the desired shape. Some pick-and-place strategies overcome this limitation by employing a forming principle in the placement stage. However, forming is considered to be typically a separate process to the pick-and-place process. Therefore, the challenges and strategies associated with forming and complex moulds are not discussed.

Fabrics typically found in literature are either unidirectional [UD], woven or Non-Crimp Fabrics [NCF]. Unidirectional fabrics have all fibers parallel while woven fabrics are mostly bidirectional. NCFs are made by stacking unidirectional fabrics in different orientations and stitching them together.

An advantage of UD and NCFs over woven fabrics is that they avoid the crimp found in woven fabrics because the fibers do not cross but lie on top of each other [16]. Compared to woven fabrics NCFs can achieve improved in-plane structural properties due to a reduction in the fiber undulation. Also, UD and NCFs have more freedom in tailoring the lay-up sequence. However, UD will have the tendency to split, tear and wrinkle under forming loads due to their low structural rigidity in directions other than the fiber direction [3, 17]. Additional advantages of NCFs include an increase in the lay-up rate due to higher masses per-unit area and a low number of defects due to material handling - even in large cut pieces [18].

An advantage of woven fabrics is however that they typically have better drapability [19]. The drapability of woven fabrics or NCFs is influenced by the knitting/stitching properties or weave type [12, 20]. Figure 2.1 gives two examples of stitches that can be used in

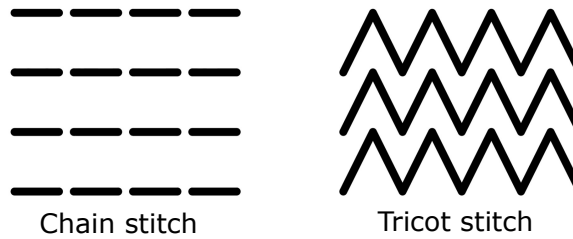


Figure 2.1: Comparison of chain and tricot type stitch

an NCF: a tricot stitch and a chain stitch. A tricot stitch will result in a low bending and shear stiffness while a chain stitch will give an NCF with high form stability [21].

Current research focuses on picking up one layer at a time. Increasing the number of layers to be handled simultaneously is a good way to increase the manufacturing output, which can result in a decrease in manufacturing cost. Handling multiple layers at once will however also introduce additional challenges. For the current work layers are defined in two different ways:

**Sub-layer** A sub-layer is defined as the layers within a NCF. The layers are attached to each other through for example stitches or an adhesive binder.

**Layer** A layer is defined as the reinforcement as a whole as supplied by the manufacturer. This can for example be an NCF, woven fabric or UD prepreg.

Increasing the number of sub-layers or layers will affect the pick-and-place process in a variety of ways. For NCFs with sub-layers the behaviour will also depend on the integrity of the binder - whether it is structural or non-structural. Non-structural stitching will consolidate the plies but, unlike structural stitching, it will not form a 3D reinforcement. In industry several non-structurally stitched NCFs are typically used to make a preform. This whole assembly is then structurally stitched to greatly improve the out-of plane stiffness and create a 3D reinforcement [22].

The draping process will also be affected by the amount of layers or sub-layers. When an out of plane curvature is applied to a reinforcement there will be a difference in path length between the inner and outer surface. This difference can result in fiber wrinkling. When multiple plies are present each ply will be subjected to this effect. Severe wrinkling will occur if the plies cannot slip over one another [23].

The processability of a stack of multiple plies can be improved by using local stitching - a so-called assembly seam. These stitches facilitate easier handling by locally fixing the layers together. It is undesirable for this assembly seam to influence the mechanical properties of the final product. Therefore, its placement needs to be optimized and its density should be minimized. The deformation behaviour of ply stacks is also affected by the stitches. The local stitching can for example reduce the ability of the plies to shear or transfer shear forces to different areas during forming [24].

Another important factor when looking at the influence of the reinforcement on the pick-and-place process is the size of the reinforcement. The number of points used to pick up the reinforcement should for example depend on the reinforcement size [25]. Increasing the reinforcement size without changing the amount and/or position of pick up points will result in a larger deformation and larger stresses at the pick-up points. This can not only make the correct placement more difficult but will also result in severe shear deformation, which will have a large influence on the resulting fiber orientations. When extreme deformation is present this could even lead to breaking or tearing of the fabric.

The reinforcements required for the manufacturing of large components can be too large for a single robot to handle. In those cases multiple robots are required to work together. This can provide challenges in terms of the robot configurations required to pick, move and place the desired cut pieces. Eckardt *et al.* [18] note that they use a geometric link between the two robots to enable them to carry out cooperating movements. Larsen *et al.* [26] describe their approach to collision-free automatic path planning for cooperating robots.

For the case where the intent is to handle multiple large layers of NCF at the same time the pick-and-place strategy is considered to be effective if:

- The pick-and-place strategy does not negatively affect the quality of the ply through e.g. contamination of the surface or permanent distortion of the ply.
- Contact between plies and mould surface and the desired fiber orientations have been achieved within tolerances.
- There are no (sub-)layers left on the cutting table after pick-up or released during movement.

## 2.3. STRATEGIES IN LITERATURE

### 2.3.1. PLY HANDLING TECHNIQUES

Literature presents a wide range of different strategies for the handling of single plies. In general, it shows that research has a tendency to focus on highly specialized end-effectors. This results in inflexible single purpose end-effectors and is not efficient when dealing with large reinforcements and complex surfaces [10]. Figure 2.2 presents the four categories as defined by Elkington *et al.* [4] that are used to aid in discussing the various strategies: Rigid, kinematic, compliant and free ply.

**Rigid (A)** Plies are picked up using grippers on a rigid frame. This way the ply also becomes rigid during the handling operation. Rigid frames are generally used to move plies from a flat table to a flat mould. Plies are generally picked up straight and placed straight down, e.g. [3, 27–29]. Alternatively, pick-up and place down is achieved through a rolling motion [19].

**Kinematic (B)** Once a ply is picked up a kinematic ply handling system can deform itself to match the shape of the mould. This makes it possible to place plies on more complex shapes. A downside of this system is that the kinematics of the

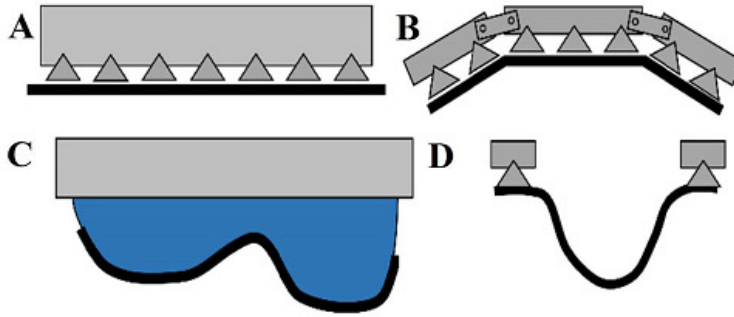


Figure 2.2: Schematics of four common ply handling methods: (A) Rigid, (B) Kinematic, (C) Compliant and (D) Free Ply. From: Elkington *et al.* [4].

end-effector dictate the complexity of the shape it can conform to. Depending on the system it might only be able to handle a few different features of the mould. Furthermore, when the components to be draped become larger and more complex the number of linkages and actuators required increases rapidly, which might limit further development. The shape of the reinforcement can be matched to the mould while suspended in the air or while placing the ply down. Plies can be picked up straight before being draped in or over the mould [11], but rolling motions are also used [12].

**Compliant (C)** The compliant ply handling method avoids the above mentioned problems from the kinematic ply handling method by using passive compliant elements that deform as the end-effector holding the ply is lowered onto the mould. Several strategies use a straight pick up before a compliant strategy to drape the ply in or on the mould [11, 30] while other strategies both pick up and place down plies through a rolling motion [31, 32].

**Free Ply (D)** Contrary to the previous methods the free ply method does not strictly dictate the shape of the ply that is held. The plies are generally held at a limited amount of points along corners or edges and left to hang. The sag that results from holding a ply this way has for example been used to dictate where the first contact between ply and mould is and to be able to place plies into a deep convex mould. This way of ply handling is also how plies are generally handled during hand lay-up. A laminator will use their hands to hold a ply and will generally pick them up at opposing edges. The free ply strategy is used for both flat [3, 25] and curved [10, 18, 33, 34] surfaces. For curved moulds they can be picked up straight before being actively draped over the mould [18, 33, 34] while other strategies use an additional roller to place the ply [10]. Björnsson *et al.* [3] performed some testing on picking up prepreg plies using a peeling motion.

Table 2.1 divides the strategies presented in literature based on the four categories as defined by Elkington *et al.* [4].

Table 2.1: Mapping of ply handling methods used in the handling of reinforcements. Based on ply handling methods described by Elkington *et al.* [4]

	Rigid	Kinematic	Compliant	Free ply
Dry	[13, 35, 36]	[9, 11, 12, 37, 38]	[11, 12, 30, 31, 37]	[10, 18, 33]
Prepreg	[3, 19, 27–29, 39]	[32, 34, 40–42]	[32]	[3, 25, 34]
Unspecified	[43]	[44]	-	-

The behaviour of dry reinforcements during handling can be very similar to that of the fabrics used in the garment/textile industry. In addition to pick-and-place operations, this industry also deals with other challenges such as separation, untangling, flattening, (un)folding, hanging and clothing assistance [45]. Despite the garment/textile industry being significantly larger than the composite industry there is not as much development of and variety in the handling strategies; the strategies will typically take a bimanual approach, mimicking a human approach to executing the task. Using the definitions given by Elkington *et al.* [4] these systems would be considered to be using free ply strategies.

To aid in the successful execution of the handling tasks required in the garment/textile industry they use a manipulation technique not found in the handling of reinforcements. This technique is regripping: during the handling process gripping points are released and placed in a different location. This is for example used to grasp a garment at the desired locations after it has been picked up at a random grasping point [46]. Regripping in this exact form is not as relevant for the handling of reinforcements due to their relatively delicate nature. It is important that these reinforcements are picked up in the appropriate areas at the start of the handling process to prevent undesired permanent deformations. However, strategic placement and release of pick-up points during the handling process can facilitate accurate placement of reinforcements.

Figure 2.3 presents an overview of the ply sizes and end-effector sizes reported in literature based on the research mentioned in Table 2.1. Most studies do not report both the ply size and end-effector size. The data for the graph can be found in Tables A.1 and A.2 in Appendix A.

Figure 2.3 shows that the largest ply size presented in literature is  $\pm 12000 \times 1500 \text{ mm}^2$ , with the majority of plies being smaller than  $\pm 1000 \times 800 \text{ mm}^2$ . Grippers are generally used to handle a variety of ply shapes and sizes. The size of the end-effector will need to be chosen such that it can fit the largest ply in the ply book. For the presented end-effectors that are larger than the largest presented ply some authors mention that the dimensions are required for the parts to be handled [13, 47] or that the end-effector can be used to grip multiple plies next to each other [31]. For strategies that use a 'Free Ply' ply handling method the end-effector can be significantly smaller than the plies that are being handled - e.g. the two collaborating end-effectors used by Eckardt *et al.* [18], Gerngross *et al.* [12] and Deden *et al.* [5] are  $210 \times 2000 \text{ mm}^2$  while the largest plies they handle are respectively  $1989 \times 1034 \text{ mm}^2$ ,  $4300 \times 1315 \text{ mm}^2$  and  $6000 \times 1220 \text{ mm}^2$ .

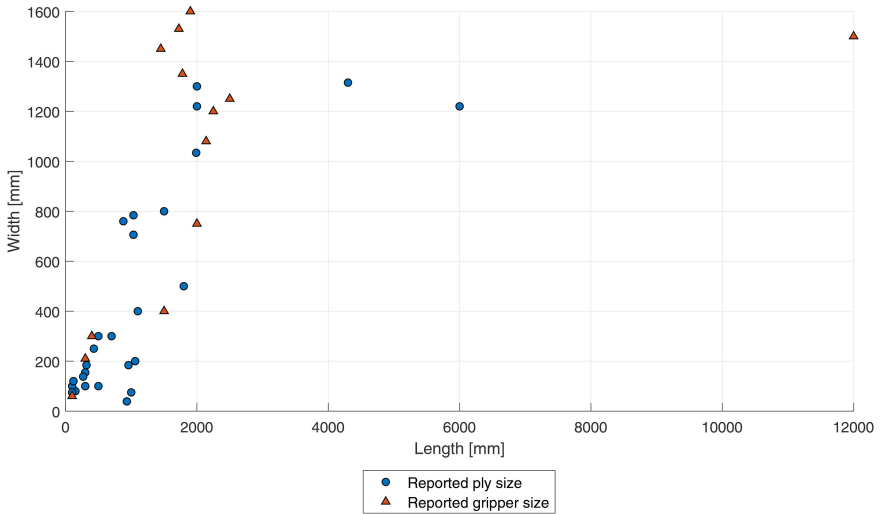


Figure 2.3: Mapping of ply sizes and end-effector sizes reported in literature

### 2.3.2. GRIPPING POINT STRATEGIES

All of the above presented ply handling strategies require a mechanism that connects the ply with the end-effector. Table 2.2 gives an overview of the positioning of these gripping points in literature. Strategies vary from grabbing the complete surface to only utilizing a minimal amount of pick-up points. Some of the presented strategies are optimized for a specific ply - e.g. [27, 32, 37, 40] - or plybook - e.g. [3, 19, 39] - while others can be used with a variety of shapes and/or sizes - e.g. [12, 13, 29–31, 38]. The optimal placement of pick-up points when handling limp materials using a limited amount of pick-up points has been studied for one-dimensional strips [48, 49] and two-dimensional parts [50, 51].

Table 2.2: Mapping of grip point distribution. Based on categories defined by Björnsson *et al.* [52].

	Grip points at edges or corners	Grip points spread over surface
Dry	[10, 11, 18, 33, 37]	[9, 12, 13, 30, 31, 35, 36, 38]
Prepreg	[3, 19, 25, 27–29, 34]	[32, 39, 41, 42]
Unspecified	-	[40, 43, 44]

There is a wide range of gripping devices that can be used to handle non-rigid materials - see e.g. [53–56]. When reviewing literature on the handling of reinforcements for composite production, six gripping technologies were found to be used: Needles, vacuum, cryo-freezing, electrostatic, gecko inspired and pinching.

**Needles:** Needle grippers can achieve high holding forces [55]. However, the penetration of the material required to pick the reinforcement up using needles can result in damage and displacement of the fibers (e.g. fiber distortion, fiber broadening and buckling [13]), thereby possibly negatively influencing the properties of the finished part [11]. Brinker *et al.* [34] do however note a spring back effect of the textile when pulling out the needles and Buckingham & Newell [25] did not measure a reduction in structural

integrity, even when unrealistically large loads were applied. The lay-up precision can however be decreased through the relative motion of the fibers. It is therefore recommended to grip in the excess material [25]. Jarvis *et al.* [36] found that unidirectional fabric in particular tended to slip after initial attachment. Lutz *et al.* [55] remark that additional disadvantages of needle grippers are their high per unit cost and the large installation space that is required.

Seliger *et al.* [56] present the following (theoretical) holding force formula for needle grippers:

$$F_h = \sigma \cdot A_N \cdot n_N = \frac{E_{z6\%} \cdot \delta}{2 \cdot S \cdot \sin \alpha_N} \quad (2.1)$$

$$A_N = \frac{\delta^2 \cdot \tan \gamma / 2}{\sin \alpha_N} \quad (2.2)$$

where,  $\sigma$  is the surface tension,  $A_N$  is the area of a needle penetrating the fabric,  $n_N$  is the amount of needles,  $E_{z6\%}$  is the Modulus of Elasticity of a Fabric with 6% Extension,  $\delta$  is the layer thickness,  $S$  is the prick distance of the needles,  $\alpha_N$  is the penetration angle and  $\gamma$  is the leading edge angle. Figure 2.4 gives a schematic of a needle gripper.

The minimum holding force required to pick up a reinforcement can be estimated using:

$$\vec{F}_{min} = m(\vec{g} + \vec{a}) \quad (2.3)$$

where,  $F$  is the gripping force,  $m$  is the mass of the part,  $g$  is the gravitational acceleration and  $a$  are any additional accelerations, which are to be included if they are significant. To pick up the reinforcement  $F_h$  will need to be at least equal to  $F_{min}$ .

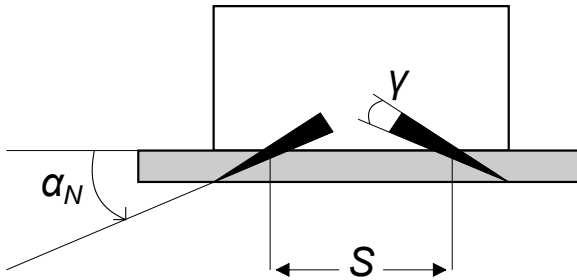


Figure 2.4: Schematic for needle gripper. Based on Seliger *et al.* [56]

An increase in the number of needles or a decrease in the penetration angle will result in an increase in the holding force of needle grippers. Seliger *et al.* [57] note that the piercing angle should be in the range of  $20^\circ$  -  $40^\circ$  for a high holding force. Smaller angles can theoretically result in a larger holding force but can be challenging to achieve. The holding force will be further influenced by properties of the reinforcement such as fiber density, relocatability of fibers and the architecture. A fabric with higher fiber density or a larger amount of crossing points will for example require less needles than one with lower fiber density and a lower amount of crossing points.

**Vacuum:** The vacuum category includes both low airflow/high pressure difference and high airflow/low pressure difference solutions. The first category includes traditional vacuum system while in the second the air flow is for example generated by electrical fans or Coanda ejectors. The use of Bernoulli grippers can result in fiber displacement and there is also a risk of deformation when suction grippers are used. Coanda grippers do however have little risk of leaving marks on the fabric. [11, 55, 58]

Traditional vacuum systems can be categorized in flat and bellow cups. The flat suction cups can generate a faster sufficient holding force due to their low internal volume and are more rigid, which results in better stability and lay-down accuracy in lateral directions. An advantage of bellow suction cups is that they can adapt to uneven surfaces and different laminate thicknesses. Flat suction cups can achieve these advantages by using spring followers to equal different thicknesses and couplings and ball joints to adapt to uneven surfaces [19, 29]. Lutz *et al.* [55] note that suction pads also have the advantage of low unit costs and a small construction space. Additionally, they make it possible to separate plies from a stack and, when compared to Bernoulli grippers, they have the advantage that there is lateral fixation of the plies.

The roughness of the surface to be picked up will influence the ability of vacuum grippers. A higher surface roughness will result in more leakage under the suction cup. To counter this a higher suction power is needed to enable more effective sealing [25]. The permeability of the fabric results in suction grippers being energetically highly inefficient [11, 55, 58]. Kühnel *et al.* [29] found that for a more porous fabric pressure charged grippers were better suited while for denser materials vacuum charged grippers is more appropriate. The difference in performance is attributed to the higher flow rate of the pressure charged grippers and the ability to better sustain vacuum of the vacuum charged grippers.

It is possible to calculate the (theoretical) handling force of a vacuum gripper. The (theoretical) holding force formula is as follows [56] :

$$F_h = A_V \cdot \eta (p_0 - p) \quad (2.4)$$

where,  $A_V$  is the area of the vacuum gripper,  $\eta$  is the efficiency,  $p_0$  is the atmospheric pressure and  $p$  is the pressure in the gripper. An increase in pressure  $p$  will result in a decrease in the holding force  $F_h$ . Kühnel *et al.* [29] tested the handling forces of vacuum grippers when picking up PEEK powder impregnated woven fabric. They found handling forces of 0.1 - 0.66 N for vacuum grippers with a vacuum charged effective area and 0.61 - 2.12 N for vacuum grippers with a pressure charged effective area. Brecher *et al.* [11] found a gripping force of  $\pm 0.2$  N per Bernoulli gripper module.

**Cryo-freezing:** To pick the fabric up the freezing medium (e.g. water vapor) is frozen using a cooling element, thereby generating a contact surface. Placement of the fabric is achieved by liquifying the frozen vapors using air pressure. The freezing medium required for cryo-freezing brings a contamination risk that can impact the final quality [37, 52]. Additional disadvantages noted by Lutz *et al.* [55] are the high cost per unit and a low process stability.

The (theoretical) handling force of a freezing gripper can be calculated using the following formula [56]:

$$F_h = \frac{W_{sl}^{ad} \cdot A_R}{\delta} = \frac{\sigma \cdot (1 + \cos\theta) A_R}{R_z} \quad (2.5)$$

where,  $W_{sl}^{ad}$  is the adhesion work,  $A_R$  is the area of the freezing gripper,  $\delta$  is the layer thickness,  $\sigma$  is the surface tension,  $\theta$  is the contact angle and  $R_z$  is the surface roughness. Seliger *et al.* [56] note that they realized holding forces of up to 40 N when handling carbon fiber preforms.

The cryo-freezing gripper is a strategy relying on an adhesive gripper principle. Adhesion between gripper and fabric can also be obtained using other media. Dutta & Schmidt-Eisenlohr [59] do for example present a patent for the adhesive handling of semi-finished fiber products using matrix material.

**Electrostatic:** An electrical field is created by applying different potentials to the gripper electrode [11]. The material is released by turning the voltage off or by leaving the material at an area with a higher electrostatic attraction. The release through turning the voltage off can be aided by an airstream coming from the gripper [58]. Electrostatic grippers allow the air-permeable reinforcements to be handled reliably and damage-free [11]. Advantages of electrostatic grippers over vacuum grippers when handling fabric plies include their light weight, an uniform surface force, ease of re-configuration, simple construction and low cost [60]. Brecher *et al.* [61] note that the specific weight of the material to be handled is the only limiting factor for the use of electrostatic grippers, with almost all materials being suitable for handling using electrostatic grippers. Jarvis *et al.* [36] do however decide against using electrostatic gripping because they believe high electrical potentials are undesirable in an environment where a lot of highly conductive carbon strands and dust can be found.

Under the assumption of a uniform field the holding force applied to a ply by a single-pole electrostatic gripper can be calculated as [47]:

$$F_h = A_E \cdot \varepsilon_1 \left( \frac{V}{d_1} \right) \quad (2.6)$$

where,  $A_E$  is the area of the electrostatic gripper,  $\varepsilon_1$  is the permittivity of the insulation layer of the electrostatic gripper,  $V$  is the voltage and  $d_1$  is the thickness of the insulation layer. Brecher *et al.* [61] find material specific gripping forces varying from 2 N/m<sup>2</sup> up to 150 N/m<sup>2</sup> depending on the voltage that is applied. The maximum lifting capacity for Interglas 92110 was  $\pm 17$  N/m<sup>2</sup> and for a carbon fiber UD-fabric  $\pm 27$  N/m<sup>2</sup>. The electrostatic pad presented by Ruffatto III *et al.* [62] can support up to 112 N or 68 kPa in shear on a glass substrate. The adhesive values are however highly dependent on the substrate. Up to 5.6 times lower values were reached for drywall, finished wood and steel substrates.

**Gecko inspired:** "Gecko grippers" are inspired by the mechanisms that aid the gecko in climbing walls and hanging upside down - van der Waals interactions enabled by the tiny hairs on their toes [63].

Dadkhah *et al.* [64] mimic the gecko gripping technology by using  $20\ \mu\text{m} \times 60\ \mu\text{m}$  triangular wedges. This results in a directional dry adhesive. Applying a shear force in the correct direction will result in the adhesive force being turned on, reversing the load will result in a release. The authors combine this adhesive with an electrostatic gripper and show that the addition of electroadhesion improves the handling force.

Brecher *et al.* [11] generate van der Waals forces by rolling the polymer sheet out on the ply to be picked up. To release the ply this process is executed in reverse. Advantages of this technology include the ability to handle most surface types and not being dependent on a power supply. However, the authors note that flexible goods risk being rolled in with the polymer sheet upon release and that the gripper is vulnerable to contamination. This technology can therefore not compete with gripper systems such as vacuum or needle grippers [11].

Chu *et al.* [65] developed an end-effector for the handling of a delicate flat surface that is able to achieve a maximum adhesion of 12.5 kPa with a preload of 0.4 N. In their work they present adhesion results for a variety of end effectors developed in recent years by other research institutes for different applications. These results show a high variability in the maximum adhesion. It should be noted that the adhesive forces that can be achieved are highly dependent on the condition of the surface to be gripped. Factors such as roughness or contamination of the surface affect the van der Waals force that is responsible for adhesion [65].

**Pinching:** Pinching grippers mimic the motions of a human hand grasping an object.

Alebooyeh *et al.* [66] developed a soft gripper that picks up carbon fiber based plies through a pinching mechanism. The material is released by opening the pinching clamps. In [66] they improve the fabric wrinkling and placement accuracy compared to their previous work for fabrics being handled using a double arm pick-and-place strategy. Additionally, the improved performance of their current design in terms of slippage and material wrinkling is presented. Further unpublished work discussing further development of the gripper can be found in Wang & Urbanic [67].

Additional gripping strategies used in the garment/textile industry are clamps - see [68] for a recent review. This review also includes pinching grippers. Additionally, Lutz *et al.* [63] note that roll grippers can be used to handle textiles and in the past adhesive grippers have been used - e.g. [66,67]. There is an interest in bringing clamping/pinching grippers to the composite manufacturing process to a larger extent: Gerngross and Nieberl [12] used toggle clamps to handle auxiliary materials. Szczesny *et al.* [69] used a clamping mechanism in the placement of tapes up to 300 mm in width.

Table 2.3 categorises these technologies according to the reinforcement type that is being handled. Each research project is mentioned once. Additionally, there are projects that focus solely on improving gripping technologies to be used with composite reinforcements for: vacuum grippers [70–72], Cryo-freezing grippers [56], Electrostatic grippers [47, 60, 64] gecko inspired grippers [64] and pinching grippers [66, 67].

Table 2.3: Mapping of gripping technologies used in the handling of reinforcements

	Prepreg	Dry	Unspecified
Needles	[27, 28]	[11, 37]	-
Vacuum	[3, 19, 25, 28, 29, 32, 34, 39, 41, 42]	[9, 10, 12, 13, 18, 30–33, 36, 38]	[43, 44]
Cryo-freezing	-	[37]	-
Electrostatic	[11]	[11, 35]	-
Gecko inspired	-	[64]	[11]
Pinching	-	[66]	-

### 2.3.3. ACCURACY IN PICK-AND-PLACE PROCESSES

The accuracy of positioning of placements is typically not reported in literature. The quality criteria that were found most often are placement accuracy or repeatability. Martinsson [19] uses an array sensor to measure the position of the edges of a placed prepreg relative to predefined points. Kuehnel *et al.* [29] use a computer vision approach to detect position and orientation of cuts before picking them up and placing them. Krogh *et al.* [42] discuss the difference between prescribed and actual boundaries for their numerical simulations of draping of woven prepreps on double curved molds. Additionally, they also report the ply-mold separation for different draping strategies. The work by Gerngross & Nieberl [12] stands out because they set tolerances for both the fiber angles ( $\pm 5^\circ$ ) and the boundary curve positions (+5 / -7.5 mm). Their preforming results are evaluated by comparing them to a laser projection.

Several strategies have been employed in literature to avoid inaccurate placement of the plies. Eckardt *et al.* [18] manually taught their dual arm collaborating robots how to place down a ply in such a way to avoid wrinkles, bridging and distortion. Brecher *et al.* [11] and Kordi *et al.* [37] employ a combination of active and passive draping - as defined by Björnsson *et al.* [52] - to keep the distance between gripping elements constant during fabric manipulation. This process ensures that fabric bridging is avoided and reinforcements can be picked up without introducing displacement or wrinkles. Additionally, Brecher *et al.* [11] mention that the electrostatic prototype they present can handle goods without distortion or shifting due to the evenly distributed surface attraction. Buckingham & Newell [25] note that for their set-up in which a free hanging ply is placed down, the initial-touch down point should generally be in the middle of the mould or at a nearby turning point. Doing so allows placement to take place outwards, thereby ensuring that bubbles and wrinkles are continuously moved out of the component. Krogh *et al.* [73–75] found that the path taken by the grippers during draping has a large influence on the accuracy of the placement of prepreg plies. Wrinkles were easily created with both the uniform draping strategy and the wave shape draping they employed. They conclude that for an accurate placement effort should be taken to determine the optimal trajectories for the grippers.

Sensor systems can be used in addition to the above mentioned solutions to control the handling and draping process, e.g. [32–34, 70, 71]. This is for example done by determining suitable placing strategies [33], measuring the position and orientation of the ply and refining the location of markers in the fixed world coordinate system [34] or force measurement and camera control [32].

## 2.4. DISCUSSION

Literature has shown that there is a wide range of strategies that can be used to handle reinforcements for composite production. These strategies consist of a combination between a ply handling method with a certain amount of gripping points. These gripping points can use a variety of gripping technologies. The different strategies are evaluated based on whether they can swiftly handle multiple large-sized layers while:

- The pick-and-place strategy does not negatively affect the quality of the ply through e.g. contamination of the surface or permanent distortion of the ply.
- Contact between plies and mould surface and the desired fiber orientations have been achieved within tolerances.
- There are no (sub-)layers left on the cutting table after pick-up or released during movement.

### 2.4.1. PLY HANDLING STRATEGIES

Picking a reinforcement up from a cutting table and moving it will result in deformations from its original flat state. The magnitude of these deformations and possibly permanent distortions will not only depend on the ply handling strategy. Other relevant factors include reinforcement size, amount of layers being handled, speed of operations including accelerations and decelerations, etc. For the discussion on reinforcement quality only the effect of the ply handling strategy is considered.

Reinforcements can be permanently distorted in different ways during handling. It is important to consider the difference between desired permanent distortions and undesired permanent distortions. Plies that are handled using kinematic or compliant strategies will be deformed to match the mould. Depending on the geometry of the mould this could result in desired permanent distortions. Undesired permanent distortions can mainly occur in the parts of the reinforcement for which there are no restrictions. Reinforcements have the most freedom for deformations in free ply strategies. Rigid and kinematic strategies will however also have unrestrained areas between the pick-up points.

Literature presents a wide range of techniques and strategies that are used to ensure correct placement of plies. Despite this, the quality of the reinforcement during handling and after placement is not typically discussed. Gerngross & Nieberl [12] do set tolerances for fiber angles and position of the boundary curve. These tolerances are however not substantiated. For the evaluation of permanent distortions during handling tolerances will first need to be established. Once tolerances have been set these can be taken into account for the design and monitoring of pick-and-place operations.

The majority of ply handling strategies presented in literature is limited in the complexity and diversity of geometries they are able to handle. A wide variety of strategies can be used for the placement of plies on flat surfaces or single curved moulds. More complex moulds will however often become challenging for most strategies. Rigid ply handling strategies are the most limited in their possible placements but kinematic ply handling strategies and compliant ply handling strategies will also both typically be limited to use with a single mould.

Some compliant ply handling strategies can handle complex and diverse mould surfaces. Examples of a compliant ply handling strategy achieving complex placements are the system presented by Ehinger & Reinhart [31] and the FormHand technology presented by Löchte *et al.* [30]. These systems are able to conform to challenging moulds thanks to their form-flexible end-effectors. The system is not limited to a single mould and can adapt itself to different mould surfaces.

An alternative strategy is a free ply strategy with (a) consolidation roller(s), as presented by Flixeder *et al.* [10] for strips of fabric. Cooperation between the pick-up points and the roller(s) ensures that the ply is gradually placed in/on the mould while the roller(s) ensure(s) proper contact - thereby mimicking the work of a laminator.

Of these two strategies, the compliant based systems are the most practical as long as you're handling single plies with limited dimensions. The compliant based systems will be able to adapt to any mould without extensive programming and will also have a higher lay-up rate. However, the dimensions of the end-effector will need to be at least equal to the dimensions of the ply to be handled. When dealing with large plies this can result in end-effectors with for example impractical dimensions, impractical weight or insufficient stiffness. Additionally, since the technique used with these systems is a vacuum-based technique, it will not be possible to lift multiple layers.

There is a wide variety of applications where moulds are not complex. Depending on the exact mould typically either kinematic, compliant or free ply handling strategies can be used. However, as discussed previously, with an increasing ply size the free ply strategy becomes more interesting. On the other hand, if more control over the ply is desired, a kinematic or compliant strategy with more pick-up points should be chosen. Adding a compliant element to a predominantly kinematic ply handling strategy - as for example used by Brecher *et al.* [11] and Kordi *et al.* [37] - can be used to improve the accuracy of the placement. Using a strategic release and placement of pick-up points inspired by the regrasping technique seen in the garment/textile industry can be used to facilitate accurate placement.

When the speed, accelerations and decelerations of handling during a pick-and-place operation are increased a strategy with more control over the ply area will have a lower risk of movement induced distortions. A free ply strategy is the least appropriate strategy for handling at high speeds since there is a large chance of ply distortion. A rigid ply handling strategy or a compliant strategy with full control over the surface will avoid movement induced distortions of the ply. A kinematic or general compliant strategy with strategically placed pick-up points can be a good compromise between a free ply and a rigid strategy.

#### **2.4.2. GRIPPING STRATEGIES**

Since most gripping principles have a chance of damaging the material they are handling it is preferable to place gripping points in the excess material as much as possible. If this is not possible because this results in excessive displacements, deflections or strains gripping points in the ply should be considered. Increasing the amount of pick-up points will reduce these stresses but will result in more complex strain patterns. In a scenario

where pick-up points in both the excess material and in the ply are required it can be worthwhile to use a combination of different gripping strategies. For the excess material needle grippers, with their possibility for high holding forces but also a risk of deformation to the material, could be used. For the ply area an alternative strategy such as electrostatic grippers or coanda grippers is preferred.

Gripping points restrict the areas they are in contact with. A limited amount of strategies is designed such that these areas can deform after gripping (e.g. [11, 30, 31]) but for most strategies these gripping areas will be rigid. The restricted area differs per gripping strategy: a vacuum gripper will for example typically restrict a larger area than a needle gripper. A gripping strategy with a larger gripping area will affect the potential deformation of the ply. This will affect the accuracy of the placement when curved moulds are used. The gripping strategy should therefore also be matched to the mould. For a mould with (relatively) high curvatures a gripping strategy with a smaller gripping area, such as needle grippers, will be more favorable.

Increasing the size of the ply does not have to affect the choice of gripping strategy but it does affect the amount and placement of the points. With an increase in ply size it becomes more important to avoid an oversized end-effector that has an unnecessary large weight and energy consumption.

There are few gripping principles suitable for the handling of multiple layers. Needle grippers make it possible to pierce and secure multiple layers. The maximum thickness of the reinforcement stack will depend on the maximum stroke of the needles. By setting an adjustable stroke to the desired dimension, as is for example possible with [76], it is also possible to pick up a predefined number of layers [55].

Vacuum grippers are not suitable for handling multiple layers. When low permeability layers are used there will be no airflow reaching the lower layers, making it impossible to handle more than one layer. For layers with a high permeability there will be a large amount of losses, which results in the process being energetically highly inefficient. The cryo-freezing, electrostatic and gecko inspired strategies will also not be appropriate: When multiple plies are present these strategies will only be able to pick up the top layer, while the other layers will remain on the cutting table.

The pinching and clamping strategies used in the textile industry are able to handle multiple layers. For scenarios where the handling of multiple layers is desired it would be interesting to further explore the possibilities these gripping strategies could bring. Disadvantages of clamping grippers include that they typically require access to both sides of the fabric and need to be able to approach the edges. Pinchers, while very effective in picking fabrics, will experience difficulty placing fabric without folds or wrinkles [77]. Additionally, the pinching gripper will apply a fold at each location where a gripping point is present. This can reduce the quality of the reinforcement being handled. Since the pinching gripper works by introducing folds it is not possible to engage pinching grippers all over the surface of a reinforcement all at once. The folds will shorten the reinforcement and pinching grippers will need to be engaged in a pattern to avoid introducing unwanted tension in the fabric. Additionally, depending on the number of layers and the material to be picked up the pinchers might struggle getting all layers.

An alternative strategy to handling multiple layers is to decouple the gripping strategy and the mechanism holding the plies together. Some solutions that can be used in the excess material to facilitate handling can include placing eyelets/grommets or using the inherent ability of the material to become one through local melting and/or curing - similar to spot welding. Figure 2.5 illustrates that these 'external fixing mechanisms' can either be placed in a way that they are separate from the gripping points (Figure 2.5(a)) or such that the fixed areas correspond with the gripping points (Figure 2.5(b)).

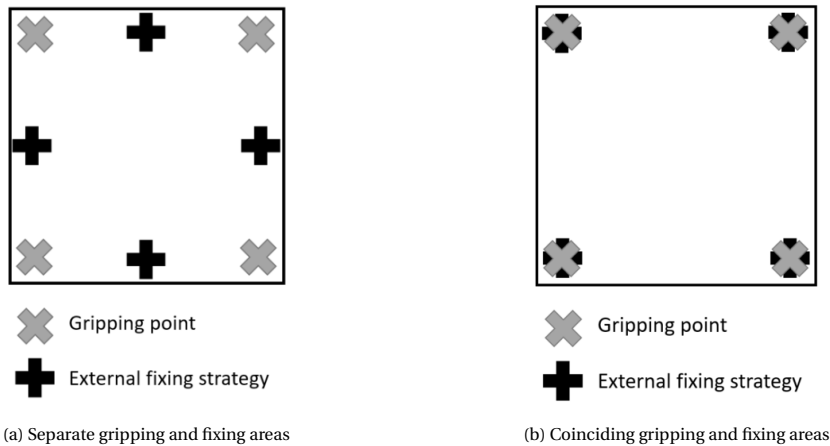


Figure 2.5: Placement of gripping points and external fixing mechanisms.

The addition of these areas in which the multiple layers are locally fixed does not result in all gripping technologies being suitable. If these fixed areas do not correspond with the gripper areas - see Figure 2.5a - the issues discussed above will still mostly be present. It might be possible to lift the stack of plies, but with the top layer being the only one connected to the pick-up points it will not be possible to control the placement. The top layer will also experience large stresses and strains since the rest of the stack will only start to lift after the distance between the pick-up points and fixed areas has tightened.

Alternatively, the pick-up points and fixed areas are designed to coincide - see Figure 2.5b. If stitches are applied such that they provide an area for the gripping mechanism to grab they do overcome the issues associated with plies being left on the table. The same can be said for a fixing strategy that is based on local melting/curing of the reinforcements. While eyelets/grommets bring advantages for the handling of multiple layers by distributing the stresses and locally stiffening the stack their placement will hinder the use of most techniques. Since eyelets/grommets remove part of the reinforcement the surface area that can be gripped is greatly reduced. They do however bring possibilities of e.g. using clamping/pinching techniques to pick up the stack at the eyelets/grommets.

Any strategy that fixes the movement of plies that are handled together can cause issues when dealing with a curved mould. The differences in path length between the inner and outer layers, combined with the plies not being able to slip over one another result

in severe wrinkling. Potter *et al.* [23] note that this would be considered to be a process induced defect. Unlike a design related defect/feature which might not be acceptable but can only be avoided/changed at the design stage a process induced defect can be avoided by changing the manufacturing process [23]. Simultaneously draping multiple layers is therefore not a suitable strategy for every mould surface. Depending on the design these drawbacks can possibly be circumvented through careful and strategic release of part of the pick-up points during the draping process. A different solution is to use a two-step process where the layers are transported using a pick-and-place process before being formed.

The risk of layers releasing during the pick-and-place process will be larger when the speed, accelerations and/or decelerations are increased due to the additional forces. The different gripping technologies will be affected differently by these additional forces. Needle grippers and pinching grippers will be less susceptible to releasing layers due to their gripping mechanism that physically holds all layers. The other gripping methods - vacuum, cryo-freezing, electrostatic and gecko-inspired are unable to handle multiple layers without external fixing mechanism. The external fixing mechanisms as described above will prevent part of the stack from detaching. However, the holding forces will still need to be increased to prevent the complete stack from falling. In general it will be preferable to use a gripping principle that is able to handle multiple layers instead of adding an external fixing strategy. As mentioned before pinching grippers result in undesirable folds in the reinforcement. This makes needle grippers the best choice out of the currently available techniques.

## 2.5. CONCLUSIONS

There is a wide variety of available strategies for the handling of reinforcements. However, if the intent is to swiftly handle large layers and/or multiple layers part of these strategies will no longer be suitable. Conclusions can be summarised as follows:

1. There is a limited amount of research that focuses on the quality of reinforcements in pick-and-place processes. For the widespread implementation of pick-and-place processes in industry it will be crucial that a guaranteed consistent quality can be achieved. Additional research is required to set tolerances for quality parameters and develop knowledge on their use in the design and monitoring of pick-and-place processes.
2. The best way to ensure the quality of plies is not affected by the pick and place operation is to grip in the excess material. Increasing the amount of pick-up points is not necessarily the best solution to decreasing the chance of damage to the plies - while the maximum stress/strain will decrease, the stress and strain patterns will also become more complex. The optimal amount and location of pick-up points depends on quality requirements and requires further research.
3. All five ply handling methods can be suitable for the handling of multiple layers of large-sized layers of reinforcement. The choice made in ply handling method will depend on e.g. the mould and reinforcement used in the manufacturing operation. As ply size increases it does however become more interesting to go more

towards a free hanging strategy.

4. When multiple layers are concerned needle grippers are the only gripping principle that is able to reliably lift all plies without an external fixing mechanism. Additional fixing strategies could be used to facilitate handling using other gripping mechanisms but it is preferred to use a gripping principle that does not require external fixing mechanisms. When fixing strategies are used the fixed area should coincide with the gripping area. The limits of handling multiple layers - both in terms of amount of layers and mould complexity - are currently unknown, research is required to study these limits.
5. The speed, accelerations and decelerations of the pick-and-place process will affect the process through the introduction of additional forces. As these parameters are increased it becomes more desirable to fix the ply - as opposed to free hanging. The additional forces resulting from increases mean a larger handling force is required. Additional research is required to quantify the effect of increasing the speed, accelerations and decelerations in pick-and-place processes on strategy choices.

## 2.6. RESEARCH GOAL AND RESEARCH QUESTIONS

Several regions of interest have been identified based on the review and discussion of the state of the art. The current work will focus on tolerances for quality parameters and the optimal amount and location of pick-up points. With the size and the amount of (sub)layers also being a research interest large-sized layers of bi-axial NCFs will be the reinforcement used in this research.

The quality criterion that is focused on in the current work is the fiber angle deviations due to in-plane shear. For flow of the chapters the justification for choosing this quality criterion is found in Chapter 3.

The research goal for the the current work will be:

The development of a framework for prediction and prevention of fiber angle deviations due to in-plane shear during handling of large-sized bi-axial NCFs

Research questions can be defined as:

RQ1: How can tolerances be set for handling induced fiber angle deviations due to in-plane shear in bi-axial NCFs?

RQ2: How can the elastic properties of a bi-axial NCF be predicted based on its dimensions and stitch pattern?

RQ3: Can the design of optimal pick-up point locations on a large reinforcement be simplified through the use of a repeating pattern of pick-up points?

Solving the initial research question will give the current and future research a way to define limits for allowable fiber angle deviations and in-plane shear strains during the handling of bi-axial NCFs. Without tolerances design choices need to be made based on

experience. Tolerances give a clear indication of the quality of a specific design in terms of fiber angle deviations and in-plane shear.

The result to the second research question will make it possible to rapidly get an indication of the elastic properties for a bi-axial NCF. Being able to predict the elastic properties based on dimensions and stitching pattern will be a huge advantage in comparing the behaviour of different NCFs or different stitching patterns during handling.

A large variety of ply handling strategies use a lot of pick-up points spread over the surface. Often there are a lot of pick-up points present, which might not be the best strategy for quality handling of the reinforcement. Ideally, it would be possible to model a single instance of a repeating pattern of pick-up points and have the results be representative of the reinforcement as a whole. This would make it a lot more efficient to compare the behaviour of reinforcements under different pick-up point patterns. The third research question aims to find if this is possible.

# BIBLIOGRAPHY

- [1] A Mills. “Automation of carbon fibre preform manufacture for affordable aerospace applications”. In: *Composites Part A: Applied science and manufacturing* 32.7 (2001), pp. 955–962.
- [2] M Elkington, Carwyn Ward and K Potter. “Automated layup of sheet prepregs on complex moulds”. In: *SAMPE Long Beach Conference*. 2016.
- [3] Andreas Björnsson et al. “Getting to grips with automated prepreg handling”. In: *Production Engineering* 11.4 (Oct. 2017), pp. 445–453. ISSN: 1863-7353.
- [4] Michael Elkington, Carwyn Ward and Aza Sarkytbayev. “Automated composite draping: a review”. English. In: *SAMPE 2017*. SAMPE North America, May 2017.
- [5] Dominik Deden et al. “Towards a fully automated process chain for the lay-up of large carbon dry-fibre cut pieces using cooperating robots”. In: *SAMPE Europe 2019* (2019).
- [6] Tobias Gerngroß, Florian Krebs and Andreas Buchheim. “Automated production of large preforms based on robot-robot cooperation”. In: (2012).
- [7] *BOEING 787 DREAMLINER*. <https://www.boeing.com/commercial/787/#/technical-specs>. Accessed: 03-9-2019.
- [8] *LM Wind Power manufactures longest wind turbine blade*. <https://www.compositesworld.com/news/lm-wind-power-manufactures-longest-wind-turbine-blade>. Accessed: 03-9-2019.
- [9] *ROBOTIC COMPOSITE FIBRE LAY-UP SYSTEM PROMISES HIGHER PRODUCTIVITY FOR WING MANUFACTURE*. <http://www.machinery.co.uk/machinery-news/carbon-fibre-reinforced-plastic-cfrp-automated-production-kuka-bombardier>. Accessed: 20-7-2018.
- [10] Stefan Flixeder, Tobias Glück and Andreas Kugi. “Force-based cooperative handling and lay-up of deformable materials: Mechatronic design, modeling, and control of a demonstrator”. In: *Mechatronics* 47 (2017), pp. 246–261.
- [11] C Brecher et al. “Handling of preforms and prepregs for mass production of composites”. In: *19 th International Conference on Composite Materials*. 2013.
- [12] Tobias Gerngross and Dorothea Nieberl. “Automated manufacturing of large, three-dimensional CFRP parts from dry textiles”. In: *CEAS Aeronautical Journal* 7.2 (June 2016), pp. 241–257. ISSN: 1869-5590.
- [13] G. Reinhart and G. Straßer. “Flexible gripping technology for the automated handling of limp technical textiles in composites industry”. In: *Production Engineering* 5.3 (June 2011), pp. 301–306. ISSN: 1863-7353.

- [14] Andreas Björnsson. “Automated layup and forming of prepreg laminates”. PhD thesis. Linköping University Electronic Press, 2017.
- [15] Gualtiero Fantoni et al. “Grasping devices and methods in automated production processes”. In: *CIRP Annals-Manufacturing Technology* 63.2 (2014), pp. 679–701.
- [16] *Fiber reinforcement forms*. <https://www.compositesworld.com/articles/fiber-reinforcement-forms>. Accessed: 20-2-2019.
- [17] SG Hancock and KD Potter. “The use of kinematic drape modelling to inform the hand lay-up of complex composite components using woven reinforcements”. In: *Composites Part A: Applied Science and Manufacturing* 37.3 (2006), pp. 413–422.
- [18] Mona Eckardt, Andreas Buchheim and Tobias Gerngross. “Investigation of an automated dry fiber preforming process for an aircraft fuselage demonstrator using collaborating robots”. In: *CEAS Aeronautical Journal* 7.3 (Sept. 2016), pp. 429–440. ISSN: 1869-5590.
- [19] Fredrik Martinsson. *Development of Robust Automated Handling of pre-impregnated Carbon Fibre (Master Thesis)*. 2018.
- [20] Joram Wiggers. “Analysis of textile deformation during preforming for liquid composite moulding”. PhD thesis. University of Nottingham, 2007.
- [21] Helga Krieger, Thomas Gries and Scott E Stapleton. “Design of Tailored non-Crimp Fabrics Based on stitching geometry”. In: *Applied Composite Materials* 25.1 (2018), pp. 113–127.
- [22] V Koissin et al. “Internal structure of structurally stitched NCF preform”. In: *Proc. of 12th European Conference on Composite Materials (ECCM-12), Biarritz, France, August 29—September 1. 2006*.
- [23] K Potter et al. “Variability, fibre waviness and misalignment in the determination of the properties of composite materials and structures”. In: *Composites Part A: Applied Science and Manufacturing* 39.9 (2008), pp. 1343–1354.
- [24] A Margossian et al. “Finite element forming simulation of locally stitched non-crimp fabrics”. In: *Composites Part A: Applied Science and Manufacturing* 61 (2014), pp. 152–162.
- [25] R.O. Buckingham and G.C. Newell. “Automating the manufacture of composite broadgoods”. In: *Composites Part A: Applied Science and Manufacturing* 27.3 (1996), pp. 191–200. ISSN: 1359-835X. URL: <http://www.sciencedirect.com/science/article/pii/1359835X96800019>.
- [26] Lars Larsen et al. “Full automatic path planning of cooperating robots in industrial applications”. In: *2017 13th IEEE Conference on Automation Science and Engineering (CASE)*. IEEE. 2017, pp. 523–530.
- [27] Christopher Bruns et al. “Process design and modelling methods for automated handling and draping strategies for composite components”. In: *CIRP Annals* (2018).
- [28] Bernd-Arno Behrens et al. “Automated stamp forming of continuous Fiber reinforced thermoplastics for complex Shell geometries”. In: *Procedia CIRP* 66 (2017), pp. 113–118.

- [29] M Kühnel et al. “Automated near net-shape Preforming of Carbon Fiber Reinforced Thermoplastics (CFRTP)”. In: *Innovative Composites Summit, JEC Europe, Paris, France* (2014), pp. 11–13.
- [30] C Löchte et al. “Form-flexible handling technology for automated preforming”. In: *Proc. of 19th intern. Conf. on Comp. Mat. (ICCM19), Montreal, Canada*. 2013.
- [31] Claudia Ehinger and Gunther Reinhart. “Robot-based automation system for the flexible preforming of single-layer cut-outs in composite industry”. In: *Production Engineering* 8.5 (Oct. 2014), pp. 559–565. ISSN: 1863-7353.
- [32] H Apmann. “Automatic handling of dry carbon fabrics and prepregs”. In: *17th International Conference of Composite Materials ICCM*. Vol. 17. 2009.
- [33] R Molfino et al. “Design of a Hyper-flexible cell for handling 3D Carbon fiber fabric”. In: *Recent advances in mechanical engineering and mechanics* 165 (2014).
- [34] J Brinker et al. “Automated Handling and Draping of Reinforcing Textiles — Challenges and Developments”. In: *New Advances in Mechanisms, Mechanical Transmissions and Robotics*. Springer, 2017, pp. 485–493.
- [35] JA Chestney and M Sarhadi. “Control and integration techniques in a fully automated manufacturing cell for carbon composites”. In: *IEE Proceedings-Control Theory and Applications* 143.2 (1996), pp. 159–163.
- [36] SDH Jarvis et al. “Design of a handling device for composite ply lay-up automation”. In: *Advanced Robotics, 1991. Robots in Unstructured Environments, 91 ICAR., Fifth International Conference on*. IEEE. 1991, pp. 790–795.
- [37] M. T. Kordi, M. Husing and B. Corves. “Development of a multifunctional robot end-effector system for automated manufacture of textile preforms”. In: *2007 IEEE/ASME international conference on advanced intelligent mechatronics*. Sept. 2007, pp. 1–6.
- [38] F Förster et al. “Manufacturing of textile preforms with an intelligent draping and gripping system”. In: *Procedia CIRP* 66 (2017), pp. 39–44.
- [39] Alfons Schuster et al. “Smart Manufacturing of Thermoplastic CFRP Skins”. In: *Procedia Manufacturing* 17 (2018), pp. 935–943.
- [40] *Online video "Fill lowflip multi-functional gripper based on Tecnacompssystem by Tecnalía"*. <https://youtu.be/vKxejyTkrx4>. Accessed: 26-11-2018.
- [41] *Integrated Composite Handling and Drape System*. <http://www.broetje-automation.de/en/equipment/fordersysteme/#handling>. Accessed: 20-7-2018.
- [42] Christian Krogh, Jens A Glud and Johnny Jakobsen. “Modeling the robotic manipulation of woven carbon fiber prepreg plies onto double curved molds: A path-dependent problem”. In: *Journal of Composite Materials* 53.15 (2019), pp. 2149–2164.
- [43] *FibreMOVE - 2D COMPOSITE GRIPPER*. <http://www.looptechnology.com/fibreMOVE-composite-gripper-system.asp>. Accessed: 16-7-2018.

- [44] *FibreFORM – A COMPLETE COMPOSITE HANDLING SYSTEM*. <http://www.looptechnology.com/fibreFORM-composite-handling-system.asp>. Accessed: 16-7-2018.
- [45] Jose Sanchez et al. “Robotic manipulation and sensing of deformable objects in domestic and industrial applications: a survey”. In: *The International Journal of Robotics Research* 37.7 (2018), pp. 688–716.
- [46] Pablo Jiménez and Carme Torras. “Perception of cloth in assistive robotic manipulation tasks”. In: *Natural Computing* 19.2 (2020), pp. 409–431.
- [47] Z Zhang, JA Chestney and M Sarhadi. “Characterizing an electrostatic gripping device for the automated handling of non-rigid materials”. In: *Proceedings of the Institution of Mechanical Engineers, Part B: Journal of Engineering Manufacture* 215.1 (2001), pp. 21–36.
- [48] S Rangunathan and L Karunamoorthy. “Genetic algorithm-based optimal locations for handling fabric materials in garment automation”. In: *International Journal of Robotics and Automation* 21.4 (2006), pp. 288–294.
- [49] Shrinivas Lankalapalli and Jeffrey W Eischen. “Optimal pick-up locations for transport and handling of limp materials: Part I: One-dimensional strips”. In: *Textile research journal* 73.9 (2003), pp. 787–796.
- [50] Shrinivas Lankalapalli and Jeffrey W Eischen. “Optimal pick-up locations for transport and handling of limp materials: Part II: Two-dimensional parts”. In: *Textile research journal* 73.10 (2003), pp. 867–874.
- [51] Fabian Johannes Ballier. *Systematic gripper arrangement for a handling device in lightweight production processes*. Shaker Verlag, 2019.
- [52] Andreas Börnsson, Marie Jonsson and Kerstin Johansen. “Automated material handling in composite manufacturing using pick-and-place systems – a review”. In: *Robotics and Computer-Integrated Manufacturing* 51 (2018), pp. 222–229. ISSN: 0736-5845. URL: <http://www.sciencedirect.com/science/article/pii/S0736584517301758>.
- [53] Panagiotis Koustoumpardis et al. “Handling of non-rigid materials with robots (XROMA), application in robotic sewing”. In: *37th International Symposium on Novelties in Textiles*.
- [54] A Karakerezis et al. “Robotic handling for flat non-rigid materials”. In: *Systems, Man, and Cybernetics, 1994. Humans, Information and Technology., 1994 IEEE International Conference on*. Vol. 1. IEEE. 1994, pp. 937–946.
- [55] Volker Lutz et al. “Automation in material handling”. In: *Automation in Garment Manufacturing*. Elsevier, 2018, pp. 165–177.
- [56] G. Seliger et al. “Automated Handling of Non-Rigid Parts”. In: *CIRP Annals* 52.1 (2003), pp. 21–24. ISSN: 0007-8506. URL: <http://www.sciencedirect.com/science/article/pii/S0007850607605216>.
- [57] G Seliger, C Gutsche and L-H Hsieh. “Process planning and robotic assembly system design for technical textile fabrics”. In: *CIRP annals* 41.1 (1992), pp. 33–36.

- [58] Andreas Björnsson, Jan-Erik Lindback and Kerstin Johansen. *Automated removal of prepreg backing paper-a sticky problem*. Tech. rep. SAE Technical Paper, 2013.
- [59] Somen Dutta and Clemens Schmidt-Eisenlohr. *Method, effector and apparatus for adhesive picking, handling and / or depositing semi-finished fiber products and carrier material-matrix material composite for use in such a method*. 2016.
- [60] X.Q. Chen and M. Sarhadi. “Investigation of electrostatic force for robotic lay-up of composite fabrics”. In: *Mechatronics* 2.4 (1992), pp. 363–373. ISSN: 0957-4158. URL: <http://www.sciencedirect.com/science/article/pii/0957415892900037>.
- [61] Christian Brecher et al. “Form-adaptive gripping system for light-weight productions”. In: *20th International Conference on Composite Materials*. 2015, pp. 19–24.
- [62] Donald Ruffatto III, Jainam Shah and Matthew Spenko. “Increasing the adhesion force of electrostatic adhesives using optimized electrode geometry and a novel manufacturing process”. In: *Journal of Electrostatics* 72.2 (2014), pp. 147–155.
- [63] Kellar Autumn et al. “Evidence for van der Waals adhesion in gecko setae”. In: *Proceedings of the National Academy of Sciences* 99.19 (2002), pp. 12252–12256.
- [64] Mohammad Dadkhah et al. “A self-aligning gripper using an electrostatic/gecko-like adhesive”. In: *2016 IEEE/RSJ International Conference on Intelligent Robots and Systems (IROS)*. IEEE. 2016, pp. 1006–1011.
- [65] Zhongyi Chu et al. “A gecko-inspired adhesive robotic end effector for critical-contact manipulation”. In: *Science China Information Sciences* 65.8 (2022), pp. 1–14.
- [66] Morteza Alebooyeh, Bowen Wang and Ruth Jill Urbanic. *Performance Study of an Innovative Collaborative Robot Gripper Design on Different Fabric Pick and Place Scenarios*. Tech. rep. SAE Technical Paper, 2020.
- [67] Bowen Wang and Ruth Jill Urbanic. “Model-based Design and Simulation of a Soft Robotic Gripper for Fabric Material Handling”. In: (2021).
- [68] Júlia Borràs, Guillem Alenyà and Carme Torras. “A grasping-centered analysis for cloth manipulation”. In: *IEEE Transactions on Robotics* 36.3 (2020), pp. 924–936.
- [69] Marko Szesny et al. “The advanced ply placement process—an innovative direct 3D placement technology for plies and tapes”. In: *Advanced Manufacturing: Polymer & Composites Science* 3.1 (2017), pp. 2–9.
- [70] Michael Brink, Jan-Hendrik Ohlendorf and Klaus-Dieter Thoben. “Development of a Handling System with integrated Sensors for Textile Preforms using Additive Manufacturing”. In: *Procedia Manufacturing* 24 (2018), pp. 114–119.
- [71] Johannes Graf et al. “An Approach for the Sensory Integration into the Automated Production of Carbon Fiber Reinforced Plastics”. In: *Procedia CIRP* 52 (2016), pp. 280–285.
- [72] D Kupzik et al. “Development and evaluation of separation concepts for the controllable release of tacky prepreg from handling devices”. In: *Procedia CIRP* 72 (2018), pp. 574–579.

- 2
- [73] Christian Krogh, Johnny Jakobsen and James A Sherwood. “Development of a Computationally Efficient Fabric Model for Optimization of Gripper Trajectories in Automated Composite Draping”. In: *International Conference on Engineering Optimization*. Springer. 2018, pp. 1107–1118.
  - [74] Christian Krogh, Jens A Glud and Johnny Jakobsen. “Modeling of prepregs during automated draping sequences”. In: *AIP Conference Proceedings*. Vol. 1896. 1. AIP Publishing. 2017, p. 030036.
  - [75] Christian Krogh and Johnny Jakobsen. “Modeling of Robot Draping Sequences with Prepreg Plies”. In: *NSCM 30 (2017)*, p. 104.
  - [76] *Needle Grippers SNG-AP*. <https://www.schmalz.com/en/vacuum-technology-for-automation/vacuum-components/special-grippers/needle-grippers/needle-grippers-sng-ap>. Accessed: 7-8-2019.
  - [77] P Koustoumpardis and N Aspragathos. “A review of gripping devices for fabric handling”. In: *hand* 19 (2004), p. 20.

# 3

## SETTING BOUNDS FOR IN-PLANE SHEAR INDUCED FIBER ANGLE DEVIATIONS IN BI-AXIAL NON-CRIMP FABRICS

### 3.1. INTRODUCTION

IMPLEMENTATION of the pick-and-place process in industry requires a consistent and acceptable product quality. Without quality criteria it is not possible to evaluate the quality of the process and final product. In the state of the art on handling of (non-crimp) fabrics using pick-and-place operations quality criteria are often overlooked. The quality criterion that is most often reported in literature is a placement accuracy/repeatability. Martinsson [1] uses an array sensor to measure the position of the edges of a placed prepreg relative to predefined points. Kuehnel *et al.* [2] use a computer vision approach to detect position and orientation of cuts before picking them up and placing them. Krogh *et al.* [3] discuss the difference between prescribed and actual boundaries for their numerical simulations of draping of woven prepreps on double curved molds. Additionally, they also report the ply-mold separation for different draping strategies. The work by Gerngross & Nieberl [4] stands out because they set tolerances for both the fiber angles ( $\pm 5^\circ$ ) and the boundary curve positions (+ 5 / -7.5 mm). Their preforming results are evaluated by comparing them to a laser projection.

One of the most important quality criteria and design parameters for fiber reinforced materials is the orientation of the fibers. A misalignment between fiber direction and

---

Parts of this chapter have been published in Chantal M. de Zeeuw, Daniël M. J. Peeters, Otto K. Bergsma & Rinze Benedictus (2022) Setting bounds for in-plane shear induced fiber angle deviations in bi-axial non-crimp fabrics, *Journal of Industrial Textile*, 52, 1-23, DOI: 10.1177/15280837221113921

loading direction will greatly reduce the mechanical properties. This is e.g. illustrated by Mouritz [5] for a UD composite loaded at different angles. The orientation of the fiber angles should be taken into account when the pick-and-place process is studied.

Fiber angles are directly influenced by in-plane shear, which is the main deformation mode during forming of reinforcements [6] and will also be the main deformation mode during handling. In-plane shear angles of the final product are a common result presented in studies focusing on forming and draping. Recent work includes the draping simulations of Guzman-Maldonado *et al.* [6] that are used to predict shear angles after forming of a hemisphere and step profile using non-orthogonal biaxial NCFs. Krieger *et al.* [7] present optically measured local shear angles for non-crimp fabrics with different stitch types and orientations draped over an elongated hemisphere. Wang *et al.* [8] produce both experimental and simulated results for the in-plane shear angle for hemispherical stamping of 3D woven composite reinforcements.

Handling a reinforcement will subject it to forces due to gravity and accelerations. These forces can result in deformations and therefore in deviations of the fiber angles. Deformations during handling using pick-and-place operations are for example presented by Krogh *et al.* [9] in the context of generating feasible gripper trajectories for the draping of prepregs. Lin *et al.* [10] and Do *et al.* [11] are examples of studies interested in predicting the deformations of reinforcements during handling in real time.

One factor that will have a large influence on the behaviour of a reinforcement that is handled is the positioning of pick-up points. Rangunathan & Karunamoorthy [12] and Lankalapalli & Eischen [13] studied the optimal positioning of pick-up points based on minimization of strain energy. Ballier [14] based the positioning of pick-up points on deflections. These parameters do however not give a clear indication of the quality of the reinforcement. With fiber angles being such an important parameter for the quality of a composite product fiber angle deviations should be taken into account when designing the pick-and-place process. Tolerances need to be set for the in-plane shear and resulting fiber angle deviations. Pick-up points need to be positioned in a way that ensures that deviations remain within the previously established boundaries.

Until now, no clear bounds have been established for fiber angle deviations during handling of different non-crimp fabrics. Therefore, the aim of this chapter is to provide a framework for the determination of acceptable criteria for in-plane shear induced fiber angle deviations in bi-axial non-crimp fabrics. Thereby answering the research question:

How can tolerances be set for handling induced fiber angle deviations due to in-plane shear in bi-axial NCFs?

For the current work the filaments within a tow are assumed to be aligned to such an extent that tow angles correspond to filament angles, factors such as in-plane waviness as a result of manufacturing are not considered. In section 3.2 and 3.3 experimental picture frame tests are used to set a tolerance for the fiber angle deviations/in-plane shear strain. The simulated shear response can be used as an indication of fiber angle deviations. The results from the current work are discussed in section 3.4. Finally, section 3.5 presents the conclusions.

### 3.2. FIBER ANGLE DEVIATIONS AND IN-PLANE SHEAR IN AN NCF

For the current work an E-glass based Biaxial  $\pm 45^\circ$  NCF with a chain stitch pattern is used. A chain-stitch type NCF has been chosen since a chain stitch gives a high form stability, making the fabric appropriate for automated handling [7]. Figure 3.1 illustrates the stitch pattern of the NCF. Table 3.1 presents the details for the NCF selected for the present work.

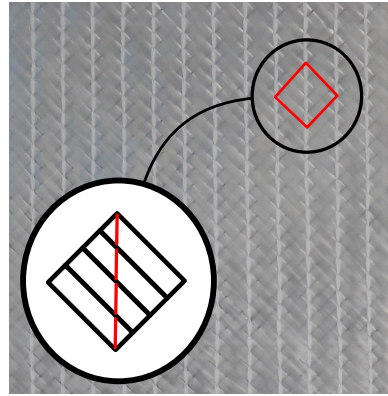


Figure 3.1: Stitch pattern of NCF. The vertical red line indicates the direction of the stitches, the diagonal black lines indicate the direction of the fibers of the top layer

Table 3.1: Specifications of selected fabric as provided by the manufacturer

Fabric type:	Biaxial $\pm 45^\circ$ NCF
Weight:	430 $g/m^2$
Fibres:	100% E-glass (300 tex)
Stitch:	Chain stitch
Finishing:	Silane treated

There is no official standard for the shear testing of biaxial fabrics like the NCF used in this work. Picture frame tests are however widely used to characterize the in-plane shear behaviour of non-crimp fabrics. Recent work using this test includes e.g. Guzman-Maldonado *et al.* [6] and Habboush *et al.* [15]. The current work will also use the picture frame test. Using a picture frame test will ensure that there is uniform shear throughout the specimen.

In a picture frame test the fabric is constrained at the edges and subjected to pure shear. Figure 3.2 shows a schematic of the aluminum frame used to clamp the fabric on four edges and both specimens with stitches loaded in tension and with stitches loaded in compression. The difference between specimens loaded in tension and in compression is the orientation of the specimen in the frame. The red stripes in the figures indicate the direction of the stitches while the blue lines indicate the direction of the fibers. The fabrics' stabilizing yarns, spaced every 45-55 mm, in the 0/90 direction are removed prior to testing while stitches are left intact.

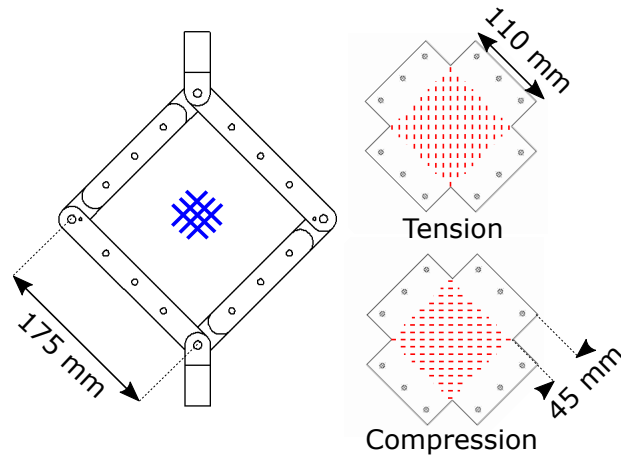


Figure 3.2: Illustration of the frame design and both a tension and compression specimen with the direction of the stitches indicated in red stripes and the direction of the fibers indicated in blue lines

Figure 3.3 shows the picture frame with a specimen clamped during testing. Several tows are highlighted using black marker to track the behaviour of the tows during testing. Pictures are taken so the tow angles can be compared to the frame angles in post-processing.

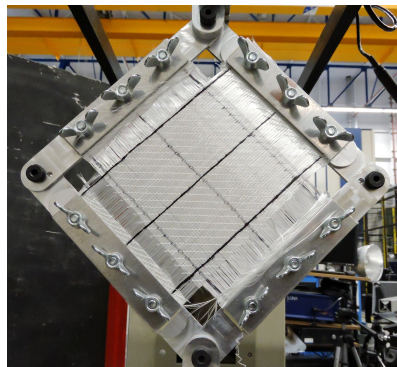


Figure 3.3: Picture frame with clamped fabric during testing

To ensure that the start of the test coincides with the start of shearing, the distance between opposite holes in the specimens is 1 mm smaller than the distance between opposite holes in the frame. Double sided tape is applied to fix the specimens to the frame, thereby reducing the possibility of slipping as much as possible. During the test the load-displacement curve is recorded using a 10 N load cell. A camera set-up is used to monitor the fabric. Specimens are tested at a speed of 10 mm/min. Machine speed is

based on the work by Lomov [16] who found no systemic variation of the shear resistance of biaxial non-crimp fabrics when using machine speeds from 10 to 1000 mm/min.

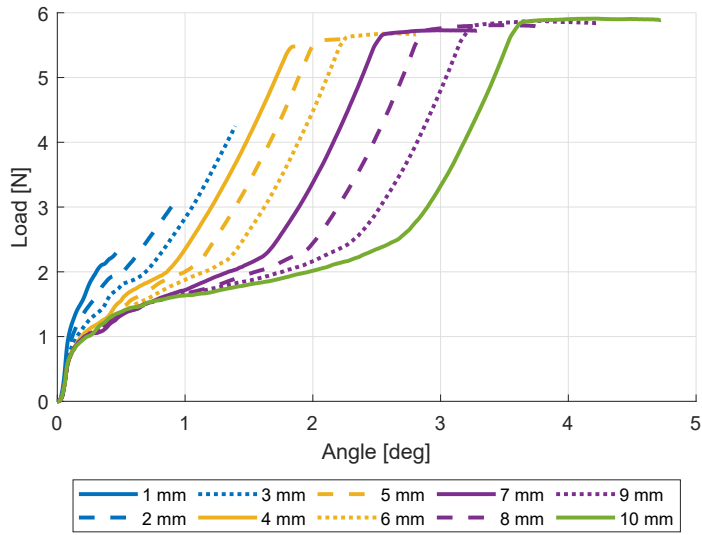
Load-displacement data is automatically recorded by the tensile testing machine. The load-displacement curve due to shear of the specimen is obtained by subtracting the load-displacement curves for each test by the relevant load-displacement curve for the empty frame. Each load cycle is repeated three times. The initial cycle will be a conditioning cycle during which the specimen settles, ensuring a uniform response of the fabric [16]. Unless noted otherwise the values presented in this chapter are the average of the second and third cycle.

The current work studies fiber angle deviations due to in-plane shear in the context of material handling in the composite manufacturing process. This means that the region of interest is different than other work carrying out picture frame tests. Typically, specimens will be tested up to the locking angle. Recent examples include the work by Fial *et al.* [17], Luxet *et al.* [18] and Santhanakrishnan *et al.* [19]. For the current work the interest lays in the unintended deviations that may occur during to the handling process. With this in mind specimens are initially tested over a range of displacements from 1 - 10 mm or frame angles from 0.47 – 4.68 degrees. Based on these results the region of interest is further narrowed down to displacements of 1 - 5 mm (0.47 – 2.34 degrees) and additional specimens are tested. Specimens are loaded up to a predefined displacement / angle, once this has been reached the machine returns to its starting position. After the starting position has been reached the next displacement / angle is applied.

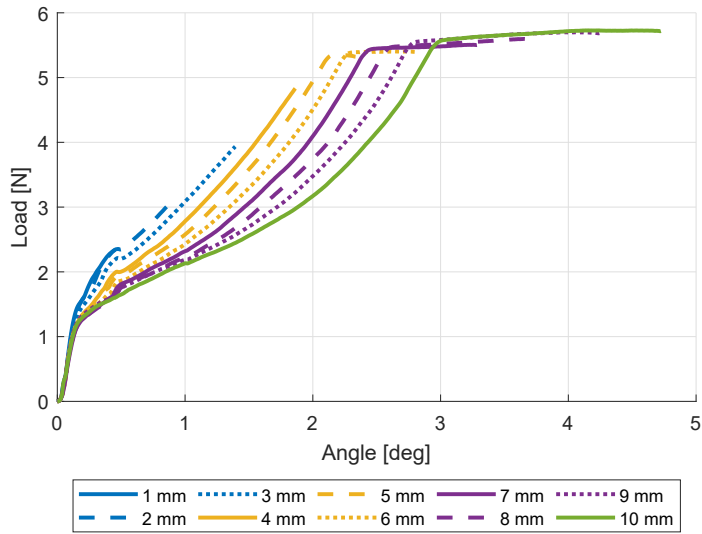
Figure 3.4 shows load-displacement graphs for a compression specimen and a tension specimen loaded from 1 - 10 mm / 0.47 – 4.68 degrees. Figure 3.5 shows three compression and three tension specimens loaded from 1 - 5 mm / 0.47 – 2.34 degrees. Larger sized figures can be found in Appendix B. Applied displacements have been converted to applied angles using basic trigonometry. For the current work the choice has been made to present results individually, as opposed to presenting a mean with standard deviations. The interest of the current work lays in setting tolerances for the fiber angle deviations based on the behaviour of the fabric. Looking at individual specimens ensures that no behaviour is missed.

The initial steep region, observed for the curves in Figures 3.4 and 3.5 is attributed to frame effects. Most frame effects have been removed from the data through subtraction of load-displacement data for empty frames. It is suggested that the presence of the pre-loaded fabric in the frame causes the frame to behave slightly different than in the empty cases. This results in the data still showing some behaviours that are not caused by shearing of the fabric.

The sudden change in trajectory at the end of the load-displacement graphs marks the point where the mechanical safety stop of the load cell is engaged. The 10 N load cell has been used despite this phenomena to ensure the highest accuracy in the load-displacement behaviour in the region of interest: low displacements corresponding to low fiber angle deviations. A 1 kN load cell is used to observe the behaviour of the specimens beyond 10 N. Figures B.7 and B.8 in Appendix B shows how the trajectory of the load-displacement graphs will continue until the set displacement is reached.

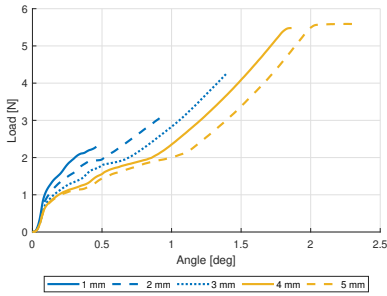


(a) Compression

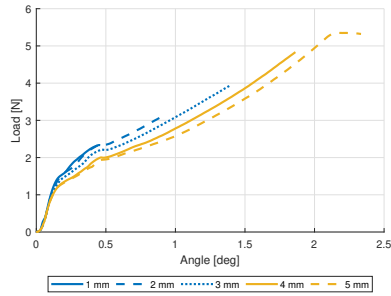


(b) Tension

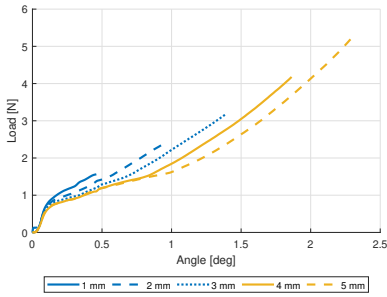
Figure 3.4: Load-displacement graph for compression 1 and tension 1 specimens for displacements of 1 - 10 mm



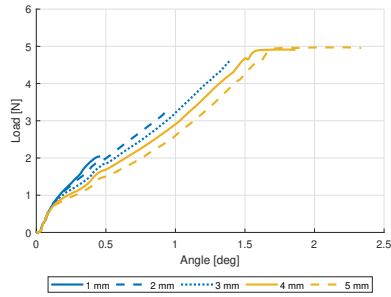
(a) Compression 1



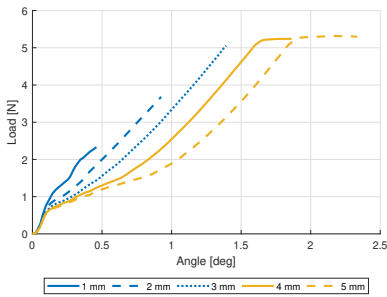
(b) Tension 1



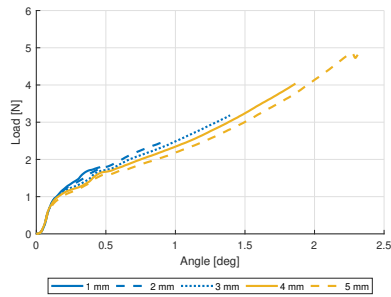
(c) Compression 2



(d) Tension 2



(e) Compression 3



(f) Tension 3

Figure 3.5: Load displacement graphs for compression and tension specimens for displacement of 1 - 5 mm. Larger versions of the image can be found in Appendix B

### 3.3. SETTING LIMITS FOR IN-PLANE SHEAR AND FIBER ANGLE DEVIATIONS BASED ON PICTURE FRAME TESTS

When setting bounds for the fiber angle deviations they should be set such that no irreversible change has occurred yet. Figure 3.6 illustrates how the behaviour of the fabric is influenced by previous shearing. The graphs present the load-displacement diagrams for applied displacements of 1, 3 and 5 mm, which corresponds to applied angles of 0.47, 1.40 and 2.34 degrees. The "5 -" notation indicates that these test cycles occurred after the frame had already been sheared up to 5 mm and returned back to the base position. The results show that the trajectory of these load-displacement graphs closely follows that of the 5 mm case. It requires significantly less force to shear the fabric to 3 mm once it has previously been sheared to 5 mm than if the fabric is new and unsheared. This behaviour can also be seen in the results presented in Figures 3.4 and 3.5. The slope for the final region of the curves for compression specimens remains consistent across the applied displacements of 1 - 10 mm. For the first region there is however a clear drop in resistance as the applied displacement increases. This is attributed to the behaviour shown in Figure 3.6.

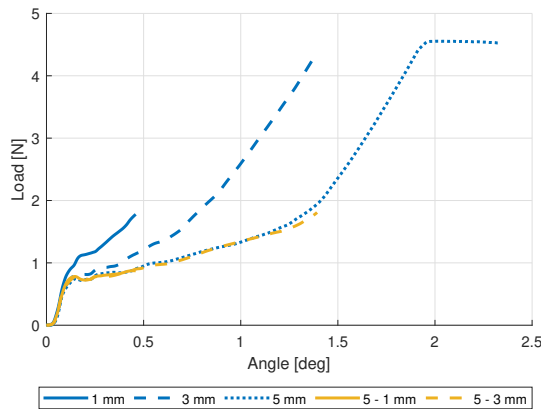


Figure 3.6: Load-displacement graph for a compression specimen that is loaded at a series of lower and higher displacements

The current work shows that even at low angles irreversible changes have already occurred in the fabric. Unloading the fabric does not return it to its previous state. Shear applied to the reinforcement at an earlier stage will always influence the behaviour at a later stage. These observations have been used to set tolerances for the fiber angle deviations and in-plane shear strains. When setting these tolerances the focus is on the behaviour the reinforcement will show when it is sheared an additional time. Since the compression load case shows the greatest reduction in initial stiffness due to previous loading this case is used to set the limits. Figure 3.4 and 3.5 show that for an applied displacement of 5 mm the initial region with a reduced stiffness will go beyond an angle of  $1^\circ$ . This means that once a displacement of 4 mm or angle of  $1.87^\circ$  has been applied the

reinforcement will easily shear again to  $1^\circ$ . With the importance of precise fiber angles in many applications of composites this is considered to be too large of an initial region of reduced stiffness. Therefore, the tolerance for the current work is set to displacements of 3 mm / angles of  $1.4^\circ$ .

Figure 3.7 shows the end values for the tension and compression specimens for displacements up to 3 mm. Additionally, it shows the linear approximation for these end values. The relationship between the end values for a specific specimen is linear but if this trend would be extrapolated to displacements of 0 mm the predicted force would be non-zero. As has been discussed before the results as presented in Figures 3.4 and 3.5 show an initial steep region that is attributed to frame effects. This can also be concluded from Figure 3.7 after extrapolation of the striped lines to zero angle.

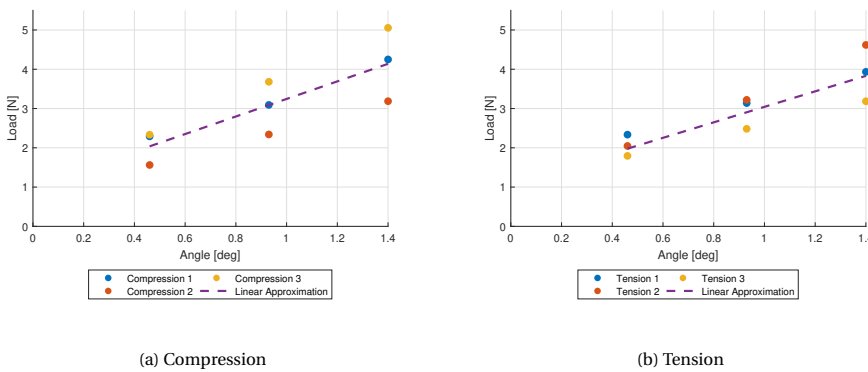


Figure 3.7: Linear approximation for end values of load-angle graphs based on experiments

Figure 3.8 shows the tows and frame arms that are used to compare the frame angles and the angles of the reinforcement during testing. For the reinforcement the angles are recorded at six different locations while for the frame the angles of all four frame arms are recorded. The angles of these six tows are individually compared to the average angle of the corresponding two parallel frame arms. The angles are measured using Inkscape. Basic trigonometry is used to convert the displacements of the picture frame to angles of the picture frame. This can then be used to calculate the in-plane shear strain.

Table 3.2 shows these results and the average observed difference between the angles of the fabric specimens and the frame. There are differences between the angles of the fabric and the frame angles. The standard deviation of the difference is also large compared to the mean value. The difference is however small enough that it is always clear to which displacement and which frame deviation the data belongs. From this it is concluded that the angles of the frame give a sufficient indication for the angles of the fabric for the current purpose.

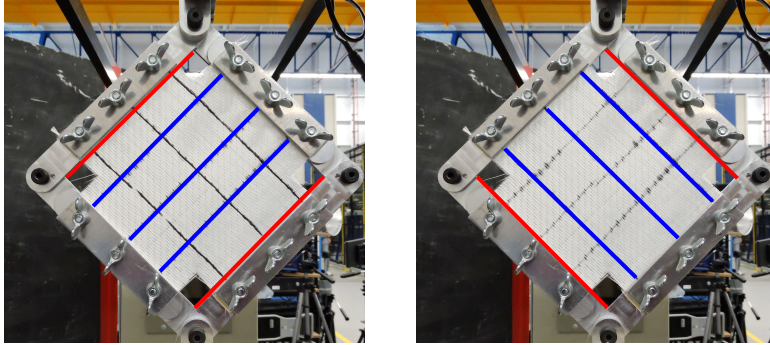


Figure 3.8: Highlighted tows and frame arms to indicate which angles are used in the comparison between frame angles and angles of the reinforcement during testing.

Table 3.2: Relationship between applied displacement, in-plane shear strain, angle of the frame and the difference between fabric and frame angles.

Displacement [mm]	Frame deviation from 90°, in-plane shear strain [°]	Difference between fabric and frame angles [°]	
		Tension	Compression
1	0.47	0.07 ± 0.09	0.02 ± 0.03
2	0.93	0.07 ± 0.08	0.07 ± 0.03
3	1.40	0.13 ± 0.09	0.07 ± 0.06

### 3.4. DISCUSSION

Figures 3.4 and 3.5 showed a clear difference between the patterns of specimens loaded in tension and compression. Patterns are consistent across multiple specimens. For specimens loaded in compression two clearly different regions are observed while specimens loaded in tension show a more consistent trend.

Creech & Pickett [20] present the key mesoscopic fabric deformation mechanisms in a biaxial NCF. Of these deformation mechanisms the direction of the stitches influences the shear behaviour of the fabric through stitch tension, frictional stitch sliding and interaction between stitching and tows. In the unloaded state of the NCF the stitches are not under tension. The deformation mechanisms of stitch tension and frictional stitch sliding will only become relevant once the stitches are loaded. Up till that point the stitches only contribute through the interaction between stitching and tows. With low displacements the stitches will also not be fully engaged yet, making the stitch-tow interaction the only contribution of the stitches.

The compression results show that there are different mechanisms at play in the reinforcement at different stages of the experiment. Two distinct regions can be defined with a transition where the material becomes significantly stiffer. The mechanisms at play before and after the kink will be discussed below. In the compression case the stitches will not be under tension and will only contribute through the interaction between (unloaded) stitches and tows. However, other deformation mechanisms such as tow com-

paction, inter-tow shear, inter-tow sliding and cross-over point sliding (as per Creech & Pickett [20]) will still be present. All mechanisms are subject to coupling and will influence each other.

The compression graphs in Figures 3.4 and 3.5 show that the deformation behaviour is dependent on the loads that have previously been applied. At the start of the series of experiments the first region with a reduced stiffness is short, but as the loads that are applied to the reinforcement become larger so does the length of the first region. With each additional applied shear load the reinforcement shears more easily to a higher angle. Unloading the reinforcement did not return it to its previous state. Instead, the fabric and its behaviour have changed over the course of the series of experiments. The response of the reinforcement to a shear load is always influenced by previous shear. This further exemplifies the importance of setting limits for the fiber angle deviations and in-plane shear strains.

It is suggested that in the lower stiffness region inter-tow shear is a dominant deformation mechanism. As the behaviour of the fabric changes, the contribution of other deformation mechanisms starts to increase. The test returns the picture frame to the original configuration with no applied displacement or angle after each loading. However, during unloading not all deformation mechanisms will work in a way that returns the fabric to the original configuration. This results in less resistance to shear when the fabric is loaded again until the different deformation mechanisms start to act on the fabric again. Additionally, as discussed by Colin *et al.* [21] the filament orientation within NCFs is not perfectly aligned with the tow direction. Within tows this can for example include a waviness of the filaments or filaments laying at an angle. For the NCF used in this work filaments have been observed to follow a path from one tow to the neighboring tow between stitching points, thereby travelling a longer path than fibers that are perfectly contained within a single tow. The middle of Figure 3.9 shows an example of this phenomenon. As the fabric is loaded these misalignments will be straightened out, upon unloading they might not go fully back to their origin resulting in part of the tows not being loaded until larger applied displacements. This contributes to the permanent changes that have been observed in the behaviour of the fabric due to shear loading.

The tension results show that the stitches are quickly under tension once a displacement is applied. No obvious differences can be observed in the trend of the graphs for loads from  $1 - 10 \text{ mm} / 0.47 - 4.68^\circ$ . It would be expected that an obvious increase in stiffness would be observed if the stitches came under tension later in the experiment. Around  $0.4 - 0.5^\circ$  a small 'bump' can be observed in the graphs in the tension graphs in Figures 3.4 and 3.5. Since a similar 'bump' is present in the reference measurements for an empty frame after testing this is attributed to frame effects. For the fabric loaded in tension it can also be observed that the fabric changes over the course of the experiment due to the previous loadings. This effect is however less dramatic than for the compression specimens. This is attributed to the stitches playing a large role in the deformation of specimens loaded in tension. For the compression case the stitches only contribute through interaction between (unloaded) stitches and tows. For the tension case the stitches also contribute through stitch tension and frictional stitch sliding. Additionally, the interaction between stitches and tows is now between loaded stitches and

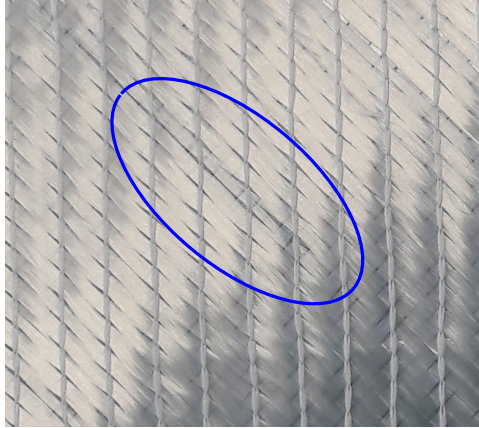


Figure 3.9: Example of filaments following a path between different tows.

tows. It is suggested that the stitches are less susceptible to permanent changes due to the mechanisms they show during deformation of the fabric than the tows are.

For this work the end values of the load-displacement graphs are of interest. As shown in Figure 3.7 the loading direction does not have a large influence on the end-values of standard specimens at displacements of 1 - 3 mm / angles of  $0.47 - 1.4^\circ$ . This suggests that at these small displacements and subsequent shear angles the direction of the stitches in the  $\pm 45^\circ$  bi-axial NCF does not significantly influence the final shearing behaviour of the fabric.

For the bi-axial NCF used in this work the maximum allowable fiber angle deviation during handling was found to be  $1.4^\circ$ . This value is specific to this fabric and cannot be assumed to be valid for other fabrics. The method by which this value has been determined can however be applied to any bi-axial NCF.  $\pm 1.4^\circ$  will be used for the remainder of this work as a tolerance for in-plane shear induced fiber angle deviations. No other work has been found that specifically looks at tolerances for the handling process. Gerngross & Nieberl [4] set a tolerance of  $\pm 5^\circ$  for picking-up, transporting, draping and positioning of the cut-pieces (dry textile weave or non-crimp fabric). This does however include draping and positioning, which are not considered in the current work.

The method for setting a tolerance for the fiber angle deviations as has been presented in the current work is of value both in designing pick-and-place processes and in monitoring them. Setting a tolerance for fiber angle deviations makes it possible to base design decisions such as pick-up point location on a criterion that directly affects the quality of the final product: the fiber angles. Real-time monitoring is most valuable when the expected variation is known. This makes it possible to check the observed variation with the expected variation. Additionally, if tolerances are found to be exceeded when monitoring the handling this can be taken into account in further manufacturing steps and/or in further iterations of the process.

### 3.5. CONCLUSIONS

The present chapter set out to provide a framework for the determination of acceptable criteria for in-plane shear induced fiber angle deviations in bi-axial non-crimp fabrics. The research question to be answered was:

How can tolerances be set for handling induced fiber angle deviations due to in-plane shear in bi-axial NCFs?

The chapter presents a case study for a specific bi-axial non-crimp fabric loaded at low shear angles. It was found that even low shear angles will result in permanent changes in the bi-axial NCF. Unloading the reinforcement did not reverse these changes. The permanent changes build upon each other as the experiments continued and the fabric was further sheared. These observations have been used to set tolerances for the fiber angle deviations and in-plane shear. For this fabric tolerances are set for the fiber angle deviations and in-plane shear strain of  $1.4^\circ$ . The methodology as shown in the current work can be repeated for any bi-axial NCF or other type of fabric.

The research goal for this research project as defined in chapter 2 is:

The development of a framework for prediction and prevention of fiber angle deviations due to in-plane shear during handling of large-sized bi-axial NCFs

The current chapter has contributed to this research goal by providing a method for setting tolerances for these in-plane shear induced fiber angle deviations. Tolerances for a specific bi-axial NCF have been set that will be used throughout the remainder of this work. These tolerances can be used with numerically predicted in-plane shear strains and fiber angle deviations for different scenario's. Chapter 4 will work towards the set up of such a numerical model by presenting a method for the determination of elastic properties of bi-axial NCFs based on their dimensions and stitch pattern. When designing a new product or pick-and-place procedure it can be valuable to for example be able to predict the influence of changes in the stitching pattern on the fiber angle deviations that occur during handling. The method presented in the next chapter will make it a relatively straightforward process to determine the effect of changes to NCF geometry or stitching pattern to homogenised elastic properties.



# BIBLIOGRAPHY

- [1] Fredrik Martinsson. *Development of Robust Automated Handling of pre-impregnated Carbon Fibre (Master Thesis)*. 2018.
- [2] M Kühnel et al. “Automated near net-shape Preforming of Carbon Fiber Reinforced Thermoplastics (CFRTP)”. In: *Innovative Composites Summit, JEC Europe, Paris, France* (2014), pp. 11–13.
- [3] Christian Krogh, Jens A Glud and Johnny Jakobsen. “Modeling the robotic manipulation of woven carbon fiber prepreg plies onto double curved molds: A path-dependent problem”. In: *Journal of Composite Materials* 53.15 (2019), pp. 2149–2164.
- [4] Tobias Gerngross and Dorothea Nieberl. “Automated manufacturing of large, three-dimensional CFRP parts from dry textiles”. In: *CEAS Aeronautical Journal* 7.2 (June 2016), pp. 241–257. ISSN: 1869-5590.
- [5] A Mouritz. “Fibre–polymer composites for aerospace structures and engines”. In: *Introduction to Aerospace Materials, 1st ed.; Woodhead Publishing Ltd.: Cambridge, UK* (2012), pp. 338–393.
- [6] Eduardo Guzman-Maldonado et al. “Experimental and numerical analyses of the mechanical behavior during draping of non-orthogonal bi-axial non-crimp fabric composite reinforcements”. In: *Materials & Design* 218 (2022).
- [7] Helga Krieger, Thomas Gries and Scott E Stapleton. “Design of Tailored non-Crimp Fabrics Based on stitching geometry”. In: *Applied Composite Materials* 25.1 (2018), pp. 113–127.
- [8] Jie Wang et al. “Mesoscopic analyses of the draping of 3D woven composite reinforcements based on macroscopic simulations”. In: *Composite Structures* 250 (2020), p. 112602.
- [9] Christian Krogh, James A Sherwood and Johnny Jakobsen. “Generation of feasible gripper trajectories in automated composite draping by means of optimization”. In: *Advanced Manufacturing: Polymer & Composites Science* 5.4 (2019), pp. 234–249.
- [10] Hua Lin et al. “3D mathematical modelling for robotic pick up of textile composites”. In: *Composites Part B: Engineering* 40.8 (2009), pp. 705–713.
- [11] Duc Do, Sabu John and I Herszberg. “3D deformation models for the automated manufacture of composite components”. In: *Composites Part A: Applied Science and Manufacturing* 37.9 (2006), pp. 1377–1389.
- [12] S Raganathan and L Karunamoorthy. “Genetic algorithm-based optimal locations for handling fabric materials in garment automation”. In: *International Journal of Robotics and Automation* 21.4 (2006), pp. 288–294.

- [13] Shrinivas Lankalapalli and Jeffrey W Eischen. "Optimal pick-up locations for transport and handling of limp materials: Part II: Two-dimensional parts". In: *Textile research journal* 73.10 (2003), pp. 867–874.
- [14] Fabian Johannes Ballier. *Systematic gripper arrangement for a handling device in lightweight production processes*. Shaker Verlag, 2019.
- [15] Ali Habboush et al. "Characterization and analysis of in-plane shear behavior of glass warp-knitted non-crimp fabrics based on picture frame method". In: *Materials* 11.9 (2018), p. 1550.
- [16] Stepan Vladimirovitch Lomov. "Deformability of textile performs in the manufacture of non-crimp fabric composites". In: *Non-Crimp Fabric Composites*. Elsevier, 2011, 117–144e.
- [17] Julian Fial et al. "Shear Characterization of Reinforcement Fabrics using Textile-applied printed Strain Sensors". In: *Procedia Manufacturing* 47 (2020), pp. 65–70.
- [18] Benedikt Lux et al. "Development of a shear forming envelope for carbon fibre non-crimp fabrics". In: *Journal of Industrial Textiles* 51.2\_suppl (2022), 2089S–2105S.
- [19] Venkateswaran Santhanakrishnan Balakrishnan et al. "Experimental and numerical investigation on draping behaviour of woven carbon fabric". In: *Journal of Industrial Textiles* 51.3\_suppl (2022), 3575S–3592S.
- [20] Gavin Creech and Anthony K Pickett. "Meso-modelling of non-crimp fabric composites for coupled drape and failure analysis". In: *Journal of materials science* 41.20 (2006), pp. 6725–6736.
- [21] David Colin et al. "Virtual Description of Non-Crimp Fabrics at the Scale of Filaments Including Orientation Variability in the Fibrous Layers". In: *Applied Composite Materials* 27.4 (2020), pp. 337–355.

# 4

## MESOSCOPIC MODELING OF NON-CRIMP FABRICS FOR THE DETERMINATION OF HOMOGENISED ELASTIC PROPERTIES

### 4.1. INTRODUCTION

THE goal of the research presented in this thesis is to provide a framework that can be used to predict and prevent fiber angle deviations in non-crimp fabrics using different pick-and-place strategies. Chapter 3 established that there is a direct link between fiber angle deviations and in-plane shear strains and set tolerances. For the prediction of the fiber angle deviations under different scenarios a numerical model will be created and material properties will need to be determined for the NCF.

A practical approach to evaluating reinforcement shear during handling is the use of existing Finite Element Analysis [FEA] software. This analysis can be carried out using a micro scale model (filament level), a meso scale model (tow level) or a macro scale model (structural level). Micro and meso scale modeling allow for close study of the effect of geometry on reinforcement behaviour. However, when processes are simulated the behaviour of a reinforcement as a whole is of interest. This makes the macro scale more favourable for these types of analyses [1]. Additionally, the macro scale is the level the end-users of reinforcements will be working with and choices at this level affect the shear experienced by the reinforcement - e.g. placement of pick-up points or the size of the reinforcement being picked up.

---

Parts of this chapter have been published in Chantal M. de Zeeuw, Daniël M. J. Peeters, Otto K. Bergsma & Rinze Benedictus (2022) Setting bounds for in-plane shear induced fiber angle deviations in bi-axial non-crimp fabrics, *Journal of Industrial Textile*, 52, 1-23, DOI: 10.1177/15280837221113921

Advantages of both meso and macro scale modeling can be combined through the use of periodic representative volume element [RVE] homogenisation. An RVE can be defined as the smallest material volume element for which the macroscopic constitutive representation is a sufficiently accurate model to represent mean constitutive response [2]. In periodic RVE homogenisation effective elastic properties are computed through imposition of uniform strains on the RVE [3]. These effective elastic properties can then be used in a macroscale model. Changes in the mesoscale RVE model will result in different effective elastic properties. This makes it possible to observe the effect of changes at the mesoscale on the behaviour at the macroscale.

Recent work on meso scale modeling of NCFs includes the work by Thompson *et al.* [4] in which meso scale modeling was used to capture the tow-stitch interactions during forming and compaction processes. Similarly, Creech & Pickett [5] use meso scale modeling to ensure their draping/forming simulation includes all important fabric deformation mechanisms. Bel *et al.* [6] use a meso-macro scale approach where the two layers in a bi-axial NCF are connected using bar elements that represent the stitches. In these forming simulations there are no limits for the in-plane shear, just observations and a desired final shape. Additionally, the simulations assume the reinforcement will be in perfect condition at the start of forming. In reality the handling process, which takes place before the actual forming process, could already result in undesired shear. Colin *et al.* [7] used RVEs with averaged periodic boundary conditions for the virtual characterisation of NCFs. Through the use of reference points and digital chain elements their model allows for the simulation of deviations in fiber angles within the layers of an NCF. The authors focus on the influence of these deviations on the compaction behaviour of the NCF. These fiber angle deviations are on a different scale than the ones of interest for the current work. The current work focuses on fiber angle deviations through reorientation of tows while Colin *et al.*'s [7] fiber deviations are at the individual filament level.

Periodic RVE homogenisation has recently been used by Benyahi *et al.* [8] to determine material properties and evolution of damage for composite material with inclusions. Zhao *et al.* [9] used RVE based finite element homogenisation to obtain effective material properties for injection molded short fiber reinforced PEEK composites. RVEs are generated using the random sequential adsorption algorithm for the fibers. Periodicity is ensured by cutting parts of the fiber that extend outside the RVE and shifting these to the opposite surface. Omairey *et al.* [3] developed and validated EasyPBC, an Abaqus plugin that can be used for the periodic RVE homogenisation of RVEs designed in Abaqus. A limitation of this plugin in relation to the current work is that it works on a single part, while the RVE for an NCF will require multiple parts to represent the tows and stitches.

The research question to be answered for the current chapter is as follows:

How can the elastic properties for a bi-axial NCF be predicted based on its dimensions and stitch pattern?

This chapter will present the work that has been done to obtain homogenised material properties using periodic RVE homogenisation. The goal for the RVE is to have it be readily adaptable to different bi-axial NCF configurations. First, Section 4.2 will go over the setting up of the RVE. This is followed by Section 4.3 which will detail how the tow

properties are obtained for the RVE material input. Section 4.4 discusses the determination of the homogenised material properties using the RVE and in Section 4.5 the RVE is validated. The work on the mesoscopic modeling of non-crimp fabrics for the determination of homogenised elastic properties is discussed in Section 4.6. Finally, Section 4.7 presents some conclusions.

## 4.2. SETTING UP THE REPRESENTATIVE VOLUME ELEMENT

Homogenised material properties are obtained through periodic RVE homogenisation. First, an RVE is designed in such a way that repeating it will give an accurate representation of the material at a larger scale. For the current work the RVE will be created at the meso scale level, with the larger scale being the macro scale. Periodic boundary conditions ensure that the deformation of the RVE happens in the same way it would if the RVE was surrounded by repeats of the same RVE. For this research node-to-node periodic conditions are used, where nodal degrees of freedom are linked to each other. For the homogenisation uniform strains are applied to the RVE. The resulting reaction forces at different reference points are then used to calculate the stresses and moduli.

The periodic RVE homogenisation implementation is based on the work by Omairey *et al.* [3]. In that work the authors present EasyPBC, an ABAQUS/CAE plugin that calculates the homogenised effective elastic properties of RVEs created by the user. However, their algorithm is not compatible with RVEs that require multiple components for a correct representation, as is the case with non-crimp fabrics, which have tows and stitches as components. For the current work the algorithm of EasyPBC 1.4 has been used as a guideline for the development of an RVE that is build up using multiple tows and stitches.

Omairey *et al.*'s [3] EasyPBC requires the user to create an RVE in ABAQUS/CAE. The plug-in can then be selected to compute homogenised elastic properties for this user generated RVE. For the current work code has been written that will create the input file for an RVE composed of eight tows with specified dimensions and a predefined stitch pattern. The EasyPBC plugin is used as a guideline in writing the code that makes it possible to apply periodic boundary conditions and uniform strains with the goal of obtaining homogenised elastic properties. Periodic boundary conditions are required to ensure the RVE deforms in a way that also takes deformation of the surrounding material into account.

The algorithm written for the current work creates two different types of files. The main file is a script file that will be read by Abaqus, additionally input files are created for Abaqus for the model and all the appropriate boundary conditions. A separate input file is created for obtaining the Young's moduli and the shear moduli. This is a result from different linear constraints equations and displacement boundary conditions being required for the two different cases. The exact constraint equations and displacement boundary conditions can be found in Appendix C.

The full python files that work together to create the script file and input files can be found on 4TU Research data [10]. Comments are provided in the code to aid in understanding. Four files are used: the 'RVE set-up file', the 'RVE functions file', the 'Constraint functions file' and the 'Scriptfile'.

The main file is the 'RVE set-up file'. This is the file where input data is given for the creation of the Abaqus input file and the script file used to run the simulations. The user can choose which of the elastic properties they are interested in and provide dimensions and material properties for the tows and stitches. Stitches are created by providing the start and end-coordinate for each segment. This main file uses the 'RVE functions file' and the 'scriptfile' to get all the information required to write the output files.

The 'RVE functions file' is the file that creates the nodes, elements, parts and instances based on the dimensions given in the 'RVE set-up file'. It is also responsible for setting the interactions and contact between the different set and surfaces. The 'RVE functions file' also creates the reference points that are used to apply the strains on the RVE. Finally, this file imports the constraint functions from the 'Constraint functions file' to create the boundary conditions necessary to ensure the deformed surfaces of the RVE stay periodic.

The 'Constraint functions file' writes all the constraints for the nodes based on the different sets that are defined by Omairey *et al.* [3]. Omairey *et al.* [3] illustrate these sets in Figure 6 of this paper. The linear constraints and load boundary conditions are given in Table 1 in their work [3]. The sets for the current work can be found in Appendix C.

The final file is the 'script file'. The basis of this file comes directly from the work by Omairey *et al.*. It has been adapted to work with the other files and with the model as created for the current research. The 'script file' writes the script file that is imported in Abaqus to run the simulations based on the elastic properties that have been chosen in the 'RVE set-up file'. This is the part of the script where the strains to be applied to the RVE are set. It is also the part where the reaction forces are obtained that are used to calculate the Poisson ratio's, Young's moduli and Shear moduli. Finally the script prints the desired results for the elastic properties and writes these to a text file.

For the current work the RVE is based on the bi-axial NCF as presented in Figure 3.1. The stitch pattern of this RVE requires that at least four tows on the top and four tows on the bottom are used. The scripts as presented in Appendix C only work for this configuration of four tows on the top and four on the bottom. They can however be adapted to increase or decrease the amount of tows.

The stitching in a non-crimp fabric [NCF] has a large influence on the shearing behavior through the stitching pattern and their placement relative to the shearing motion [11–13]. Therefore, care has to be taken that the stitching pattern in the RVE is a good representation of the real life pattern. Figure 4.1 shows a reproduction of the chain stitch. On the front of the stitch there is a loop, on the back of the stitch there is a single thread. This is taken into account in the creation of the stitch pattern in the 'RVE set-up file' by allocating twice the surface area for the top representation of each individual stitch.

Figure 4.2 shows the stitch pattern in the RVE in red. Figure 4.3 shows the RVE with a top tow removed to show the bottom tows. In this figure the top part of stitches can still be seen as a diagonal line. Within the model, tows are free to move relative to each other within the constraints of the boundary conditions used for periodic RVE homogenisation. The stitches are connected to the tows at each corner.

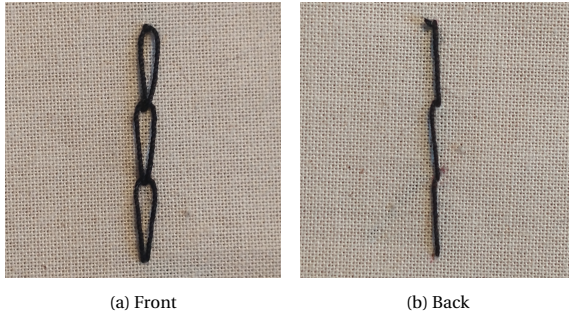


Figure 4.1: Reproduction of chain stitch

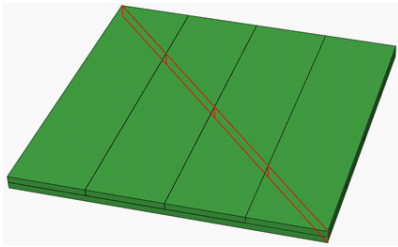


Figure 4.2: The stitches in RVE are indicated in red

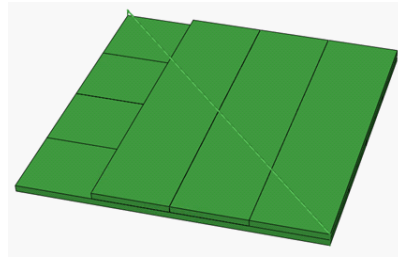


Figure 4.3: RVE with a top tow removed to show the bottom tows

Table 4.1 shows the dimensions that have been obtained for the tows and stitches using a micrometer and caliper. For the stitches a Young’s Modulus of 2.8 GPa is used for the PES material [14].

Table 4.1: Dimensions for tows and stitches obtained using micrometer and caliper

Tow width	1.89 mm
Tow height	0.168 mm
Stitch diameter	0.045 mm

Figure 4.4 shows the meshed RVE model with dimensions. The tows are meshed using C3D8R elements with a size of 1/3 of the tow height, which is 0.056 mm. This mesh size is based on a convergence study for the calculated material properties. For the stitches T3D2 elements are used, with element size being equal to the dimensions of the individual stitch parts.  $a$  is the tow width.  $b$  is four times the tow width and is 7.56 mm.  $h$  is twice the thickness of a tow and is 0.336 mm. The surface area of a truss is obtained using  $\pi \times r^2$  and is 0.00159 mm<sup>2</sup>. The surface area for the top truss is double this value.

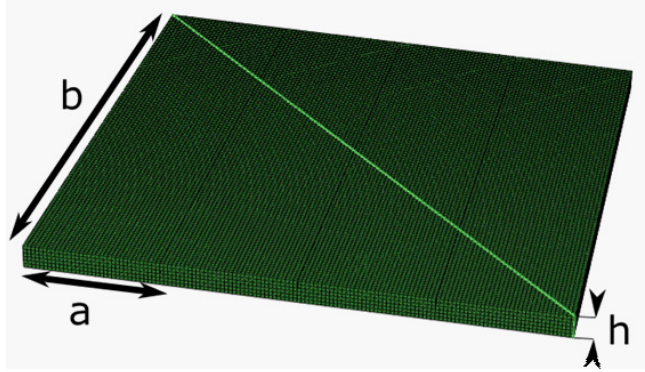


Figure 4.4: Meshed RVE model with dimensions

### 4.3. OBTAINING TOW PROPERTIES FOR RVE INPUT

A flexural rigidity test based on ASTM D1368 is used to approximate the longitudinal stiffness of the tow that ensures correct bending behavior. Similar approaches have previously been used by Creech & Pickett [5], Pabst *et al.* [15] and Döbrich *et al.* [16] to calibrate mechanical properties to ensure correct behavior. A tow consists of thousands of filaments. These filaments are held together through a small amount of coating or through twisting of the filaments. The resulting stiffness of a tow is therefore not equal to the material stiffness but reduced depending on the connection between the filaments in the tow.

Figure 4.5 shows how a tow is slid over a block with a  $41.5^\circ$  slope until the tow hits the slope.  $L_{residual}$  and  $L_{slope}$  are recorded with an accuracy of 1 mm based on a ruler connected to the surface. These values are used to calculate  $L_{over}$  and  $\delta$ . Next, Euler-Bernoulli beam theory is used to obtain an initial approximation for the effective  $E_{11}$ .

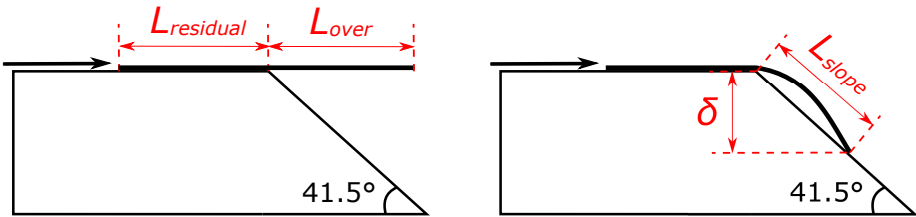


Figure 4.5: Flexural rigidity test block and tow with dimensions recorded during testing

Eleven specimens have been tested using the procedure described above. From these experiments the resulting  $L_{over}$  is  $133 \pm 6$  mm. The recorded  $L_{slope}$  is  $129 \pm 6$  mm. The measured deflection,  $\delta$  is  $85 \pm 4$  mm. This value is used to calibrate the Young's moduli of the tows to be used in the remainder of the work.

The value for  $E_{11}$  obtained using the flexural rigidity test and Euler-Bernoulli beam theory is taken as an initial value.  $E_{11}$  is further calibrated using Abaqus/CAE 2017 through

a non-linear shell model of the beam deflection test. In the model one end of the tow is fixed in all rotational and translational degrees of freedom and a gravitational load of  $9.81 \text{ m/s}^2$  is applied. The model is meshed using S4R elements with a mesh size equal to the tow width of 1.89 mm. Figure 4.6 shows a schematic of the model used for the overhang test simulations. The width  $a$  and thickness  $h$  of the model are equal to tow dimensions and respectively 1.89 mm and 0.168 mm. Length  $b$  is the mean overhang length recorded during the experiments and is 133 mm.

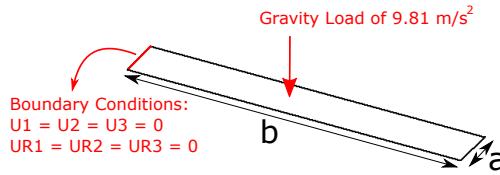


Figure 4.6: Schematic of overhang test simulation

The longitudinal stiffness is varied until the tow deflection matches the experimental work. Table 4.2 demonstrates the limited influence variations in  $E_{22}$  and  $E_{33}$  have on the tow deflection.

Table 4.2: Influence of variations in  $E_{22}$  and  $E_{33}$  on the maximum deflection of a simulated tow

	Max deflection [mm]
$E1 = E2 = E3$	85.42
$0,1 * E1 = E2 = E3$	85.47
$0,01 * E1 = E2 = E3$	85.48
$0,001 * E1 = E2 = E3$	85.48

Based on the observations that the deflection is virtually independent on the magnitude of  $E_{22}$  and  $E_{33}$  these stiffnesses are set at  $E_{11} / 10$ . This represents the fact that in reality the stiffnesses in the 22 and 33 direction of a tow are much smaller than in the 11 direction.

Figure 4.7 shows the simulation results compared to the average measurements for the tow end. For the simulation with elastic properties based on linear elastic beam theory  $E_{11} = 2.48 \text{ GPa}$  and  $E_{22}, E_{33} = 248 \text{ MPa}$ . The calibrated Young’s moduli are  $E_{11} = 1.57 \text{ GPa}$  and  $E_{22}, E_{33} = 157 \text{ MPa}$ . This is indeed considerably lower than a typical Young’s modulus for E-glass of 72 GPa.

The explanation for the difference between the typical Young’s modulus and the calibrated Young’s modulus is twofold. Firstly, this typical Young’s modulus is an axial modulus. This modulus will only be identical to a Young’s modulus calibrated for bending if the material behaves perfectly linear. The second part of the explanation lays in the construction of a tow. A tow is not solid E-glass: it is made up of a bundle of E-glass filaments. When loaded in tension the bundle of filaments might act very similarly to solid E-glass with the same dimensions. However, for bending the internal mechanisms between the two cases will be different. For solid E-glass the bending will purely come

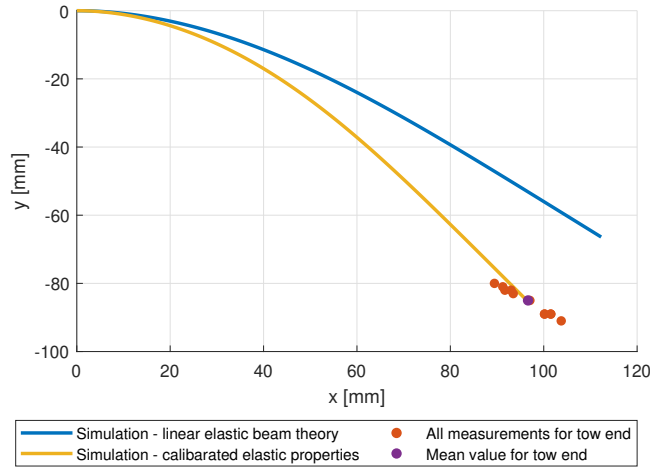


Figure 4.7: Simulation results compared to experimental measurements of the tow end deflection

from bending of the material. The filaments in the tows will have a low resistance to bending due to their small dimensions. Friction between the filaments causes them to connect and show a larger resistance to deformation. The combination between bending of individual filaments and the friction results in the effective bending stiffness for a tow.

For the tows a constant volume assumption is used which gives Poisson's ratio's  $\mu_{12}, \mu_{23}, \mu_{13} = 0.5$ . Crech [5] found it suitable to take all shear moduli to be equal.

The shear moduli of the tows are calibrated by looking at the homogenised in-plane shear modulus of the NCF. In real life an NCF will not have any resistance to in-plane shear without the stitches, the response of the RVE should reflect this. The tow shear moduli are varied until the RVE gives the desired response: matching the real life behavior as close as possible while ensuring computational time is kept reasonable. This results in shear moduli for the tows of 0.65 MPa.

Table 4.3 summarizes the final tow input values that are used.

Table 4.3: Tow elastic properties used in RVE

$E_{11}$ [MPa]	$E_{22}$ [MPa]	$E_{33}$ [MPa]	$\mu_{12}$ [-]	$\mu_{13}$ [-]	$\mu_{23}$ [-]	$G_{12}$ [MPa]	$G_{13}$ [MPa]	$G_{23}$ [MPa]
1570	157	157	0.5	0.5	0.5	0.65	0.65	0.65

## 4.4. DETERMINATION OF HOMOGENISED MATERIAL PROPERTIES USING RVE

Table 4.4 shows the homogenised properties calculated using the RVE based on tow and stitch properties as determined previously. This section will go over the elastic properties and where required will update these initial results.

Table 4.4: Homogenised elastic properties as determined by the RVE based on previously determined tow and stitch properties.

$E_{11}$ [MPa]	$E_{22}$ [MPa]	$E_{33}$ [MPa]	$\mu_{12}$ [-]	$\mu_{13}$ [-]	$\mu_{23}$ [-]	$G_{12}$ [MPa]	$G_{13}$ [MPa]	$G_{23}$ [MPa]
804	800	0.156	0.02	0.31	0.32	2.39	$4.01 \times 10^{-9}$	$1.64 \times 10^{-7}$

The RVE determines elastic properties by applying displacements in the 1, 2 and 3 direction. It is unable to determine properties calibrated for bending. Therefore, the  $E_{11}$  and  $E_{22}$  presented in Table 4.4 are an overestimate.  $E_{11}$  and  $E_{22}$  calibrated for bending can however be estimated by looking at  $EI$  instead of  $EA$ . The method is also shown for the standard axial stiffness to demonstrate the validity of properties determined using these steps.

The stiffness  $E_{11}$  for the tows has been determined to be 1570 MPa. With the definitions chosen for the RVE the tows lay in the 1 and 2 direction. It is assumed that tows perpendicular to the loading direction will not contribute. This means that only half the height of the fabric will be available in both the  $A$  in  $EA$  and the  $I$  in  $EI$ . If the full height would contribute, the  $E_{11}$  of the fabric would be the same as the  $E_{11}$  of a tow. With only half the height contributing  $EA$  can be written as  $E \cdot \frac{1}{2} h \cdot b$  or  $\frac{1}{2} EA$ . Since in the homogenised part, the full area is used, the E-modulus has to be halved, leading to  $E_{11} = 785$  MPa, which is close to the 800 MPa found by the RVE. The same can be done for  $EI$ . Writing  $EI$  out results in  $E \cdot b \cdot (\frac{1}{2} h)^3 / 12$  or  $\frac{1}{8} EI$ . This results in an  $E_{11}$  and  $E_{22}$  calibrated for bending to be used in further simulations of  $\frac{1}{8} \cdot 1570 = 196$  MPa.

Crech [17] showed that a constant volume assumption is valid for an NCF with a tricot stitch. The current work includes an NCF with a chain stitch. It is assumed that the constant volume assumption, which is typically used in commercial fabric models [17], can be used for the NCF used in the current work. To account for this  $\mu_{12}$ ,  $\mu_{13}$ ,  $\mu_{23}$  are updated from the values in Table 4.4 to 0.5.

As mentioned previously there are two load cases for the fabric, one with the stitches in tension and one with the stitches in compression. The  $G_{12}$  in Table 4 of 2.39 MPa is for stitches loaded in tension. For stitches loaded in compression the RVE gives a value for in-plane shear stiffness of 0.53 MPa. This loading direction is defined as 21, so  $G_{21} = 0.53$  MPa. This value for  $G_{21}$  is significantly lower than the value for  $G_{12}$ . With the orientation of the chain stitch in the fabric and the definitions chosen when setting up the RVE the stitches are in tension when loaded in 12 and under compression when loaded in 21. To match the real life behaviour of the stitches, the trusses used in the simulation cannot be loaded in compression and will therefore not contribute to the stiffness.

Table 4.5 shows the homogenised elastic properties as determined by the RVE and where relevant updated as described above.

Table 4.5: Homogenised elastic properties as determined by the RVE and described above.

$E_{11}$ [MPa]	$E_{22}$ [MPa]	$E_{33}$ [MPa]	$\mu_{12}$ [-]	$\mu_{13}$ [-]	$\mu_{23}$ [-]	$G_{12} / G_{21}$ [MPa]	$G_{13}$ [MPa]	$G_{23}$ [MPa]
196	196	0.16	0.5	0.5	0.5	2.39 / 0.53	$4.01 \times 10^{-9}$	$1.64 \times 10^{-7}$

## 4.5. VALIDATION OF THE RVE

### 4.5.1. FLEXURAL RIGIDITY TEST USING WIDE FABRIC SPECIMENS

As an initial step in validating the RVE the flexural rigidity test and the corresponding simulations are repeated with 50 mm wide strips of NCF. Before the experiments the stabilizing yarns in the  $0^\circ/90^\circ$  directions which are present in the NCF at an interval of around 5 cm are removed from the specimens. Figure 4.8 shows the three cut-outs that were used. In the figures the fiber directions are indicated in blue while the stitch directions are indicated in red. For Figure 4.8a and Figure 4.8b the tows are  $\pm 45^\circ$ . For Figure 4.8c the tows are  $0/90^\circ$ . Three specimens have been tested per scenario.

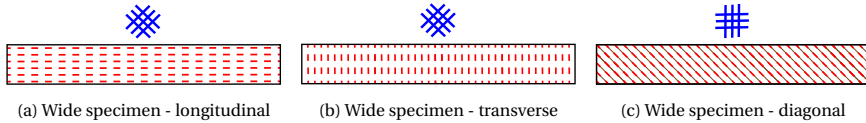


Figure 4.8: Illustration of stitch directions (red lines) and fiber direction (blue lines) for wide specimens.

For the specimens with longitudinal stitches the test results show that  $L_{over}$  is  $100 \pm 0$  mm,  $L_{slope}$  is  $95 \pm 1$  mm and  $\delta_{avg}$  is  $63 \pm 1$  mm. For transverse stitches  $L_{over}$  is  $93 \pm 2$  mm,  $L_{slope}$  is  $90 \pm 1$  mm and  $\delta_{avg}$  is  $60 \pm 1$  mm. Finally, for specimens with diagonal stitches  $L_{over}$  is  $105 \pm 1$  mm, the recorded  $L_{slope}$  is  $103 \pm 1$  mm and the measured deflection,  $\delta_{avg}$  is  $68 \pm 1$  mm.

The flexural rigidity test is simulated as described above for the beam deflection test of a single tow. The dimensions as shown in Figure 4.6 are as follows:  $a$  and  $h$  are constant across all three simulations, with  $a = 50$  mm and  $h = 0.336$  mm.  $b$  is dependent on the scenario. For specimens with longitudinal stitches  $b = 100$  mm, for transverse stitches 93 mm and for diagonal stitches 105 mm. These values are based on the experimental work.

For these simulations the  $G_{12}$  value has been used for both  $G_{12}$  and  $G_{21}$ . To avoid numerical instabilities the  $G_{13}$  and  $G_{23}$  were set to 0.24 MPa after numerical trials. This results in updated homogenised elastic properties as shown in Table 4.6. Table 4.7 shows the experimental and simulated results for the beam deflection test of wide strip specimens.

The results in Table 4.7 show that for the specimens with longitudinal and transverse stitches the simulation is able to reproduce the experimental results with a margin of 10%. For specimens with diagonal stitches the simulation is off by more than 10%. The

Table 4.6: Homogenised elastic properties as determined by the RVE and described above.

$E_{11}$ [MPa]	$E_{22}$ [MPa]	$E_{33}$ [MPa]	$\mu_{12}$ [-]	$\mu_{13}$ [-]	$\mu_{23}$ [-]	$G_{12} / G_{21}$ [MPa]	$G_{13}$ [MPa]	$G_{23}$ [MPa]
196	196	0.16	0.5	0.5	0.5	2.39 / 0.53	0.24	0.24

Table 4.7: Experimental and simulated results for beam deflection test of wide strip specimens.

	Experimental [mm]	Simulation [mm]
Wide specimen - longitudinal	60	54
Wide specimen - transverse	63	64
Wide specimen - diagonal	68	60

observed underestimation is attributed to the way the material is modeled. The numerical model does not consider individual tows and stitches but uses homogenized elastic properties. The load cases that are used to determine homogenized elastic properties are quite basic. A bi-axial NCF does however have a variety of mesoscopic fabric deformation mechanisms [5]. These different mechanisms and their coupling will not all be caught through application of these basic loading conditions on the RVE.

#### 4.5.2. PICTURE FRAME TESTS OF FABRIC SPECIMENS

A second step in validating the RVE is by looking at the experimental shear behavior of NCF. This behavior is observed using picture frame tests. These experimental results are compared to results obtained from a simulated picture frame test. The picture frame model is created using Abaqus/CAE 2017. Figure 4.9 shows this model. The inner square of the specimens, which is the area that will shear due to the applied load, is simulated using S4R elements with a size of 5 mm. Figure 4.10 highlights this area (note: this is a repeat of Figure 3.2 in Chapter 3 for clarification purposes). Correct load application is achieved through the addition of tows along the edges. For these trusses T3D2 elements are used. Boundary conditions are applied to prevent out of plane movement. The displacements are applied on one corner while the reaction forces are recorded at the opposite corner that has been restricted.

In the experimental work displacements are applied on the picture frame. If this displacement was constant throughout the whole setup there would just be a rigid body motion. Instead, the applied displacement results in a larger actual displacement at the point of load application than more towards the middle of the frame. This is illustrated in Figure 4.11. For this validation only the inner square of the NCF sample is modeled and not the whole set-up. Applying a displacement of 1 mm to this inner square would result in the application of a larger angle to the NCF than in the case where the 1 mm displacement is applied to the frame. To correct for this, the dimensions of 175 mm and 110 mm as shown in Figure 4.10 are used to scale the displacements of 1, 2 and 3 mm. This results in displacements of 0.629, 1.258 and 1.887 mm to be used for the validation.

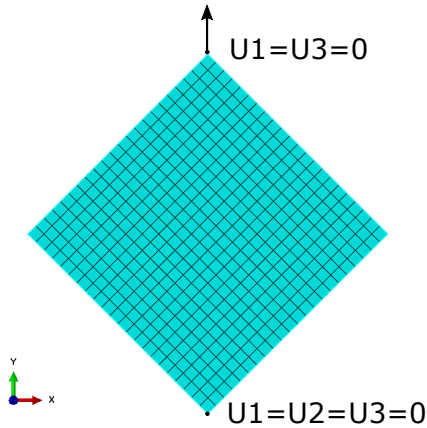


Figure 4.9: Picture frame model

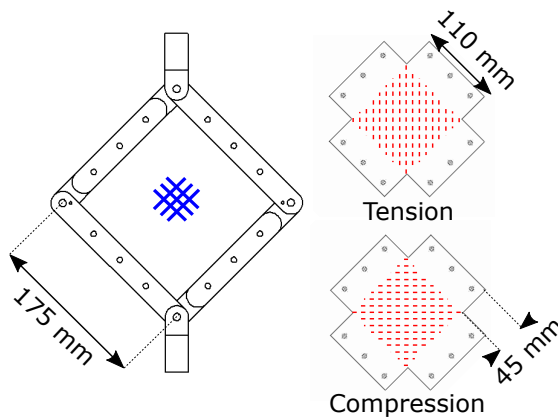


Figure 4.10: Illustration of the frame design and both a tension and compression specimen with the direction of the stitches indicated in red stripes and the direction of the fibers indicated in blue lines.

The homogenised elastic properties as determined using the RVE should be able to reproduce the results found during the picture frame tests. For the current chapter the linear approximations of the end-force-values as presented in Figure 3.7 are compared to the reaction forces in the picture frame test simulation.

For the experimental picture frame tests it was concluded that part of the observed results originates from frame effects, including the initial steep region. The numerical model will not be able to predict these frame effects. To test whether the simulations can predict the behaviour of the fabric they are compared to the slope of the linear approximation shown in Figure 3.7. Figure 4.12 presents the comparison between this linear approximation and the simulated end values predicted using both  $G_{12}$  and  $G_{21}$ .

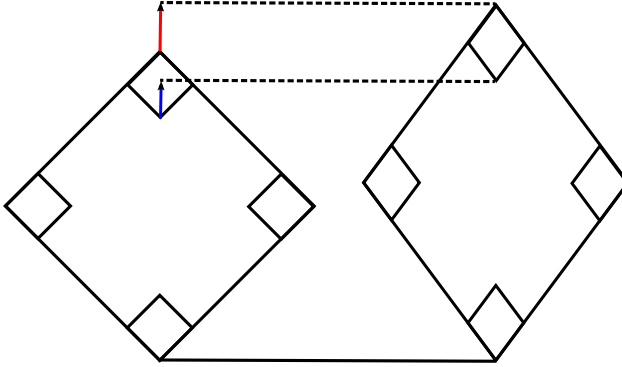


Figure 4.11: Illustration of the picture frame and the different displacements at different points in the frame. Red showing the displacement as applied to the frame, blue showing the displacement of the inner square.

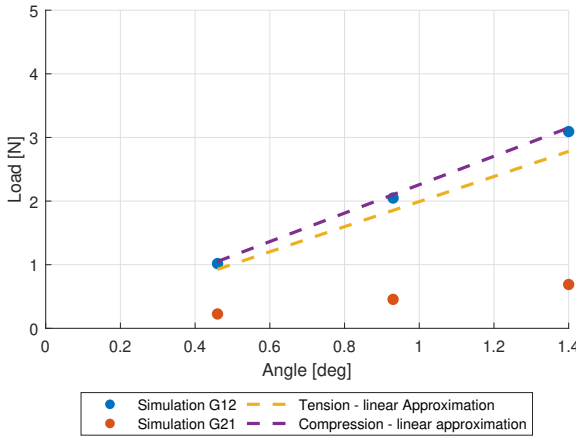


Figure 4.12: Comparison between linear approximations and simulation for end values

Figure 4.12 shows how the load case with  $G_{12}$  results in a simulation that reproduces the response for standard compression specimens very closely. Additionally, it shows that the load case with  $G_{21}$  is not able to accurately predict the actual behavior.

The experimental values for compression and tension specimens for low displacements as shown in Figure 4.12 are relatively close. Based on these results, the homogenised material properties determined using the RVE with  $G_{12}$  are able to give a good representation of the shear behavior of the fabric for low displacements, regardless of the loading direction.

## 4.6. DISCUSSION

In the current work periodic RVE homogenisation is used to determine homogenised elastic properties for a biaxial NCF. To get from the NCF to the RVE assumptions and simplifications had to be made. As mentioned before the current work assumes that the filaments within a tow are aligned to such an extent that tow angles correspond to filament angles. It does not consider factors such as in-plane waviness and twist as a result of manufacturing. The models are however build up from the tow level, using a series of tows to calibrate the material properties. The mechanical properties for the tows do therefore account for part of the irregularities that might influence bending behavior. Additionally, the results from the RVE were validated using wide fabric strips and small displacement picture frame tests.

4

The elastic properties for the tows have been calibrated for bending using overhang tests based on ASTM D1368. Using a typical axial modulus would result in a huge overestimation of the bending stiffness of a tow. When loaded under tension a bundle of filaments will behave the same as a solid beam out of the same material with the same dimensions. In bending the behaviour will however be different. This is attributed to the filaments in a tow not behaving as a single entity. There will be some friction between filaments which is increased by the silane treatment used during manufacturing of the NCF. Filaments will however still be able to behave independently. Calibration of the elastic properties was required to take the interactions between filaments into account in predicting the behaviour of the tow as a whole.

Similarly to the elastic properties of the tows the homogenised elastic properties  $E_{11}$  and  $E_{22}$  for the NCF had to be calibrated for bending as well. The method used to obtain the homogenised elastic properties uses displacements in the 11 and 22 direction to obtain these Young's moduli. This results in the determination of an axial modulus instead of one calibrated for bending. This shows that periodic RVE homogenisation is not an appropriate method for determining these properties. Calibrated properties were manually obtained using the calibrated  $E_{11}$  for tows and  $EI$  instead of  $EA$ . Alternatively, the method used to obtain estimates for the calibrated  $E_{11}$  and  $E_{22}$  on the NCF level could have already been pre-programmed in the python scripts for ease of use.

The algorithm written for this work makes the RVE customizable to a large degree, making it possible to study the influence of for example different stitch patterns on the homogenised elastic properties of the fabric. For now a case study for a single fabric with one specific type of stitch is presented. Extensive validations of different types of NCFs is required before the framework is to be used outside the current scenario.

The shear moduli of the tows are calibrated by looking at the behaviour of the RVE with no stitches present. This has resulted in  $G_{12} = G_{13} = G_{23} = 0.65$  MPa. The NCF used in this work is silane treated. This binder provides additional friction between the tows. Additionally, the friction between the filaments within the tows will contribute to a tows perceived shear modulus. The value of 0.65 MPa for the shear modulus of tows is therefore considered to be reasonable. If no silane treatment would have been present a value even closer to 0 would have been found. In real life an NCF without stitches will not have any resistance to shear, this cannot be perfectly represented in simulations. When

a sample is clamped in the picture frame and stitches are removed the tows will not remain in their perfectly aligned position. There will be a large loss of contact between tows in the  $45^\circ$  layer and the  $-45^\circ$  layer and the tows within a layer might also partially lose contact. This results in a large loss of tow-tow interactions that can contribute to the shear resistance. An RVE will always start the simulations with tows perfectly aligned. However, while an NCF without stitches will not have any resistance to shear, a single tow will.

The simulated picture frame tests carried out for  $G_{12}$  accurately predicted the end values for compression specimens.  $G_{12}$  simulations should have predicted end values for tension specimens only. However, for the region of interest of the current work, end values for compression and tension specimens were close to each other, as has also been shown and discussed in Chapter 3. Due to this observation the RVE is still considered to provide elastic properties that are acceptable to be used in further chapters.

The values predicted by the simulations with  $G_{21}$  were much lower than found for either compression or tension specimens. This low value can be explained by an inability of the trusses in the RVE to be loaded under compression. This was a purposeful design choice based on the threads in the NCF that cannot be loaded in compression. However, the experimental results show that compression specimens have a higher resistance to in-plane shear than would be expected. At these low displacement/fiber angle deviations the behaviour under compression is very similar to the behaviour under tension.

The RVE is a simplified representation of the NCF that is not able to catch all the real life mesoscopic fabric deformation mechanisms. Creech & Pickett [5] present the key mesoscopic fabric deformation mechanisms in a biaxial NCF as: Tow compaction, inter-tow shear, inter-tow sliding, cross-over point sliding, stitch tension, frictional stitch sliding and interaction between stitching and fiber tows. These mechanisms do not just act alone but are also subject to coupling. Not all of these mechanisms are present in the RVE. Inter-tow sliding and cross-over point sliding are not possible due to the periodic boundary conditions. Frictional stitch sliding is not present in the RVE due to the way the stitches are represented. It is suggested that some of these mechanisms that are not represented in the RVE and/or coupling of behaviours that are not accurately enough represented in the RVE result in an underestimate of the shear resistance under compression.

The homogenised elastic properties resulting from the RVE are able to predict linear behaviour at low displacements/fiber angle deviations. For the current work the region of interest is low fiber angle deviations up to  $1.4^\circ$  and the relationship between force and displacement/angle was found to be linear. This makes the approach used appropriate for the current work. It can however not be used for higher displacements/angles where the relationship between force and displacement/angle becomes non-linear.

The method presented in this chapter makes it possible to make relatively straightforward comparisons for the homogenised elastic properties of different (variations of a) bi-axial NCF(s). In the design process of a new product or pick-and-place procedure it can be valuable to for example study the influence a different stitching pattern would have on the behaviour of the reinforcement. Previously, the elastic properties for differ-

ent variations of an NCF would need to be determined separately and experimentally. The current work makes it possible to obtain elastic properties numerically based on dimensions, tow and stitch elastic properties and stitching pattern. This makes it possible to do rapid comparisons between different NCF configurations.

## 4.7. CONCLUSIONS

The research question to be answered in this chapter is:

How can the elastic properties for a bi-axial NCF be predicted based on its dimensions and stitch pattern?

This chapter showed how periodic RVE homogenisation can be used to determine homogenised elastic properties for bi-axial NCFs. The resulting homogenised elastic properties have been validated using flexural rigidity tests and small displacement picture frame tests.

The scripts have been set up in a way that allows for customization of the RVE. The methodology presented in the current work can be used with these scripts for any bi-axial NCF as long as the tow directions lay perpendicular to each other and the stitch pattern can be represented using four top and four bottom tows. If more tows are required the scripts can be adapted to include additional tows.

The presented framework opens up the possibility for rapid comparison of the elastic properties for different NCF architectures. This is valuable in NCF design, product design and design of handling processes. Predictions made using this method can be further improved through further research on the mesoscopic fabric deformation mechanisms and how to capture these in an RVE.

The research goal for this research project is:

The development of a framework for prediction and prevention of fiber angle deviations due to in-plane shear during handling of large-sized bi-axial NCFs

The current chapter has contributed to this research goal by providing a method for obtaining elastic properties for bi-axial NCFs based on their dimensions, tow and stitch elastic properties and stitch pattern. The method has been used to calculate elastic properties for a specific bi-axial NCF that will be used for the remainder of this work. These elastic properties can be used in a numerical model for the prediction of in-plane shear strains and fiber angle deviations. Chapter 5 will make the step from the mesoscale used in the current chapter to the macroscale and set up models for the determination of in-plane shear strains. These in-plane shear strains and the corresponding fiber angle deviations can then be evaluated using the tolerances set in chapter 3.

# BIBLIOGRAPHY

- [1] Oliver Döbrich, Thomas Gereke and Chokri Cherif. “Modeling the mechanical properties of textile-reinforced composites with a near micro-scale approach”. In: *Compos Struct* 135 (2016), pp. 1–7. ISSN: 02638223.
- [2] Walter J Drugan and John R Willis. “A micromechanics-based nonlocal constitutive equation and estimates of representative volume element size for elastic composites”. In: *Journal of the Mechanics and Physics of Solids* 44.4 (1996), pp. 497–524.
- [3] Sadik L Omairey, Peter D Dunning and Srinivas Sriramula. “Development of an ABAQUS plugin tool for periodic RVE homogenisation”. In: *Engineering with Computers* 35.2 (2019), pp. 567–577.
- [4] Adam J. Thompson et al. “Modelling process induced deformations in 0/90 non-crimp fabrics at the meso-scale”. In: *Compos Sci Technol* 168 (Nov. 2018), pp. 104–110. ISSN: 02663538.
- [5] Gavin Creech and Anthony K Pickett. “Meso-modelling of non-crimp fabric composites for coupled drape and failure analysis”. In: *Journal of materials science* 41.20 (2006), pp. 6725–6736.
- [6] S. Bel et al. “Finite element model for NCF composite reinforcement preforming: Importance of inter-ply sliding”. In: *Compos. - A: Appl. Sci. Manuf.* 43.12 (Dec. 2012), pp. 2269–2277. ISSN: 1359835X.
- [7] David Colin et al. “Virtual description of a biaxial 0°/90° non-crimp fabric with normally distributed filament directions”. In: *AIP Conference Proceedings*. Vol. 2113. 2019, p. 20004. ISBN: 9780735418479.
- [8] Karim Benyahi et al. “Periodic homogenization and damage evolution in RVE composite material with inclusion”. In: *Frattura ed Integrità Strutturale* 15.58 (2021), pp. 319–343.
- [9] Jian Zhao et al. “Effective mechanical properties of injection-molded short fiber reinforced PEEK composites using periodic homogenization”. In: *Advanced Composites and Hybrid Materials* 5.4 (2022), pp. 2964–2976.
- [10] Chantal de Zeeuw. “Set-up files for the determination of homogenised elastic properties of bi-axial NCFs using periodic homogenisation of an RVE”. In: (Dec. 2022). URL: [https://data.4tu.nl/articles/software/Set-up\\_files\\_for\\_the\\_determination\\_of\\_homogenised\\_elastic\\_properties\\_of\\_bi-axial\\_NCFs\\_using\\_periodic\\_homogenisation\\_of\\_an\\_RVE/21777422](https://data.4tu.nl/articles/software/Set-up_files_for_the_determination_of_homogenised_elastic_properties_of_bi-axial_NCFs_using_periodic_homogenisation_of_an_RVE/21777422).
- [11] Stepan V Lomov. *Non-crimp fabric composites: manufacturing, properties and applications*. Elsevier, 2011.

- [12] AC Long et al. "Effects of fibre architecture on reinforcement fabric deformation". In: *Plastics, rubber and composites* 31.2 (2002), pp. 87–97.
- [13] Helga Krieger, Thomas Gries and Scott E Stapleton. "Design of Tailored non-Crimp Fabrics Based on stitching geometry". In: *Applied Composite Materials* 25.1 (2018), pp. 113–127.
- [14] A Gómez et al. "MECHANICAL BEHAVIOUR OF THERMOPLASTIC (PES, PBT) CARBON NANOFIBRE COMPOSITES". In: *ICCM*. Vol. 17. 2009.
- [15] Simon Pabst et al. "Seams and Bending in Cloth Simulation." In: *VRIPHYS* 382.1 (2008), pp. 24–41.
- [16] Oliver Döbrich et al. "Decoupling the bending behavior and the membrane properties of finite shell elements for a correct description of the mechanical behavior of textiles with a laminate formulation". In: *Journal of Industrial Textiles* 44.1 (2014), pp. 70–84.
- [17] G Creech. "Mesoscopic finite element modelling of non-crimp fabrics for drape and failure analyses". PhD thesis. Cranfield University, 2006.

# 5

## USING UNIT CELL PICK-UP POINT PATTERNS TO EVALUATE IN-PLANE SHEAR STRAINS

### 5.1. INTRODUCTION

PAST research on the automated handling of fabrics and the behaviour of these fabrics during handling has been approached in a variety of different ways. Early examples include the work published by Brown III *et al.* [1] who in 1990 set out to develop and validate a computer model that predicts the behaviour of a fabric during automated handling. Another example is the 1993 work by Eischen & Kim [2] who formulated a FEM model to simulate fabric drape, manipulation and contact for pick-and-place operations. The work by Larsen *et al.* [3] takes a similar 2D approach to these works by modeling the reinforcement as a catenary fixed at both ends. This model is used in the collision-free path planning for two cooperating robots that pick-up, move and place dry reinforcements. 2D approaches can only predict the general shape of the reinforcement as seen from the side. It is not possible to evaluate what is happening on the surface.

A different approach that does make it possible to evaluate the surface is to use 3D models to study the behaviour of reinforcements and fabrics. This includes the works by Do *et al.* [4] and Lin *et al.* [5] who developed a 3D deformation model for rectangular plies held using different boundary conditions under gravity loading. These works report predicted deflections but do not set tolerances or make any judgements about the observed behaviour. Krogh *et al.* [6] present and model a draping strategy where the prepreg is preshaped before draping it on the mould. The pick-up points in their FEM

---

Parts of this chapter have been published in Chantal M. de Zeeuw, Daniël M. J. Peeters, Otto K. Bergsma & Rinze Benedictus (2022) The effect of pick-up point location on fibre angle deviations in Non-Crimp Fabrics, Proceedings of the 20th European Conference on Composite Materials: Composites Meet Sustainability. Lausanne

model are adapted to the mould shape by variations in the z-displacement and in orientation. Simulated drape results are compared to experimental drape results. The in-plane shear strain required to achieve the desired shape is reported but no tolerances are set.

Pick-up points are an important feature in the pick-and-place process. They connect the reinforcement to the end effector at the end of the robot arm that is responsible for the manipulation during handling. In chapter 2 the different ways in which end effectors and pick-up points can operate are discussed. One factor in which the ply handling techniques can differ is the positioning of pick-up points over the surface of the reinforcement. The amount and positioning of pick-up points has a large influence on the behaviour of reinforcements during handling. Ragunathan & Karunamoorthy [7] and Lankalapalli & Eischen [8] used the criteria of minimization of strain energy to study optimal positioning of pick-up points while Ballier [9] aimed to minimize deflections. While the strain energy and deflections do give information about the behaviour of the reinforcement, they do not give an indication of possible reductions in quality of the reinforcement due to handling. A factor that does give important information about the quality of the reinforcement is the fiber angle deviations. The current research uses the tolerances established previously in Chapter 3 as a criterion for pick-up point positioning.

5

In the state of the art pick-up points are typically distributed in a consistent pattern across the surface of the reinforcement. The design process through which this pattern was established is however typically not discussed. The process of evaluating different pick-up point patterns to establish whether they work with a specific reinforcement can be (computationally) time consuming, especially when dealing with large reinforcements. Ideally, a single quick simulation should be able to predict whether a repeating pattern would work for a specific reinforcement. The current chapter wants to investigate whether this is possible. Therefore, the research question to be answered through this chapter is:

Can the design of optimal pick-up point locations on a large reinforcement be simplified through the use of a repeating pattern of pick-up points?

Section 5.2 starts by presenting the experimental work with gravity loaded reinforcements. The set-up for the experimental work is discussed and results are presented. The experimental work is used to obtain data for the validation of the numerical model and to get a better understanding of the behaviour of the NCF material during handling. Next, Section 5.3 presents the numerical work that has been carried out for gravity loaded reinforcements. First, the set up of a basic model and the validation of this model will be discussed. This is followed by a presentation of the additional set up work that has been done for the more elaborate models that will be used during the analysis. The section will finish with a presentation of the results for the numerical work. In Section 5.4 the experimental and numerical work is discussed. Finally, conclusions are given in Section 5.5.

## 5.2. EXPERIMENTAL WORK WITH GRAVITY LOADED REINFORCEMENTS

### 5.2.1. SET-UP FOR EXPERIMENTAL WORK

Basic experimental work is carried out on gravity loaded reinforcements. This section is used to get a better understanding of the behaviour of the NCF material during handling and for the validation of the numerical model that is discussed in section 5.3. The reinforcements that are used are the same type as presented in section 3.2.

During the experiments  $\pm 45^\circ$  NCFs of 300 x 300 mm and 550 x 550 mm are subjected to gravity while being suspended from a fixed pick-up point in each corner. These pick-up points are then attached to a frame. Figure 5.1 shows an illustration of this set-up. Figure 5.2 shows one of these tests.

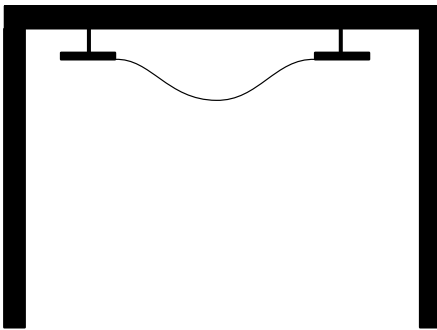


Figure 5.1: Illustration of the set-up for the experimental work with gravity loaded reinforcements



Figure 5.2: Frame with a 550 x 550 mm reinforcement suspended from the pick-up points

For these experiments the in-plane positioning of the pick-up points is accurate up to 0.5 mm. The pick-up points have a diameter of 46 mm and are attached to the reinforcements using double sided tape. From the moment the NCF is delivered on a roll to when the reinforcements are attached to the frame care is taken that they are always fully supported to avoid any preliminary in-plane shear or other deformations. Reinforcements are transported on top of an aluminum plate. This plate is then placed on a laboratory jack. The jack is moved up to connect the reinforcements to the pick-up points. Once the specimens are suspended from the frame the deflection of the reinforcement is obtained using a coordinate measuring machine. For this the laser line probe of the FARO®Quantum ScanArm is used. Using this scanarm and the laser line probe the coordinates of the whole surface of the reinforcement are measured from the bottom side of the reinforcement.

Two different testing configurations are used. This is done to determine whether an NCF can be treated as a single layer reinforcement or should be treated as multiple layers when selecting gripping strategies. In the first series the specimens are tested as is. For the second series a round piece of foil is adhered to the bottom side of the specimens at the location of the pick-up points using an silane modified polymer based adhesive.

Care is taken that the adhesive fully penetrates the fabric to ensure the two layers of the NCF are fixed together.

Specimen dimensions are chosen with a pick-up point diameter of 50 mm in mind. For the 300 x 300 mm specimens this would result in a distance between the centers of two pick-up points of 250 mm. For the 550 x 550 mm specimens this distance would be twice as large, 500 mm. The 50 mm diameter knobs that were ordered for the current work did however turn out to have a diameter of 46 mm on the side that is attached to the reinforcement.

### 5.2.2. RESULTS FOR EXPERIMENTAL WORK

Figure 5.3a shows a color map of the point cloud obtained for one of the 550 x 550 mm specimens from the first series. This first series did not include the adhesive bonding the layers together in the corners. The deflection pattern is not the one expected for  $\pm 45^\circ$  as the deformation in the  $+45^\circ$  differs from the deformation in the  $-45^\circ$  direction. In this figure the tows of the top layer lay in the direction indicated with a solid line. The tows of the bottom layer lay in the direction indicated with a dashed line.

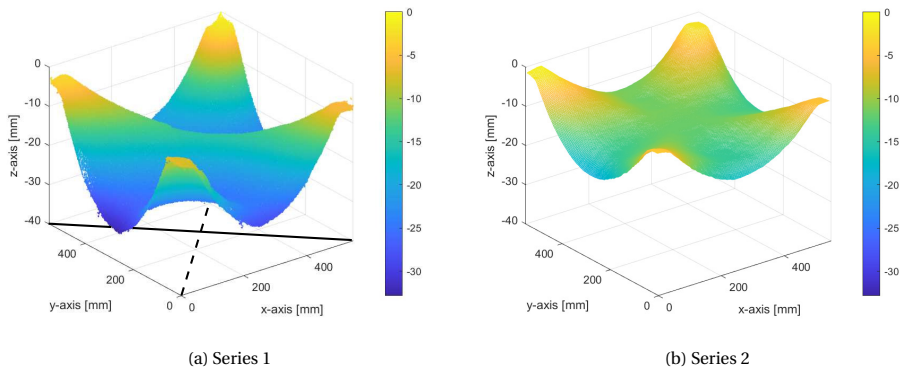


Figure 5.3: Point cloud with color map for one of the specimens from series 1 and series 2

Figure 5.3b shows the deformation result for one of the 550 x 550 mm specimens from the second series. The second series did include the adhesive gluing the layers together at the corners. For these specimens the deflection pattern is as expected for a  $\pm 45^\circ$  fabric. The pattern is symmetrical, with a lower deflection in the direction of the tows between two diagonal corners and a larger deflection between two adjacent corners. The series 2 specimens show a smaller deflection than the specimens without adhesive applied at the corners.

The results show that the method chosen to grip the reinforcement is important for the behavior during handling. For the first series as shown in Figure 5.3a the double sided tape results in a firm connection between the pick-up point and the upper layer of the reinforcement. Within the NCF the two layers are held together by the stitches. The tows in the bottom layer are however free to slide, the stitches do not prevent movement along the tows. With the tows of the bottom layer not being fixed they are unable to resist the

gravity load and slide, resulting in the observed pattern. For the second series both layers are fixed at the pick-up point, resulting in a symmetric deformation pattern as shown in Figure 5.3b.

The observed sliding behaviour has implications for the modeling of NCFs under gravity loading. The deformation pattern shown in Figure 5.3a can only be realized if the layers in the NCF are modeled separately and allowed to move individually. For the approach taken in the current work the NCF is modeled as a single layer, with the assumption that individual movement of the layers will not be significant. Therefore, the models used in this chapter will not be able to predict the behaviour shown in Figure 5.3a. These models will only be valid for scenarios where all layers are fixed at the pick-up point, resulting in results as shown in Figure 5.3b.

### 5.3. NUMERICAL WORK WITH GRAVITY LOADED REINFORCEMENTS

#### 5.3.1. BASIC MODEL SET-UP AND VALIDATION

The numerical models for the simulations of gravity loaded reinforcements are created using Abaqus/CAE 2021. Material properties are as defined in Table 5.1. The reinforcement is modeled as a shell using S4R elements. A gravity load of  $9.81 \text{ m/s}^2$  is applied to the whole model. The pick-up points are not modelled separately but are created using a partition on the surface of the shell. Boundary conditions are applied to these partitions. Figure 5.4 shows illustrations for the 300 x 300 mm model and the 550 x 550 mm model.

Table 5.1: Homogenised elastic properties as determined by the RVE and described in Chapter 4

$E_{11}$ [MPa]	$E_{22}$ [MPa]	$E_{33}$ [MPa]	$\mu_{12}$ [-]	$\mu_{13}$ [-]	$\mu_{23}$ [-]	$G_{12} / G_{21}$ [MPa]	$G_{13}$ [MPa]	$G_{23}$ [MPa]
196	196	0.16	0.5	0.5	0.5	2.39 / 0.53	0.24	0.24

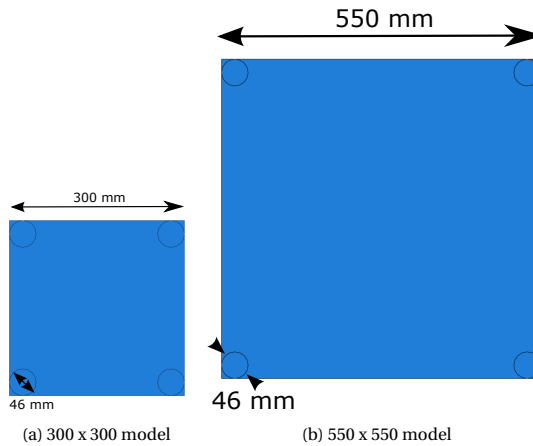


Figure 5.4: Illustrations of the 300 x 300 mm model and the 550 x 550 mm model

The numerical models are validated using the experimental work presented in Section 5.2. This validation is based on deformations and on in-plane shear strains. Numerically predicted deformations can be directly compared to deformations observed in the experimental work. For the validation based on in-plane shear strains the experimentally observed deformations first need to be converted to corresponding in-plane shear strains.

## DEFORMATION

The experimental results present two different series. The first series is with specimens as-is. For the second series the corners have been adhered to prevent the sublayers of the NCF to behave independently at the point of pick-up. The current model set-up will result in a prediction of the behaviour for the scenario of the second series. Therefore the initial validation step is done using the deformation results from the second series experiments. This is done by comparing the deflections along the diagonal of the numerical and experimental results.

5

In practice the pick-up points used during the numerical work showed some offsets in the vertical direction. Additionally, they were not perfectly parallel with the table the set-up was placed on. The exact orientation of the pick-up points during the experimental work is obtained using the point cloud of coordinates for the surface of the reinforcement. This orientation is then used as translation and rotational displacement boundary condition for the pick-up points in the numerical work.

For the numerical model data is collected along the diagonal. The displacement along the diagonal for the experimental results is obtained as follows: First the obtained point cloud of coordinates for the surface of the reinforcement is loaded in Matlab 2019b. This is then mapped to 300 x 300 mm and 550 x 550 mm grids with a mesh size of 2.5 mm. The values along the diagonal can then be obtained using the data file for this grid.

Figure 5.5 and 5.6 show this comparison for respectively the 300 x 300 mm specimens and the 550 x 550 mm specimens. Table 5.2 shows the values for the maximum deflection and the absolute error of the numerical result compared to the experimental values. Overall the specimens from the experimental work show great repeatability. However, specimen '300 x 300 #3' behaved obviously different. A possible explanation for this large deviation will be discussed below.

	Max deflection [mm]	Max predicted deflection [mm]	Error  [%]
300 x 300 #1	-4.66	-4.57	1.9
300 x 300 #2	-4.68	-4.57	2.4
300 x 300 #3	-3.25	-4.57	40.6
550 x 550 #1	-9.58	-11.64	21.5
550 x 550 #2	-10.4	-11.64	11.9
550 x 550 #3	-9.96	-11.64	16.9

Table 5.2: Experimental and predicted numerical deflection results and error. Error is calculated as a percentage of the experimental deflection

The results show that the numerical prediction for deflections along the diagonal is closer to reality for the 300 x 300 mm specimens than for the 550 x 550 mm specimens.

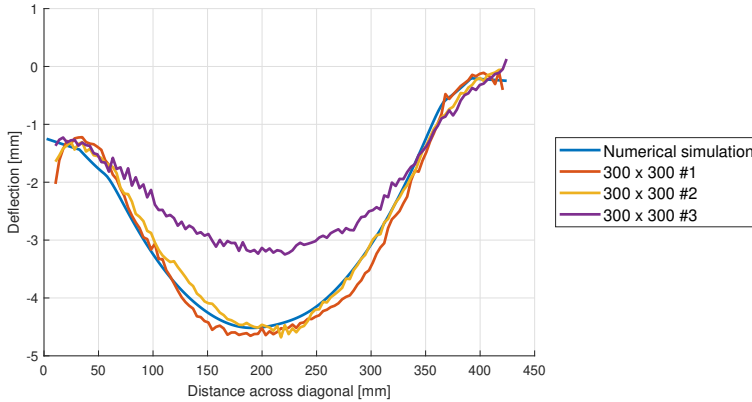


Figure 5.5: Comparison between numerical and experimental results for dimensions of 300x300 mm

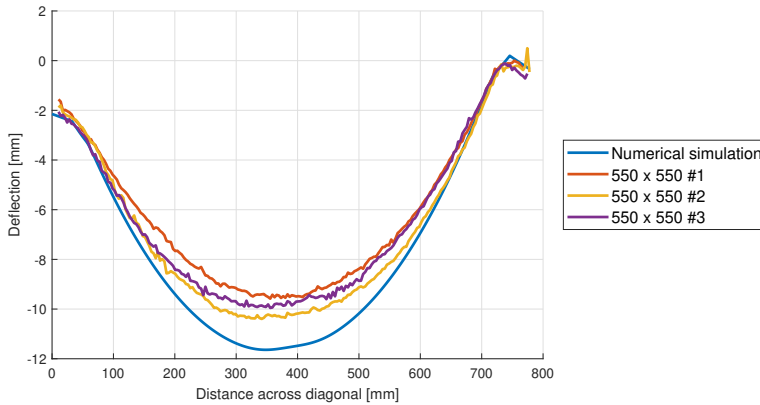
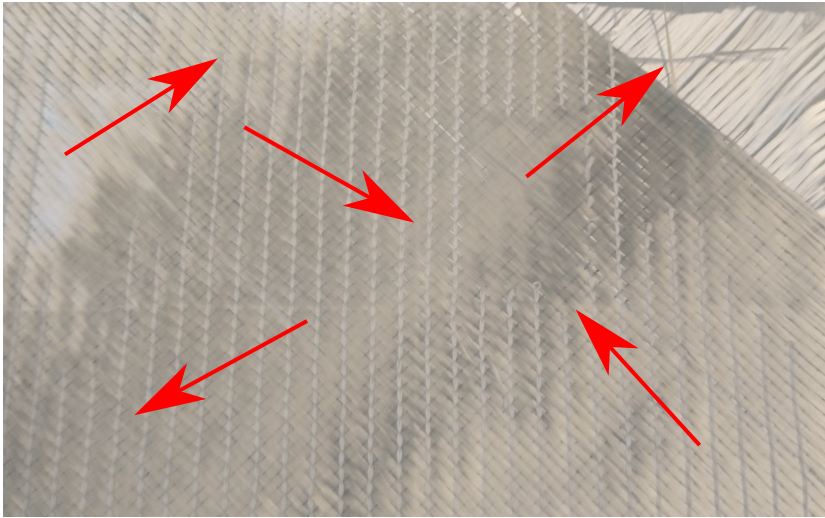
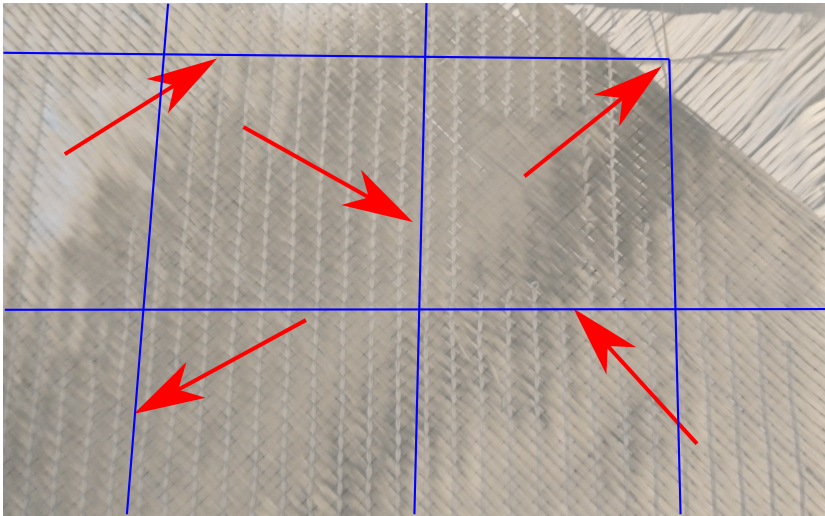


Figure 5.6: Comparison between numerical and experimental results for dimensions of 550x550 mm

For the two 300 x 300 mm specimens that do match the numerical results the average error for the predicted maximum deflection is 2.2% while for the 550 x 550 mm specimens the average error is 16.8%. An important difference between the experimental and numerical work is that the reinforcements used in the experimental work have stabilizing tows in the 0/90 direction every 45-55 mm. These stabilizing tows are not present in the numerical work. Figure 5.7 indicates the stabilizing yarns that are present in the fabric. To further investigate the influence of these stabilizing yarns on the deflections in the reinforcements the experimental and numerical results for deflections in the direction perpendicular to the reinforcement (U3) will be compared. To be able to make a direct comparison several additional steps are taken.



(a) Stabilizing yarns indicated with arrows



(b) Stabilizing yarns indicated with arrows and lines

Figure 5.7: Stabilizing yarns present in the NCF indicated with arrow and lines.

A script is written to convert the grid data for the coordinates of the reinforcement surface to an input file for Abaqus. When this input file is imported in Abaqus it will create a shell based model that uses the grid data as prescribed displacements. Running this model gives the results as presented in Figure 5.8 and 5.9. Legends have been adapted to ensure a direct comparison can be made between experimental and numerical results.

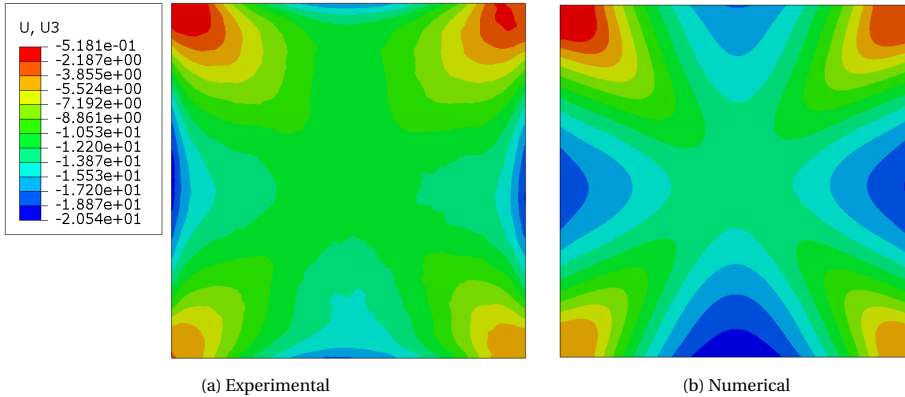


Figure 5.8: Deformations in U3 for reinforcements of 550 x 550 mm

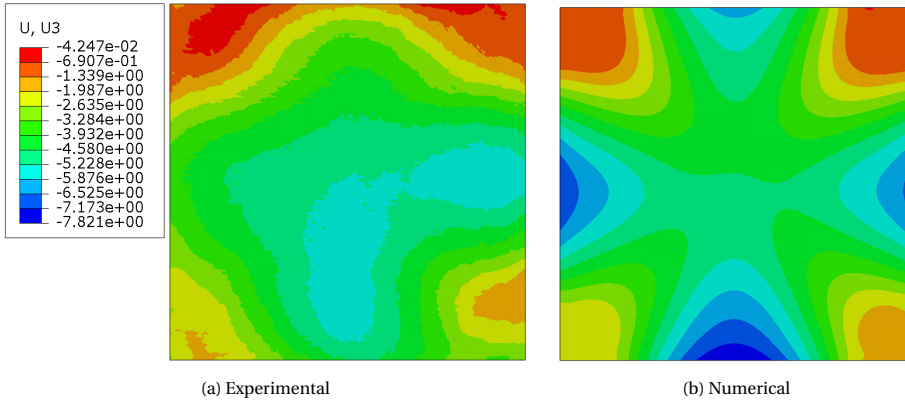


Figure 5.9: Deformations in U3 for reinforcements of 300 x 300 mm #1

Figure 5.8 and 5.9 show clear differences between the experimental and numerical results. These differences are attributed to the stabilizing yarns. With pick-up points with a diameter of 46 mm there is a high probability that the pick-up point area overlaps with stabilizing yarns. When these stabilizing yarns are fixed on both ends they will act as a support and prevent the reinforcement from deforming in the expected way.

For the 550 x 550 mm case the experimental deformation pattern shows similarities to the numerical deformation pattern. Deflections are roughly symmetric but due to the stabilizing yarns they can't extend as far towards the middle of the reinforcement as observed in the numerical case. Instead, the main deflections will be between the outer

edge and the stabilizing yarns. The experimental deformation pattern observed for the 300 x 300 mm case is however distinctly different from the numerically predicted deformations.

Figure 5.10 compares the deformations in U3 for three 300 x 300 mm specimens. All three specimens show different deformations patterns. This is attributed to the placement of the stabilizing yarns not being consistent across specimens, giving some specimens more freedom to deform than others. This non consistent placement of stabilizing yarns within the three specimens can also be used to explain the outlier result for the 300 x 300 #3 case as presented in Figure 5.5. For the 300 x 300 #1 and 300 x 300 #2 cases the stabilizing yarns are present in such a way that larger deformations are still possible. The stabilizing yarns in the 300 x 300 #3 specimen are theorized to be present in a position that is more restricting to the deflections of the NCF.

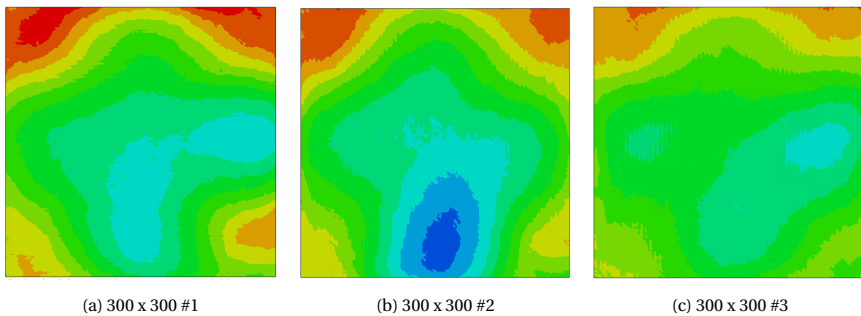


Figure 5.10: Comparison of the experimentally obtained deformations in U3 for reinforcements of 300 x 300 mm

### IN-PLANE SHEAR STRAINS

The second part of the validation is done using in-plane shear strains. Figures 5.11 and 5.12 show the experimental and numerical in-plane shear strains for reinforcements of respectively 550 x 550 mm and 300 x 300 mm. The range of the legend has been scaled so results can be directly compared. Overall, the numerical model is able to predict the pattern and magnitude of the in-plane shear strains. Differences between the experimental and numerical work can be explained by the stabilizing yarns present in the reinforcements.

Based on the numerical and experimental results for deflections and in-plane shear strains the model is considered to be validated for reinforcements with dimensions of 550 x 550 mm. Deviations from the observed experimental results can be explained by the presence of stabilization yarns. The model is able to give a conservative estimate for the deflections along the diagonal. Moreover, despite the stabilizing yarns not being present in the numerical model, the model is able to give a good prediction for the pattern and magnitude for in-plane shear strains.

For reinforcements with dimensions of 300 x 300 mm the model is able to give an accurate prediction for deflections along the diagonal. The maximum deflection along

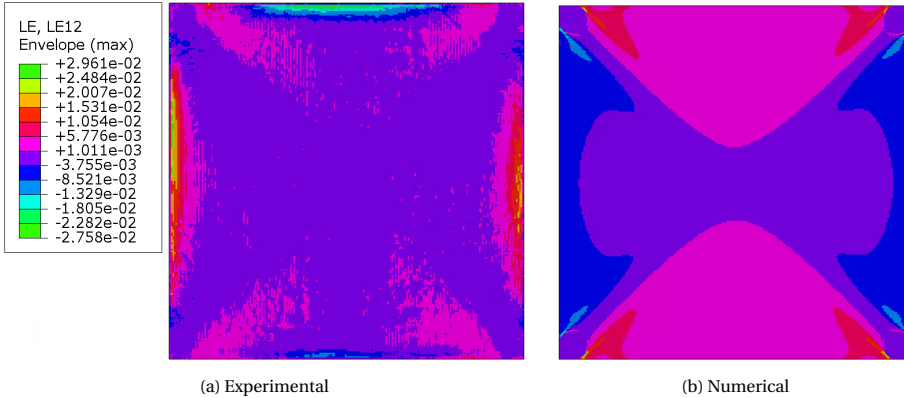


Figure 5.11: In-plane shear strains for reinforcements of 550 x 550 mm

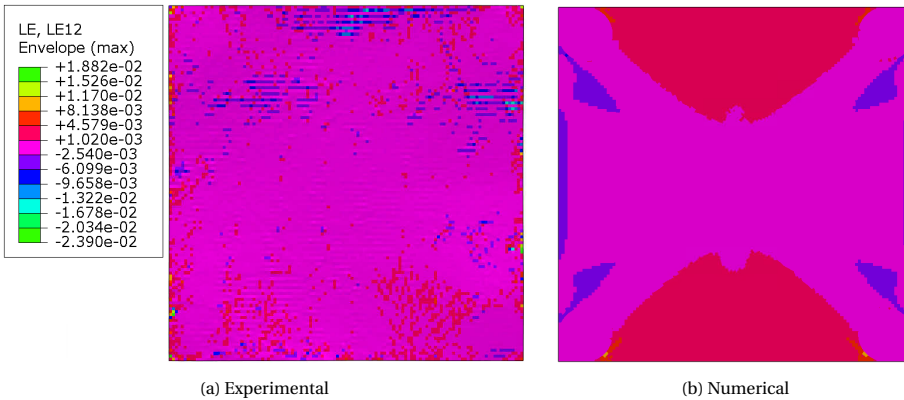


Figure 5.12: In-plane shear strains for reinforcements of 300 x 300 mm

the diagonal was predicted with an average error of only 2.2%. The overall predicted deformation pattern does however deviate significantly from their experimentally obtained counterparts. These differences can be explained by the stabilizing yarns that are not present in the numerical models. The effect of these stabilizing yarns on the observed behaviour is larger for the 300 x 300 mm case than for the 550 x 550 mm case due to the size difference. However, despite the stabilizing yarns the numerical prediction for the in-plane shear strains still gives a good prediction for the magnitude of the in-plane shear strains. Additionally, the general region of the red areas on the top and bottom and a rough indication of the locations of the purple on the left and right can be distinguished.

### 5.3.2. ADDITIONAL MODEL SET-UP FOR SIMULATIONS

#### LOCAL AND GLOBAL IN-PLANE SHEAR STRAINS

The goal of the current work is to study the influence of the positioning of the pick-up points, not to study the influence of the shape or size of the pick-up points. The interest lays in the effect of pick-up point location on the global in-plane shear strains, not on the local in-plane shear strains directly around the pick-up points. Trials have been carried out to determine the area outside which the shape of the pick-up point will no longer affect the in-plane shear strains. The in-plane shear strains in this inner area will be considered the local in-plane shear strains while the in-plane shear strains in the rest of the reinforcement are considered global in-plane shear strains.

Figure 5.13 shows the boundary conditions that have been used to trial the effect of pick-up point shape on in-plane shear strains. The highlighted area indicates the area that is restricted in all translational and rotational degrees of freedom. The two models share the same X- and Y-symmetry boundary conditions along the right and the bottom side. The models are meshed using S4R elements with a mesh size of 2.5 mm. The in-plane shear strains are recorded along three paths as indicated in Figure 5.14.

5

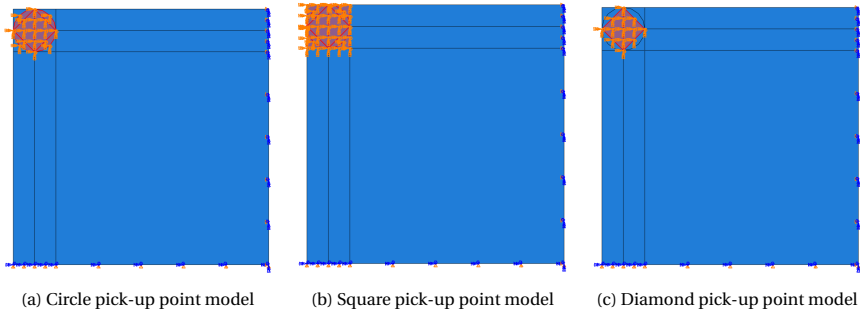


Figure 5.13: Boundary conditions for the circle pick-up point model, square pick-up point model and the diamond pick-up point model used to determine the end of the region of local in-plane shear strains

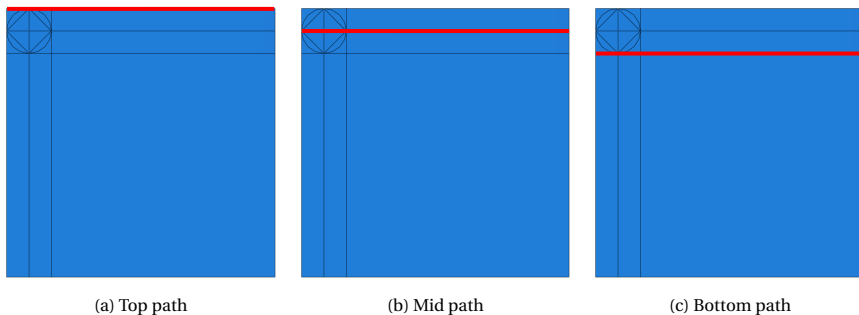


Figure 5.14: Three paths along which the in-plane shear strains are recorded determine the end of the region of local in-plane shear strains

Figure 5.15 shows the in-plane shear strains that were found for the scenario's shown in Figure 5.13 along the paths shown in Figure 5.14. These results show that it is indeed possible to define an area outside which the shape of the pick-up point does not affect the in-plane shear strains. Based on a criteria of the difference between the in-plane shear strains being less than 10% of the maximum value a distance of 115 mm along these three paths is used. This results in a definition for the local in-plane shear strain areas as shown in Figure 5.16.

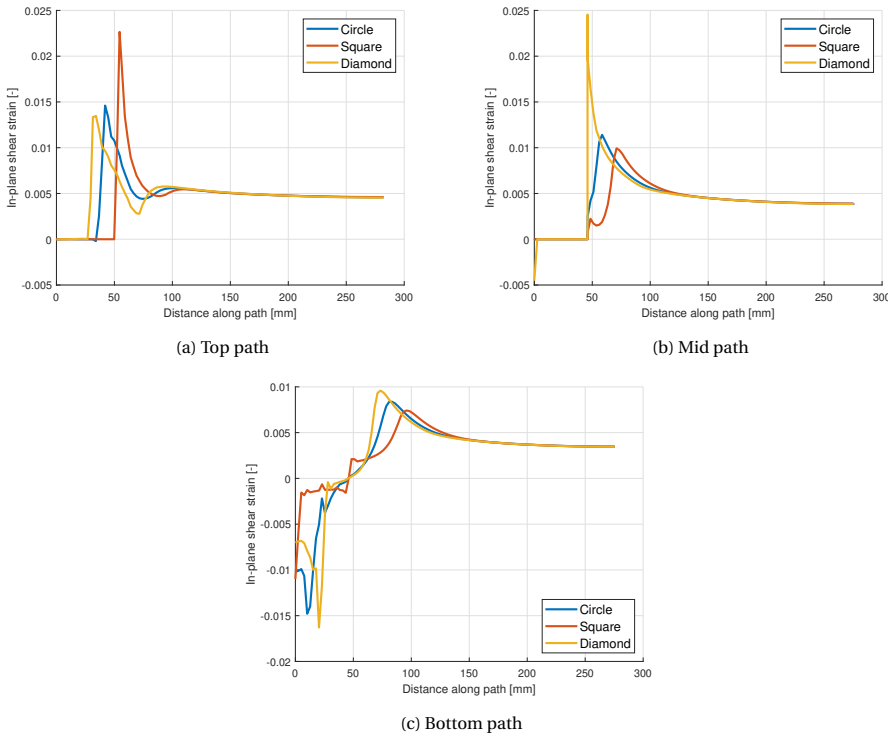


Figure 5.15: In-plane shear strains for the scenario's presented in Figure 5.13 for the paths presented in Figure 5.14

The current work aims to investigate the possibility of using a unit cell square pick-up point pattern to predict the effect of pick-up point positioning on in-plane shear strains and resulting fibre angle deviations. For the current work pick-up point patterns are always square and reinforcements are rectangular. For these conditions six different boundary condition scenario's are possible depending on the location of the pattern instance in the reinforcement. Edges can either be free or they can be connected to an adjacent pattern. Figure 5.17 illustrates the different boundary condition scenario's.

Three different models are used to study the influence of the different boundary conditions presented in Figure 5.17 on the in-plane shear strains. The first model is a basic 550 x 550 mm square with four pick-up points. The second is 550 x 1558 mm with eight

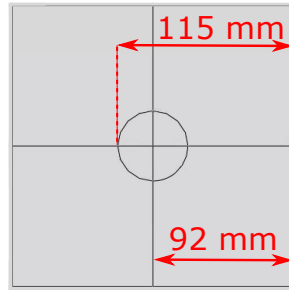


Figure 5.16: Illustration for the definition of the local in-plane shear strain area as will be used throughout this work.

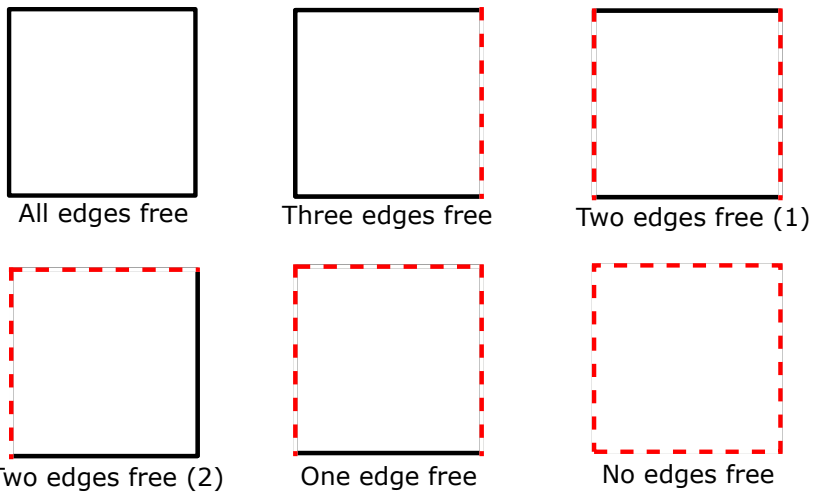


Figure 5.17: Illustration of the different boundary condition scenarios for pick-up point patterns. Black edges mean the edge is free, red edges mean the edge is connected to at least one additional unit cell.

pick-up points to simulate three repeats of the pick-up point pattern in a row. Finally, the third model is 1558 x 1558 mm with 16 pick-up points to simulate three repeats in the horizontal and three in the vertical direction. Then finally, a unit-cell pick-up point pattern model will be used that should be able to predict the worst case in-plane shear strain behaviour that will result from the different possible boundary conditions. For all these scenarios the distance between the centre of the pick-up points is 504 mm.

Figure 5.18 presents the unit cell pick-up point pattern model. While the whole surface is used during the analysis, the green areas in the figures indicate the areas that are observed for the current work. Different section assignments have been used to simplify the inclusion and exclusion of areas during the analysis of the results. Figures 5.19 - 5.21 illustrate the models that are used to determine the in-plane shear strains that will occur under the boundary conditions as presented in Figure 5.17.

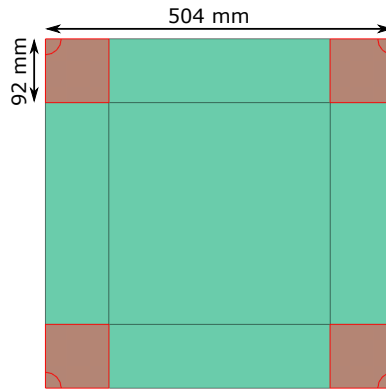


Figure 5.18: Illustration of the dimensions for the unit cell pick-up point pattern model. Areas excluded from the results are highlighted in red.

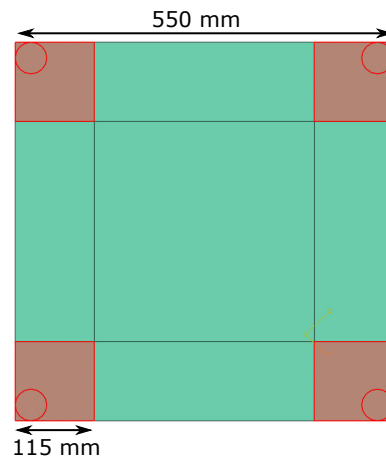


Figure 5.19: Illustration of the dimensions for the 550 x 550 mm model that is used to observe the in-plane shear strains under the boundary condition of all edges free. Areas excluded from the results are highlighted in red.

Figure 5.19 shows the model that is used to obtain results for the 'all edges free' boundary condition. Figure 5.20 shows the model that is used to obtain results for the 'Three edges free' and 'Two edges free (1)' boundary condition. Finally, figure 5.21 shows the model that is used to obtain results for the 'Two edges free (2)', 'One edge free' and 'No edges free' boundary conditions.

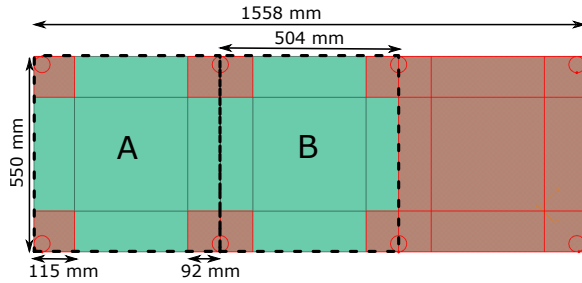


Figure 5.20: Illustration of the dimensions for the 550 x 1558 mm model that is used to observe the in-plane shear strains under the boundary conditions of (A) three edges free and (B) two edges free (1). Areas excluded from the results are highlighted in red.

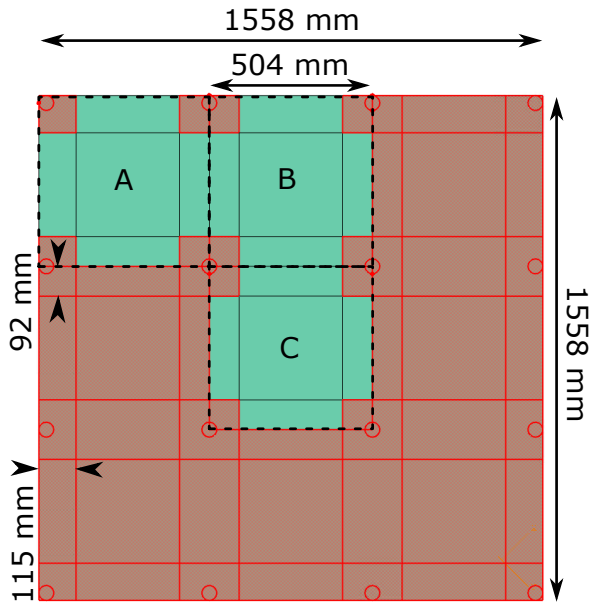


Figure 5.21: Illustration of the dimensions for the 1558 x 1558 mm model that is used to observe the in-plane shear strains under the boundary conditions of (A) two edges free (2), (B) one edge free and (C) no edges free. Areas excluded from the results are highlighted in red.

5

### 5.3.3. RESULTS FOR NUMERICAL WORK

Figure 5.22 shows the results from the simulations performed with the three models as presented in Figures 5.19 - 5.21. These results are plotted on undeformed shapes. Figure 5.26 shows the corresponding deflection results plotted on deformed shapes with a scale factor of 10. The simulations are performed with the whole models, then predefined sections are used to present the in-plane shear strains for a specific repeat of the pick-up point pattern.

The results in Figure 5.22 show that 'Two edges free (2)' is the worst case boundary condition and would lead to a conservative maximum size of the pick-up point pattern. This worst case corresponds to the four corners of the 1558 x 1558 mm model shown in Figure 5.21. A unit cell as presented in Figure 5.18 is used to determine whether it is possible to use a unit cell pick-up point pattern model to predict these worst case in-plane shear strains. Figure 5.23 presents the boundary conditions that are used to represent the scenario of 'Two edges free (2)'. Pick-up points are restricted in all degrees of freedom and symmetry boundary conditions are used along the left and bottom edge.

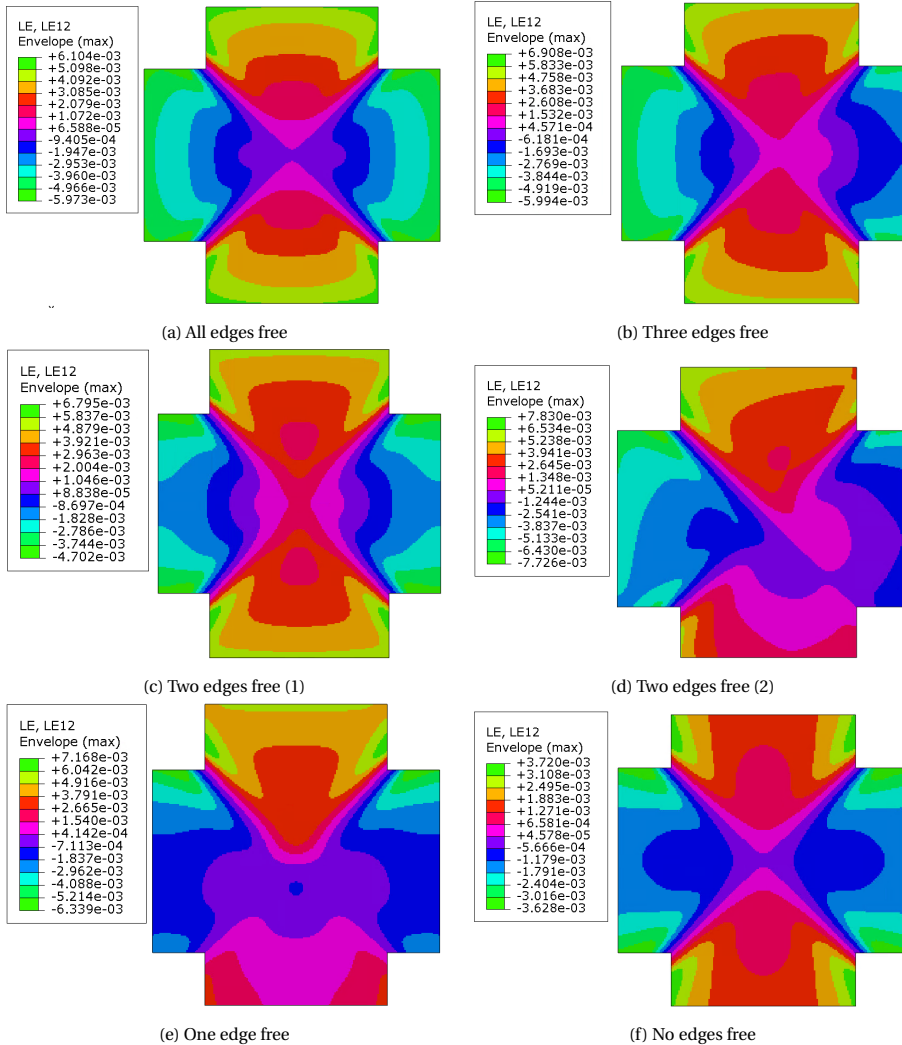


Figure 5.22: Numerical in-plane shear strain results for the different boundary conditions as defined in Figure 5.17 simulated using the models presented in Figures 5.19 - 5.21. Contours plotted on undeformed shapes.

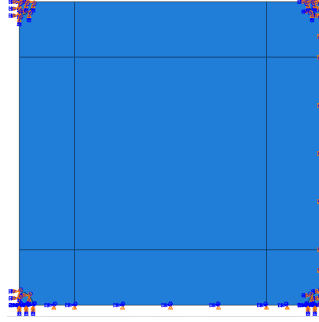


Figure 5.23: Boundary conditions for the unit cell pick-up point pattern model to simulate the worst case for in-plane shear strains. Pick-up points restricted in all degrees of freedom and symmetry boundary conditions along the left and bottom edge.

5

Figure 5.24 compares the results for the unit cell pick-up point pattern model to the results for the top left corner of the 1558 x 1558 mm model. To ensure repeatability the unit cell model only models a quarter of the pick-up point. Because of this the results from the top left of the 1558 x 1558 mm as presented in Figure 5.22 have an additional narrow edge of 23 mm on the top and the left. For ease of comparison this narrow edge is excluded in Figure 5.24. The results predicted by the unit cell pick-up point pattern model in Figure 5.24a are a match for the results predicted by the top left of the 1558 x 1558 mm model in Figure 5.24b. The results in Figure 5.24b are slightly different than previously presented in 5.22d. This difference is attributed to the additional partition required to easily remove the narrow edge section in the results resulting in a slightly different mesh. Figure 5.25 illustrates the difference between the model used to obtain the results in Figure 5.22 and the results in Figure 5.24b.

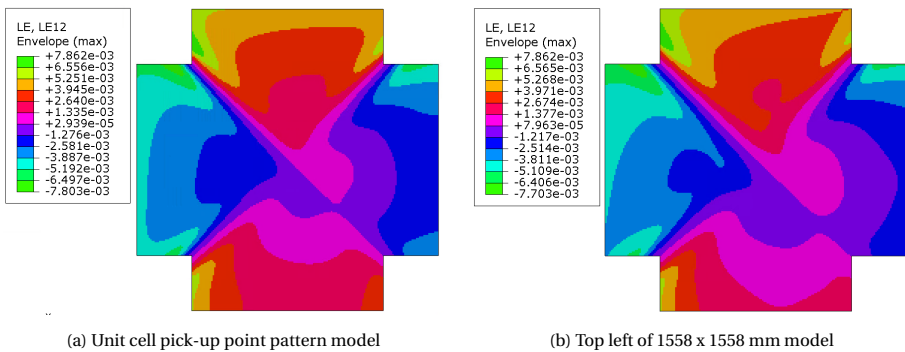
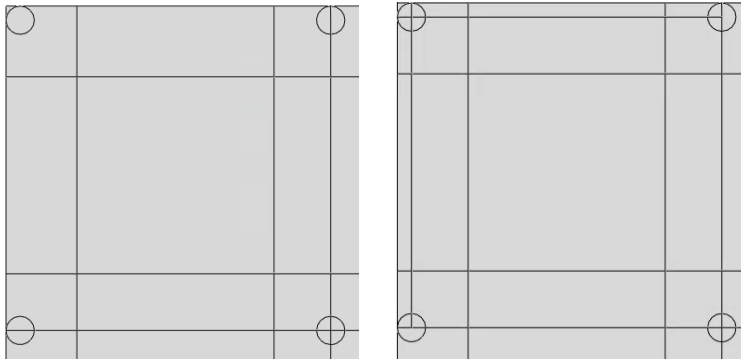


Figure 5.24: Numerical in-plane shear strain results for 'two edges free (2)' boundary condition as defined in Figure 5.17. On the left are the numerical results for the unit cell model using boundary conditions as presented in Figure 5.23 and on the right the results determined using a 1558 x 1558 mm model as shown in Figure 5.21. The contours are plotted on undeformed shapes.



(a) Model as used to obtain the results presented in Figure 5.22 (b) Model as used to obtain the results presented in Figure 5.24b

Figure 5.25: Comparison between the partitions in the model used to predict the results as presented in Figure 5.22 and the results as presented in Figure 5.24b.

Figure 5.26 shows the deformation results for the different boundary conditions. These results are plotted on deformed shapes with a scale factor of 10. This scale factor is applied to make the response of the edges to the deformations more visible. These results show that while the boundary condition case with the lowest in-plane shear strains also has the lowest deflections, the boundary condition with the highest in-plane shear strains does not correspond to the highest deflections. All edges free, which is on the lower end in terms of in-plane shear strains has the highest deflections. These observations can be explained by the way the surrounding fabric affects the behaviour of an instance of the pick-up point pattern. In figure 5.26a with all edges free the edges curve inward. This behaviour is much less obvious in figure 5.26f with no edges free. The surrounding fabric in the case with no edges free restricts the edges from translating inward. When the edges are restricted from going inward the maximum deflection of the reinforcement due to the gravity load is reduced. This does however not automatically mean that the in-plane shear strains will also be reduced. If there is at least one edge free, the in-plane shear strains will be larger than for the case with all edges free or no edges free. The edges that are not free are restricted in their movement by the surrounding reinforcement. A free edge will move down and inwards, this also results in a pull on the other edges. When other edges are free the reinforcement can deform more globally. With restricted edges these deformations need to come from different deformation mechanisms, which includes the in-plane shearing of the fabric.

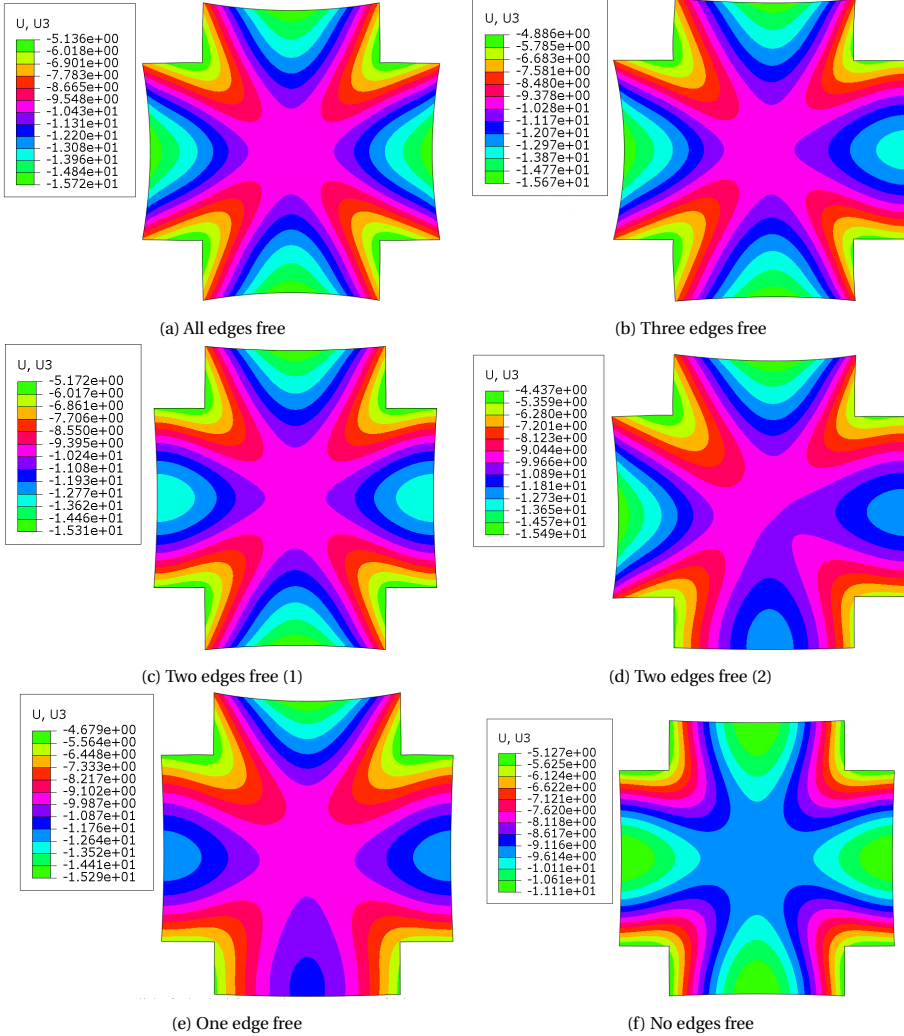


Figure 5.26: Numerical displacement results for the different boundary conditions as defined in Figure 5.17 simulated using the models presented in Figures 5.19 - 5.21. Contours plotted on deformed shapes with a scalefactor of 10.

## 5.4. DISCUSSION

### 5.4.1. EXPERIMENTAL WORK WITH GRAVITY LOADED REINFORCEMENTS

The experimental results in section 5.2 showed that the sublayers in an NCF will be free to move if they are not restricted at the pick-up points. This resulted in an unexpected deformation pattern and higher deformations than for the case where the NCF was restricted at the pick-up points. These results demonstrate that when handling a dry non-crimp fabric it is important that both layers are supported to ensure a predictable deformation pattern and less deformations. The stitches of the NCF used in this work could not solely be relied on to ensure the bottom layer stays in place. The current stitching is non-structural: it does prevent separation of the the plies but it does not create a 3D reinforcement. Using structural stitching would create a 3D reinforcement but would not mitigate the observed sliding of the bottom layer. For structural stitching yarns materials such as E-glass [10], aramide [11] or carbon [12] have been used with varying stitching patterns. While these structural yarns do for example greatly improve the out-of-plane stiffness and delamination resistance [12] they do not fully restrict movement of the tows relative to each other. Restricting this movement would lead to a reduction in the ability of the reinforcement to conform to the moulds they are placed in or on. Measures to prevent the behaviour that results from the bottom layer being unsupported will therefore either need to be applied locally at the point of pick-up or the gripping mechanism will need to be able to support all the layers.

The idea of gripping points and external fixing strategies has previously been discussed in Section 2.4.2. When unit cell pick-up point patterns are used pick-up points will typically also be present in the product material, not only in the excess material. Therefore, an important criteria when choosing an external fixing strategy is that it does not disturb the fabric in a way that affects quality of the reinforcement. A drawback of external fixing strategies is that their application results in extra steps and more risks for complications. The ideal solution would therefore be a gripping technology that can reliably grip all layers without external mechanisms. Of the various gripping strategies discussed in chapter 2, needle, clamping or pinching grippers are the only one that can reliably hold multiple layers. Clamping grippers will only be practical if all gripping points are along the edges. Needle grippers and pinching grippers can pick the reinforcement up at any desired location. Pinching grippers introduce folds in the material, which is not desirable in reinforcements. Needle grippers will typically work by using multiple needles, thereby holding the reinforcement at multiple points at each pick-up point. Needle grippers are considered to be the best choice for handling multiple layers but it is expected that they will not fully mitigate the undesired deflection behaviour resulting from unsupported layers in a bi-axial NCF.

While the current work does not focus on deflections, they are important to consider when designing the pick-and-place process. Care should always be taken that there is enough clearance between the reinforcement and any surfaces. Additionally, with a larger deflection the effect of in-plane movement and accelerations on the fiber angle deviations could be more severe.

### 5.4.2. NUMERICAL WORK WITH GRAVITY LOADED REINFORCEMENTS

Six different boundary conditions have been defined that can occur in pick-up point patterns (Figure 5.17). Using these boundary conditions it has been shown that it is indeed possible to predict the worst case scenario in terms of in-plane shear strains using a unit cell square pick-up point pattern.

Round, square and diamond shaped pick-up points have been used to study the influence of pick-up point shape on the in-plane shear strains. The results from these analyses are used to divide in-plane shear strains in a local and a global component. The local in-plane shear strains are influenced by the shape of the pick-up point while the global in-plane shear strains are not. The different models have been partitioned into various sections to exclude the regions with local in-plane shear strains in the post-processing of results. The reason for this is that the current work wants to focus on the influence of the location of the pick-up points on the global behaviour of the reinforcement, not on the local behaviour that is heavily affected by pick-up point shape. There are many more possibilities for pick-up point shape than the shapes considered in this work. For the current work these three shapes have been chosen to get extremes in terms of sharp edges in the pick-up point. Since the size of a pick-up point will also have an effect on the in-plane shear strains in the surrounding region the areas of the different pick-up point shapes are kept as similar as possible. In real life the reinforcements will experience the local in-plane shear strains and they will need to be taken into account in the design process for pick-and-place operations.

The numerical work is validated using two different criteria: deflections and in-plane shear strains.

The numerical model gives a better prediction for deflections along the diagonal for the 300 x 300 mm case than for the 550 x 550 mm case. For the 550 x 550 mm case the numerical model overestimates the deflection. For practical reasons it is more desirable to overestimate the deflections than to underestimate them. This does for example ensure that there will always be enough clearance between the reinforcement and other surfaces. However, the prediction for the overall deformation pattern was closer for the 550 x 550 mm case than for the 300 x 300 mm case.

The model presented by Do *et al.* [4] calculates the deformed profile of rectangular composite plies. For their validation the deflection of 300 x 300 mm plies of various carbon and glass fabrics is compared to the predicted maximum deflection. Depending on the material their error varied between 5.7-9.6 % for the smallest grid size of 2.5 x 2.5 mm. Lin *et al.* [5] compare maximum deflections calculated using their energy based 3D mathematical model for the deformation of woven reinforcements with a FEM simulation. Sample sizes of 200 x 200 mm, 300 x 300 mm and 400 x 400 mm are used with boundary conditions of 'four corners clamped', 'two edges clamped' and 'four edges clamped'. For the case of 'four corners clamped' errors between the two are 1.86 - 4.6 %.

The current numerical model has been able to predict the maximum deflection along the diagonal for 300 x 300 mm with an accuracy of 2.2%. Compared to the work by Do *et al.* [4], the model appears to give a better prediction for plies of these dimensions. Additionally, the accuracy is comparable to Lin *et al.* [5] who compared their mathemat-

ical model with FEM simulations. The 550 x 550 mm case was predicted with an average error of 16.7%. These results can not be compared to the results of either Do *et al.* [4] or Lin *et al.* [5] since it is not known how well their models would perform on a larger scale.

The overestimation observed for the 550 x 550 mm case is attributed to the way the material is modeled. The numerical model does not consider individual tows and stitches but uses homogenized elastic properties. These homogenized elastic properties are obtained as described in chapter 4. The load cases that are used to determine homogenized elastic properties are quite basic. A bi-axial NCF does however have a variety of mesoscopic fabric deformation mechanisms [13]. These different mechanisms and their coupling will not all be caught through application of these basic loading conditions, as has previously been discussed in chapter 4. The experimental work shows that the actual mesoscopic fabric deformation mechanisms give the reinforcement a larger resistance to deflections. It is suggested that these fabric deformation mechanisms and couplings do not scale linearly as the size of the reinforcement is increased, resulting in a larger deviation for the 550 x 550 mm case than for the 300 x 300 mm case.

The reinforcements used in the experimental work have stabilizing yarns in the 0/90 direction every 45-55 mm. These stabilizing yarns are not included in the numerical work. The experimental work indicated that there is a large chance of two adjacent pick-up points picking up these stabilizing yarns. The stabilizing yarns stabilized the deflections for the experimental work. The deflections along the diagonals are the least affected by the presence of these yarns. This explains why the numerical work was still able to give a reasonable prediction for the deflections along the diagonal. The numerical work gives a conservative prediction for deflections in a reinforcement with stabilizing yarns present.

The stabilizing yarns also affect the in-plane shear behaviour of the reinforcements. In general the presence of these yarns has stabilized the deformations and thus also the in-plane shear strains. The stabilizing yarns did however also result in high experimentally observed in-plane shear strains along the edges. In general the numerical model for the 550 x 550 mm case gave a good prediction for the pattern and magnitude of the in-plane shear strains. The model is unable to predict the high in-plane shear strains that occur along the edges but gives a conservative prediction for the overall in-plane shear strains.

Six different boundary conditions have been defined that represent all positions an instance of the pick-up point pattern can have in the reinforcement. Three different models have been used to simulate the behaviour of the pick-up point pattern at different locations. From this it followed that 'two edges free (2)' is the worst case scenario in terms of in-plane shear for reinforcements subjected to gravity loading. In this boundary condition case two perpendicular edges are free and two perpendicular edges are connected to the rest of the reinforcement. The scenario with the lowest in-plane shear strains is the scenario with no edges free. When handling very large reinforcements this will be the scenario at play for the majority of the surface.

The scenario with no edges free has the lowest in-plane shear strains and the lowest deflections. This corresponds to a region in a reinforcement that is fully surrounded by other repetitions of the pick-up point pattern. The surrounding fabric prevents the reinforcement from exhibiting larger in-plane shear strains and deflections. For these parts

of the reinforcement it would therefore be possible to increase the distance between pick-up points without the risk of exceeding tolerances. Limiting the amount of pick-up points has several advantages. Predicted in-plane shear strains are highest around the pick-up points. Additionally, the gripping mechanism used by the pick-up point will generally also have a risk of damaging the fabric material. Reducing the amount of pick-up points will reduce the area of the reinforcement directly affected these factors.

## 5.5. CONCLUSIONS

The research question the current chapter set out to answer is:

Can the design of optimal pick-up point locations on a large reinforcement be simplified through the use of a repeating pattern of pick-up points?

The current chapter showed that it is possible to predict the suitability of a repeating pick-up point pattern for a specific reinforcement in terms of in-plane shear strains using a single quick simulation.

5

The experimental work presented in the chapter confirmed that bi-axial NCFs need to be treated as multiple layers when depending on the gripping mechanism for the pick-up points. The tows in layers that are not supported will be free to slide leading to unexpected deformations. Needle grippers are expected to be the best current available choice handling multiple layers. This gripping mechanism is able to pick-up multiple layers without external fixing mechanisms, can be used at any desired location on the surface of the reinforcement and does not introduce undesired folds. It is however expected that needle grippers cannot fully mitigate the undesired sliding behaviour. Future research on novel gripping techniques that can fully support all layers is recommended.

In the current set-up only the global in-plane shear strains are taken into account since the focus was on the location of the pick-up points and not on the influence of the type of pick-up point. However, reinforcements will also experience these local in-plane shear strains that are highly dependent on the specific pick-up point. It is recommended that the effect of specific gripping strategies on in-plane shear strains is studied in future work.

The numerical work confirms that deflections/deformations and in-plane shear strains are not coupled. Higher deflections do not necessarily result in higher in-plane shear strains. To get an indication of the in-plane shear strains and the corresponding fiber angle deviations the focus needs to be on the in-plane shear strains and not on the deflections.

The research goal for this thesis as formulated in Chapter 2 is:

The development of a framework for prediction and prevention of fiber angle deviations due to in-plane shear during handling of large-sized bi-axial NCFs

The current chapter has contributed to this research goal by presenting a model that can be used to predict in-plane shear induced fiber angle deviations for different pick-up point configurations. The use of the appropriate boundary conditions and a unit cell

pick-up point pattern allow for rapid evaluation, even for large reinforcements, as long as a repeating pattern is used to handle the reinforcement. The current work can however not be directly implemented in industry. Chapter 6 will discuss the current work and explore some of the additional steps that could be taken for industrial implementation of this work.



# BIBLIOGRAPHY

- [1] PR Brown III, DR Buchanan and TG Clapp. "Large-deflexion bending of woven fabric for automated material-handling". In: *Journal of the Textile Institute* 81.1 (1990), pp. 1–14.
- [2] JW Eischen and YG Kim. "Optimization of fabric manipulation during pick/place operations". In: *International Journal of Clothing Science and Technology* (1993).
- [3] Lars Larsen et al. "Full automatic path planning of cooperating robots in industrial applications". In: *2017 13th IEEE Conference on Automation Science and Engineering (CASE)*. IEEE. 2017, pp. 523–530.
- [4] Duc Do, Sabu John and I Herszberg. "3D deformation models for the automated manufacture of composite components". In: *Composites Part A: Applied Science and Manufacturing* 37.9 (2006), pp. 1377–1389.
- [5] Hua Lin et al. "3D mathematical modelling for robotic pick up of textile composites". In: *Composites Part B: Engineering* 40.8 (2009), pp. 705–713.
- [6] Christian Krogh, Jens A Glud and Johnny Jakobsen. "Modeling the robotic manipulation of woven carbon fiber prepreg plies onto double curved molds: A path-dependent problem". In: *Journal of Composite Materials* 53.15 (2019), pp. 2149–2164.
- [7] S Ragnathan and L Karunamoorthy. "Genetic algorithm-based optimal locations for handling fabric materials in garment automation". In: *International Journal of Robotics and Automation* 21.4 (2006), pp. 288–294.
- [8] Shrinivas Lankalapalli and Jeffrey W Eischen. "Optimal pick-up locations for transport and handling of limp materials: Part II: Two-dimensional parts". In: *Textile research journal* 73.10 (2003), pp. 867–874.
- [9] Fabian Johannes Ballier. *Systematic gripper arrangement for a handling device in lightweight production processes*. Shaker Verlag, 2019.
- [10] N Himmel and H Heß. "Mechanical properties of structurally stitched non-crimp fabric composites". In: *Non-Crimp Fabric Composites*. Elsevier, 2011, pp. 335–359.
- [11] Vitaly Koissin et al. "On Surface Fibre-Free Zones and Irregularity of Piercing Pattern in Structurally Stitched NCF Preforms". In: *Advanced composites letters* 15.3 (2006), p. 096369350601500302.
- [12] V Koissin et al. "Structurally stitched NCF preforms: quasi-static response". In: *Composites science and technology* 69.15-16 (2009), pp. 2701–2710.
- [13] Gavin Creech and Anthony K Pickett. "Meso-modelling of non-crimp fabric composites for coupled drape and failure analysis". In: *Journal of materials science* 41.20 (2006), pp. 6725–6736.



# 6

## GUIDELINES FOR MOVING TOWARDS INDUSTRIAL IMPLEMENTATION

**T**HE research as presented in the previous chapters cannot be directly implemented in industry as is. This chapter will explore some of the possibilities generated by this work and some guidelines for industrial implementation.

The current research not only generates new opportunities in the design of pick-and-place processes but also for implementation of industry 4.0 through the smart factory concept. In a smart factory, machinery and production systems are fully connected and continuously share data [1]. This continuous monitoring and interconnectedness contributes to product quality and consistency.

The current research project will be discussed and recommendations will be given based on the three research chapters. First, setting tolerances for in-plane shear strain induced fiber angle deviations will be discussed. This is followed by mesoscopic modeling for the determination of homogenised elastic properties. The chapter will finish with the use of unit cell pick-up point patterns to evaluate in-plane shear strains.

### **6.1. SETTING TOLERANCES FOR IN-PLANE SHEAR STRAIN INDUCED FIBER ANGLE DEVIATIONS**

Chapter 3 showed that even small deviations in the fiber angle will already have a permanent effect on the behaviour of the reinforcement. Therefore, the prevention of undesired deviations should already start before the pick-and-place process begins. Care needs to be taken at every phase of the manufacturing process. This does also include the phase of preparing the reinforcement to be cut at a cutting table for example.

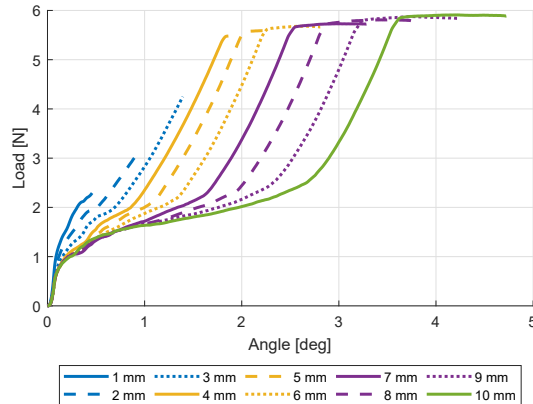


Figure 6.1: Load-displacement graph for compression 1 specimens for displacements of 1 - 10 mm

## 6

Two loadcases were considered for the biaxial NCF used in the current work: stitches loaded in tension and stitches loaded in compression. The behaviour of the NCF was shown to be more affected by previous loading for the loading direction with stitches loaded in compression than for stitches loaded in tension. Tolerances for fiber angle deviations should always be set based on the loading direction that is most affected by previous loading. If reinforcements show a load-displacement graph with two different stiffnesses, as was observed for the compression specimens in the current work (see Figure 6.1), the initial lower stiffness region should generally be used to set tolerances.

The current work chose to set tolerances based on how the reinforcement would behave after it was unloaded and loaded again. The strategy for determining tolerances is not fixed and chosen tolerances might vary depending on the application and industry. When setting tolerances allowable material property deviations need to be kept in mind. This does for example mean that for a primary structure the deviations will be tighter than for a secondary structure. It could potentially be possible to set guidelines for the tolerances for fiber angle deviations/in plane shear strain based on a database for a wide variety of specimens, thereby reducing the need for experimental work. More testing is required to research the possibility of such guidelines.

As long as the in-plane shear strains can be monitored it will be possible to monitor the fiber angle deviations. Implementation of the current research in a smart factory setting would require the placement of sensors capable of monitoring in-plane shear strains in the end-effectors handling the reinforcements. Different approaches could be taken when placing these sensors. One strategy would be to place sensors in such a way that the whole surface is monitored. Alternatively, placements could be focused on locations with the highest predicted in-plane shear strains. Continuous monitoring of the in-plane shear strains could for example make it possible for the pick-and-place process to adapt when in-plane shear strains are at risk for exceeding tolerances. These adaptations could

work in various ways. Fiber angle deviations could for example possibly be decreased due to translations of the pick-up points, decreasing the speed of the handling or by placing the reinforcement down and picking it up using a different handling strategy.

## **6.2. MESOSCOPIC MODELING FOR THE DETERMINATION OF HOMOGENISED ELASTIC PROPERTIES**

### **6.2.1. ELASTIC PROPERTIES FOR BI-AXIAL NCFs**

The current work uses an RVE to determine homogenised elastic properties. While this approach gave the desired result for the current research it might not always be the recommended choice for an industrial application. This section will discuss the current strategy for determining elastic properties and how it could be adapted to be more suitable for use in industry.

The aim for this work was to have all elastic properties rooted in engineering and physics. Preferably, no arbitrary correction factors should have to be applied to obtain the desired result. However, modeling all the tows and stitches on the full scale model would result in a model that is very computationally expensive. For the most part the aim to have all elastic properties rooted in engineering and physics has succeeded. However, the approximation for the elastic properties for the tows as determined in section 4.3 using the flexural rigidity test and linear Euler-Bernoulli beam theory resulted in an overestimation for the actual values. This is explained by the behaviour of the tows not conforming to the bending behaviour predicted by Euler-Bernoulli beam theory.

When working with Euler-Bernoulli beam theory fundamental assumptions that are made are that plane sections that are perpendicular to the neutral axis before bending remain plane and perpendicular after bending and that deformed angles are small. Additionally, Euler-Bernoulli beam theory assumes the material is linear elastic isotropic. The Euler-Bernoulli beam theory ignores effects of shear deformation, which is typically a fair assumption in long slender beams. A tow, which is composed of a large amount of separate filaments, will not behave like a solid material. Filaments are not fixed together and will be able to behave independently of each other. Bending of the tow will not force the upper filaments in tension and the bottom filaments in compression as would be required to abide by the first assumption. Instead, filaments will slide over each other as they deflect due to the gravity load. This results in a transverse shearing behaviour in the tow. Unlike with a typical solid beam the resistance of the individual filaments and the silane coating to this shear deformation is very low. This results in the shearing behaviour becoming an important component in the final deformation of the tows. This results in the Euler-Bernoulli beam theory not being able to give an accurate prediction of the elastic properties.

An obvious alternative to the Euler-Bernoulli beam theory is the Timoshenko beam theory, which is better able to describe beams for which shear deformations cannot be ignored. Fundamental assumptions of Timoshenko beam theory are slightly different than for Euler-Bernoulli beam theory. Deformed angles are still assumed to be small and the material is still assumed to be linear elastic isotropic. The first assumption is however

different since Timoshenko beam theory allows for shear deformations: plane sections that are perpendicular to the neutral axis before bending are assumed to remain plane but not necessarily perpendicular after bending. Derivations of Timoshenko beam theory could be used to predict the deflections of the beam and approximate the elastic properties. This would give a better approximation of the elastic properties of the tows than Euler-Bernoulli beam theory is capable of. The properties of the tows do however not fully fit in the assumptions of Timoshenko beam theory. As described above tows do not behave as a solid material. The shearing behaviour within tows is therefore also different than would be expected from a solid material. The shear within a tow is very large compared to what would be seen in a typical beam. Therefore, While elastic properties obtained using this theory will be closer than the ones obtained using Euler-Bernoulli beam theory, they will still require some calibration to account for these differences. Therefore, it is recommended that instead it is accepted that the tow elastic properties require calibration through a numerical model after they have been estimated using Euler-Bernoulli beam theory.

Using an RVE to determine homogenised elastic properties also gives the opportunity to observe the effect of changes in the tow geometry, stitching geometry and pattern and/or tow and stitching elastic properties without having these NCFs available. This could aid in optimizing the design of an NCF for handling using pick-and-place operations. However, in practice the choice of reinforcement might already be fixed. For these cases determining the elastic properties from the tow up might not give any advantages over determining elastic properties at a macroscale level.

Another reason to consider determining elastic properties on the macroscale instead of the mesoscale for application in industry is the inability of the RVE to capture all mesoscopic fabric deformation mechanisms and couplings as discussed in chapter 4 and 5. While simulating all the tows and stitches in a full scale model could aid in being able to capture more of these mechanisms and couplings, this would also result in a computationally heavy model, especially for the large sized reinforcements the current work is interested in. When the fabric is used to experimentally determine elastic properties more of these mechanisms couplings will automatically be included in the results. With elastic properties determined on the macroscale it will still be important to use elastic properties that are calibrated for bending behaviour. Table 6.1 shows the proposed methods and guidelines for obtaining elastic properties on the macroscale for bi-axial NCFs.

Table 6.1: Proposed methods and guidelines for obtaining elastic properties on the macroscale for NCFs

Elastic property	Method
$E_{11}, E_{22}$	Flexural rigidity test and FEM analysis
$E_{33}$	10% of $E_{11}, E_{22}$
$\mu_{12}, \mu_{13}, \mu_{23}$	Constant volume assumption
$G_{12}$	Picture frame test
$G_{13}, G_{23}$	10% of $G_{12}$

Two tests would need to be done to obtain elastic properties on the macroscale: a flexural rigidity test and a picture frame test. The picture frame test would be required in any case to set tolerances for the in-plane shear strains and fiber angle deviations. The deflection results from the flexural rigidity test or a similar overhang test are necessary to calibrate

the Young's moduli  $E_{11}$  and  $E_{22}$  to bending. For this a simple finite element simulation as described in section 3.3 can be used.

Ideally, guidelines would be set for the relationship between the actual Young's modulus and the one calibrated for bending. This would omit the requirement for flexural rigidity or other overhang tests and calibration using FEM analysis. In section 4.4 it was shown that for an NCF with tows in the 1 and 2 direction a calibrated  $E_{11}$  and  $E_{22}$  for the NCF as a whole can be estimated as 1/8th of the calibrated  $E_{11}$  of a tow. This does however still require a calibrated  $E_{11}$  for the tows in the NCF. For the E-glass used in the current work a typical Young's modulus is 72 GPa, the calibrated value for the tow  $E_{11}$  is 1.57 GPa. Creech *et al.* [2] used Toray T700 fibres. The reported axial modulus for these fibres is 230 GPa while the one calibrated for bending is 0.07 GPa. These different tows show a very different relationship and cannot be used to give a guideline. The differences between the two values can possibly be explained by the slightly different procedures used in the simulation used to calibrate the modulus. Unlike the model used in chapter 3, Creech [3] used numerical viscous damping in their model. Additionally, the current work used the obtained deflection to calibrate the axial modulus while Creech [3] used the angle between the horizontal and inclined plane to which the tow deflects. For a true comparison between different tows a standard procedure would be required. Another explanation for the large differences between the tows could be a difference in treatment. More research is required on the different materials and possible treatments and how they affect the bending  $E_{11}$ .

Alternatively, a database and guidelines could be set up for the relationship between actual moduli and moduli calibrated for bending for the NCF as a whole. It is however expected that this will be more complicated due to the interactions between tows and stitches. Different NCFs based on the same material can have a very different bending response due to fiber orientation and stitching. It should however still be possible to develop guidelines as long as all the factors contributing to the behaviour are taken into account. Factors that would need to be taken into account would be tow material, tow orientation, stitch material, stitching pattern and any treatments or binder material.

The guideline of  $E_{33} = 10\%$  of  $E_{11}$ ,  $E_{22}$  is based on a dry NCF without structural stitching and will need to be reconsidered for prepreg NCFs and/or NCFs with structural stitching. However, since the case of a dry reinforcement is the conservative case it would also be possible to keep the conservative estimate for  $E_{33}$ . Moreover, table 4.2 in chapter 4 shows that the magnitude of  $E_{22}$  and  $E_{33}$  has a very limited influence on the deflection of tows. With this limited influence of  $E_{33}$  on the bending behaviour using the estimate of  $E_{33} = 10\%$  of  $E_{11}$ ,  $E_{22}$  is considered to be a valid assumption.

The constant volume assumption for the Poisson's ratio's  $\mu_{12}$ ,  $\mu_{13}$ ,  $\mu_{23}$  implies that  $\mu_{12}$ ,  $\mu_{13}$ ,  $\mu_{23} = 0.5$ . This assumption is already used in commercial models, such as PAM-FORM. For prepreps this will generally be a valid assumption, while for dry fabrics the validity depends on the shearing angle. Initially, shearing of the fabric will result in inter-tow air voids being filled with the thickness of the fabric remaining constant. When shearing continues once the air voids are filled the fabric will start to thicken with the area of the fabric being reducing [4]. Figure 6.2 shows that for the current work the Pois-

son's ratio does not have a significant influence on the in-plane shear strains.  $\mu_{12}, \mu_{13}, \mu_{23} = 0.5$  is therefore considered to be a valid assumption.

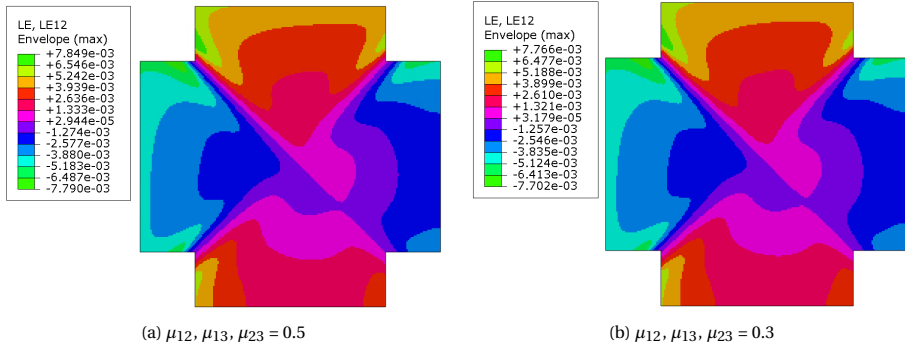


Figure 6.2: Numerical in-plane shear strain results for 'two edges free (2)' boundary condition as defined in Figure 5.17. On the left are the numerical results for the unit cell model with  $\mu_{12}, \mu_{13}, \mu_{23} = 0.5$  and on the right the results for the unit cell model with  $\mu_{12}, \mu_{13}, \mu_{23} = 0.3$ . The contours are plotted on undeformed shapes.

## 6

Picture frame tests are used to characterize the in-plane shear behaviour. Both in terms of the in-plane shear modulus  $G_{12}$  and for setting tolerances for the in-plane shear strains and fiber angle deviations. There are alternative methods for testing fabrics in shear, such as the Kawabata evaluation system for fabrics and bias-extension tests. Both of these tests do however have the drawback that they will not load the specimen under uniform shear [5]. It is therefore recommended to always use a picture frame test. For anisotropic materials the user needs to be aware that the fabric might not be loaded under uniform shear stress, with for example couplings between normal stress and in-plane shear deformation taking place due to the picture frame forcing the fabric in uniform shear deformation.

The in-plane shear behaviour of an NCF will be different depending on the loading direction. This is a result of the stitches being loaded differently. Therefore, an NCF will have a  $G_{12}$  and  $G_{21}$ . For the most accurate representation of the behaviour a numerical model would need to be able to include both these shear stiffnesses. However, the current work showed that for small shear angles  $G_{12}$  is a valid approximation for  $G_{21}$ . Further testing is required to determine whether this holds true for different NCFs. If it does, a single shear modulus can be used for ease of simulation as long as only small shear angles are considered.

### 6.2.2. MULTI-AXIAL NCFs

The current work focuses on bi-axial NCFs since those are most vulnerable to in-plane shear fiber angle deviations. However, for real-life applications multi-axial NCFs and multiple layers of bi-axial NCF stitched together using structural stitches are also of interest. To use the current work with these other types of reinforcements some adaptations would have to be made in the modeling of the RVE and tests to be done to characterize material properties.

When an industry project is interested in the use of multi-axial NCFs and does want to use the strategy of using an RVE to obtain homogenised elastic properties the RVE can be expanded to include additional sublayers of tows. Creating additional tow parts makes it possible to simulate different non-perpendicular tow directions. Additional stitch definitions can be added to make it possible to simulate different types of stitches. This would for example make it possible to differentiate between a non-structural stitch and a structural stitch, which can both be present in a reinforcement. This would make it possible to determine homogenised elastic properties for a different type of NCF.

The procedure for the picture frame tests used in the current work includes the removal of stabilizing yarns in the 0/90 direction, stitches are untouched and remain in place. Specimens are cut and placed in such a way in the picture frames that they are loaded under pure shear deformation. This procedure can be repeated in the same way for other NCF configurations with perpendicular tow directions. For bi-axial NCFs with non-perpendicular tow direction an alternative specimen shape and starting point for the frame can be chosen to ensure measured deformations stem from in-plane shear of the tows. However, removing stabilizing yarns in the 0/90 direction will remove the coupling between normal stress and shear behaviour that is present in the fabric. This will affect the behaviour of the fabric and should be taken into account.

While the picture frame test is ideal for working with bi-axial fabrics it can also be used with multi-axial ones. However, when dealing with multi-axial NCFs, the loading direction will have to be chosen carefully to ensure specimens are loaded in the direction most susceptible to shear. It is recommended to create a shear stiffness graph for the relationship between angle and shear stiffness. This can then be used to determine the angle at which the stiffness is the lowest.

### 6.2.3. STABILIZING YARNS

The current work did not take the stabilizing yarns into account that are present in the 0/90 direction of the NCF, resulting in a conservative estimate. However, for implementation in industry it is important that all parts of the fabric are taken into account. While being on the conservative side is fine, being too conservative can for example make the process not as efficient as possible. In general safety factors will need to be applied to the design, being too conservative in predictions will only further increase the difference between actual values and values required to be used.

For this research yarns are removed for the picture frame tests in chapter 3 and also not taken into account in the RVE from chapter 4. However, on the scale of the 300 x 300 mm and 550 x 550 mm specimens in chapter 5 it was not possible to remove these yarns without damaging the NCF. The stabilizing yarns are interwoven in the NCF, and just like the regular tows they might cross from one path to another. While some yarns are easily removed, others are connected to the surrounding tows and stitches and upon pulling them get stuck and result in wrinkles and other damage. The presence of these stabilizing yarns in the experiments resulted in mismatches in the numerical prediction of deflections and in-plane shear strains. Without the consideration of stabilizing yarns the numerical prediction will give a conservative estimate. For a more accurate prediction the stabilization yarns will need to be included in simulations.

Two possible ways of including the stabilizing yarns in analyses for implementation in industry are proposed: taking them into account in the material properties or modeling them separately. The stabilizing yarns are present in the NCF at an interval of 45-55 mm. Assuming that the general stabilizing effect can be considered to be consistent across the NCF the stabilizing yarns could be 'smeared out' over the full surface of the NCF. This could be represented numerically using an appropriately sized 0 and 90 layer in the RVE. Instead of the current two layers (+45°, -45°) the RVE would have four layers (+45°, -45°, 0, 90). The main stabilizing effect does however occur if a yarn is supported on both ends, as was observed in the experimental work in chapter 5. This cannot be taken into account in an RVE using the smearing methodology and will have to be modeled separately on the macroscale. For the modeling of stabilizing yarns on the macroscale it is recommended that three scenarios are considered: stabilizing yarn at the edge of the reinforcement, stabilizing yarn in the middle of the pick-up point, and stabilizing yarn on the edge of the pick-up point towards the middle of the reinforcement. This will make it possible to observe the effect of the stabilizing yarn on the general behaviour of the reinforcement and on the behaviour of the edges.

It is expected that the smearing methodology will give an accurate prediction of the behaviour of the NCF as long as stabilizing yarns are not caught between two pick-up points. If it is possible to ensure this will never happen this would be a good modeling strategy. However, if it is a possibility for the stabilizing yarns to get caught between two pick-up points the stabilizing yarns will need to be modeled separately to ensure their behaviour is captured.

### **6.3. USING UNIT CELL PICK-UP POINT PATTERNS TO EVALUATE IN-PLANE SHEAR STRAINS**

#### **6.3.1. UNEXPECTED DEFORMATIONS DUE TO SLIDING OF BOTTOM LAYERS**

Section 5.2 presented experimental results that showed that NCFs will exhibit atypical deformation patterns if the pick-up points do not support all layers being handled. Needle grippers are considered to be the best choice of gripping strategy for handling multiple layers. However, since needle grippers will not fully support the layers there will still be a risk of tows sliding while the reinforcement is being handled. For implementation in industry the behaviour of the reinforcements being handled should be typical and predictable. This requires either a gripping mechanism that will support all layers or a reinforcement that will not slide.

There is currently no gripping strategy available that is appropriate for the handling of reinforcements that will be fully able to prevent sliding of the bottom layer(s). While external fixing mechanisms are not ideal they will aid in preventing unexpected deformations. An example of an external fixing mechanism that could be used is the same resin that will be used in the finished composite product. Careful accurate application of the resin at the pick-up point locations will prevent the undesired sliding behaviour. Future research is recommended on the development of gripping strategies that are able to handle multiple layers while fully supporting them.

The current work focused on dry reinforcements as opposed to pre-preg. Dry reinforcements are more challenging to handle than pre-pregs due to their lower rigidity, thereby making it a more challenging case study. Industry does however widely use pre-pregs. It is expected that the issue of the sliding bottom layer(s) will not be (as) present in the handling of pre-pregs due to the presence of the matrix. This makes pre-pregs a more appropriate kind of reinforcement to handle with the currently available gripping strategies.

### 6.3.2. LOCAL IN-PLANE SHEAR STRAINS

In section 5.3 three shapes representing pick-up point areas were used to divide the reinforcements in areas of local in-plane shear strains and global in-plane shear strains. Local in-plane shear strain areas are areas for which the in-plane shear strains are affected by the shape of the pick-up point. Global in-plane shear strain areas are not affected by the shape of the pick-up point. For the current work local in-plane shear strain areas were excluded from the analyses. The reinforcements will however experience these in-plane shear strains. Moreover, as section 5.3 showed the highest in-plane shear strains will occur in the local in-plane shear strain areas, which are around the pick-up points. For industrial application of the current work these local in-plane shear strains will need to be taken into account.

It is not possible to give direct guidelines for dealing with local in-plane shear strains based on the current work. However, some observations were made when setting the limit for local vs global in-plane shear strains. One of the factors contributing to the in-plane shear strains in the local area around the pick-up points is the shape of the pick-up point. Peak in-plane shear strains were observed at sharp corners in the pick-up point shape. Another factor that will influence in-plane shear strains is the size of the pick-up point. However, based on the current work no comments can be made on the influence of the size of the pick-up point on the in-plane shear strains. Experimental work is recommended to observe what the actual in-plane shear strains will look like around a pick-up point when using currently available gripping strategies. Based on this experimental work guidelines can be set for dealing with the numerically predicted peak in-plane shear strains around pick-up points. A solution could for example be to, similarly to the current work, set a region around the pick-up point that will not be taken into account during evaluation because it is not representative for the actual behaviour. Additionally, it is recommended that it is investigated how (new) gripping strategies would be able to pick-up reinforcements without introducing high local in-plane shear strains.

### 6.3.3. PICK-UP POINT PLACEMENT

Chapter 5 showed that it is possible to use a pick-up point pattern unit cell to predict the largest in-plane shear strains that will occur in a gravity loaded reinforcement for a chosen rectangular pick-up point pattern. By using the right boundary conditions for this unit cell in-plane shear strains can be predicted for any location in a reinforcement consisting of 1x1, 1x3 or 3x3 repeats of the pick-up point pattern.

While this constant repetitive pick-up point pattern will work for handling basic cases, real life applications will often be more complicated. The state of the art presented

in chapter 2 mainly focuses on the mould the reinforcement is to be draped in or on when designing the pick-and-place process. The current research has taken the opposite direction and only focuses on the reinforcement. In industrial applications both need to be taken into account. Choosing to place a pick-up point in a specific location always requires the consideration if the potential damage caused by the pick-up point and the higher local in-plane shear strains are worth the decrease in global in-plane shear strains. However, sometimes a mould will require pick-up points in specific locations for the reinforcement to be able to be placed correctly. Alternatively, pick-up points might need to be avoided in a specific location. These decisions will need to be made at the start of the design process and the pick-up point pattern will need to be made around such restrictions. The current work cannot design a pick-up point pattern around restrictions. It can however be used to evaluate options for the different distances between pick-up points and be used to set a maximum allowable distance.

The current work also shows that the behaviour of the reinforcement in a pick-up point pattern repetition is dependent on the surrounding reinforcement. Regions around the edges require a smaller distance between pick-up points to guarantee in-plane strains remaining below set tolerances than regions in the middle of the reinforcement. This can be used in the design of the pick-and-place process to minimize the amount of pick-up points and thereby the effect of pick-up points on the reinforcement by increasing the distance between pick-up points in the center.

## 6

The placement of pick-up points can be exact in numerical work but in experimental work and in real life applications tolerances will need to be set. Translations and rotations away from the ideal position will influence the in-plane shear strains and fiber angle deviations experienced by the reinforcement. Tolerances will not only need to be set for the in-plane positioning of pick-up points, but also on their out-of-plane translations and on rotations. Multiple simulations with slightly different pick-up point placements will give insight into the sensitivity of pick-up point location.

### 6.3.4. VERTICAL AND HORIZONTAL ACCELERATIONS

The current work started with the basic case of reinforcements loaded under gravity, thereby only considering one state of the pick-and-place process: picked-up and held still. In reality the pick-and-place process will have several other states: being picked up, accelerating/moving vertically, accelerating/moving horizontally and being placed down. These different phases of the pick-and-place process will introduce different forces on the reinforcement. This section will discuss the different forces that will be relevant for accelerating/moving vertically and accelerating/moving horizontally. The forces resulting in in-plane shear strains and fiber angle deviations will determine the speed that can be used for the pick-and-place process. When dealing with industrial implementation picking up and placing down will also be an important part of the process. This is however considered to be mostly outside scope of the current work so it will only be touched on briefly.

The forces and resulting in-plane shear strains introduced during the picking up and placing down phase will be highly dependent on the shape of the reinforcement and the specific strategy that is used. For this discussion only rectangular shapes are considered.

As discussed in chapter 2 the reinforcements can for example be picked up (and placed down) straight - e.g. [6–14] - or a rolling motion can be used - e.g. [15–18]. The placing down phase will typically involve the draping of the reinforcement, which is considered to be a separate process for the current interest of in-plane shear strain induced fiber angle deviations during handling. The in-plane shear strains and fiber angle deviations introduced during draping will be intentional. The ones that occur during handling are not and have not previously been considered.

The forces introduced by straight picking up of reinforcements will be very similar to the ones that are introduced due to moving vertically. Moving a reinforcement vertically will not just introduce movement but also positive and negative accelerations to get it moving at the desired speed. Table 6.2 summarizes how these accelerations will interact with the gravitational acceleration. Moving a reinforcement horizontally will also result in additional horizontal accelerations, reinforcements that are moved horizontally will also always have the vertical component of the gravitational acceleration. Here aerodynamical forces can play a role as well.

Table 6.2: Summary of the interactions between gravitational acceleration and the vertical accelerations as a result from the pick-and-place process

Accelerations		Direction	
		Upwards	Downwards
	Positive	Add	Subtract
	Negative	Subtract	Add

In terms of efficiency it is desired to handle as many reinforcements per hour as possible. This would include handling them at the highest possible speeds and accelerations. The gantry presented by CMA/Flodyne/Hydradyne [19] for the handling of sheet metal is used as an example. For this gantry the maximum reported speed and acceleration in the vertical direction is respectively 84 in/s (2.13 m/s) and 0.75G (7.36 m/s<sup>2</sup>). The maximum reported speed and acceleration in the horizontal direction is 210 in/s (5.33 m/s) and 3G (29.43 m/s<sup>2</sup>). In real life applications it might be more desirable to use lower accelerations and accelerate for longer instead of using the maximum possible acceleration. Additionally, at certain speeds aerodynamical forces can come into play, resulting in undesirable behaviour of the reinforcement.

For the example gantry the maximum vertical accelerations on the reinforcement are -9.81 m/s<sup>2</sup> - 7.36 m/s<sup>2</sup> = -17.17 m/s<sup>2</sup>. The minimum vertical accelerations are -9.81 m/s<sup>2</sup> + 7.36 m/s<sup>2</sup> = -2.45 m/s<sup>2</sup>. Different vertical accelerations have been applied to a pick-up point pattern unit cell with boundary conditions 'two edges free (2)' as defined in Figure 5.17 and dimensions of 550 x 550 mm. Figure 6.3 compares the predicted in-plane shear strains that result from these different accelerations. As expected there will be an increase in the maximum in-plane shear strains with an increase in the applied accelerations. Reducing the accelerations results in a decrease of the in-plane shear strains. The maximum in-plane shear strain in Figure 6.3 is below the tolerance that has been set as 1.4° or in radians 2.44 × 10<sup>-2</sup>. Based on these simulations and the assumption that validation holds for accelerations beyond gravity this type of bi-axial NCF can therefore safely be transported in vertical direction using accelerations over 0.75G for dimensions

of 550 x 550 mm.

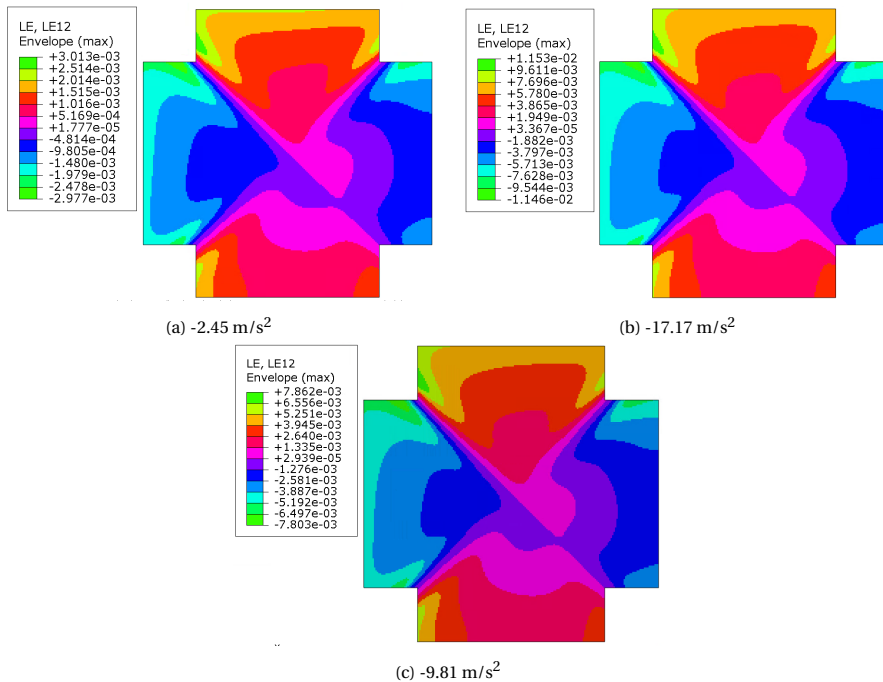


Figure 6.3: Numerical in-plane shear strain results for applied vertical accelerations of  $-2.45 \text{ m/s}^2$ ,  $-17.17 \text{ m/s}^2$  and  $-9.81 \text{ m/s}^2$ . Contours plotted on undeformed shapes.

Pick-and-place operations will not only work vertically but will also have a horizontal component. This results in the accelerations having a vertical and a horizontal component. The horizontal components will consist of the applied horizontal accelerations. For the vertical component there will be a part gravitational acceleration and potentially a part applied vertical acceleration.

The effect horizontal accelerations have on the in-plane shear strains in a specific part of the reinforcement will be dependent on the direction of the accelerations. Figure 6.4 shows an example for the 'all edges free' boundary condition. It should however be noted that the numerical model has not been validated for these type of loads. This should merely be considered to be an illustration demonstration of a concept. It is not possible to use the symmetry boundary conditions that are for example used to model 'two edges free (2)' with horizontal accelerations. With the current available model it would be required to model the whole surface when interested in horizontal accelerations.

Figure 6.4 shows the predicted in-plane shear strain results for the boundary condition case of 'All edges free'. The results demonstrate that when dealing with the prediction of in-plane shear strains due to horizontal accelerations the direction will need to be considered. A top left repetition of the pattern will for example respond differently to a left to right acceleration than a top right repetition of the pattern. Therefore, future

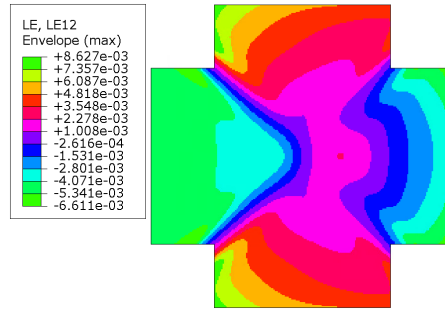


Figure 6.4: Numerical in-plane shear strain results for applied horizontal accelerations of  $29.43 \text{ m/s}^2$  on boundary conditions of 'all edges free'. Contours plotted on undeformed shapes.

research is recommended to study the possibility of using a pick-up point pattern unit cell for the evaluation of horizontal accelerations and movement.

### 6.3.5. PRE-TENSION STRATEGY

The current work focuses on a pick-and-place strategy with static pick-up points in a fixed location. It is acknowledged that pick-up points can potentially damage the reinforcement and that in-plane shear strains will be highest around pick-up points: both arguments for minimizing the amount of pick-up points and preferably placing them in the excess material. However, with this traditional static pick-up point strategy the possible size of reinforcements would be severely limited if pick-up points could only be placed along the edges. An alternative ply handling strategy could work by placing a minimal amount of pick-up points along the edges of the reinforcement and applying a pre-tension to aid in handling of the material and minimizing in-plane shear strains. Applying a pre-tension ensures the reinforcement(s) can be handled with reduced deflections and in-plane shear strains while using a limited amount of gripping points. With this approach care is to be taken that the tension is applied in the directions of the fibers. A misalignment between the fiber direction and the direction of the pre-tension will result in a force being applied in a direction with low resistance to deformation - resulting in undesired deformation. When multiple fiber directions are present - as with a woven fabric or NCF - care needs to be taken that the pre-tension is applied in such a way that all fiber directions are taken into account. While the pre-tension strategy could in theory aid in handling large layers more accurately, the accuracy required for successful application of the desired pre-tension also adds extra difficulty to the handling process.

For the implementation of a pre-tension strategy in industry research would be required on the exact method of application for the pre-tension, e.g. a pre-strain with a pre-tension limit or a pre-tension with a pre-strain limit. For this it would also be required to have an indication for the required magnitude for the pre-tension. A study would need to be done on currently commercially available products that would be able to attain and hold this pre-tension. If no such equipment exists the equipment would need to be designed and produced. Research would need to be done on the effect of slight misalignments in the pre-tension on the fabric to set tolerances for pick-up point positioning.



# BIBLIOGRAPHY

- [1] Philipp Osterrieder, Lukas Budde and Thomas Friedli. “The smart factory as a key construct of industry 4.0: A systematic literature review”. In: *International Journal of Production Economics* 221 (2020), p. 107476.
- [2] Gavin Creech and Anthony K Pickett. “Meso-modelling of non-crimp fabric composites for coupled drape and failure analysis”. In: *Journal of materials science* 41.20 (2006), pp. 6725–6736.
- [3] G Creech. “Mesoscopic finite element modelling of non-crimp fabrics for drape and failure analyses”. PhD thesis. Cranfield University, 2006.
- [4] Anthony Pickett. *Model calibration Composites material model 140 for draping simulation*. Tech. rep. ESI GmbH/Institute for Aircraft Design, Stuttgart, 2012.
- [5] MJ Clifford and AC Long. “Intra-ply shear of textile composites”. In: *FRC 2000–Composites for the Millennium*. Elsevier, 2000, pp. 211–218.
- [6] Christopher Bruns et al. “Process design and modelling methods for automated handling and draping strategies for composite components”. In: *CIRP Annals* (2018).
- [7] Bernd-Arno Behrens et al. “Automated stamp forming of continuous Fiber reinforced thermoplastics for complex Shell geometries”. In: *Procedia CIRP* 66 (2017), pp. 113–118.
- [8] M Kühnel et al. “Automated near net-shape Preforming of Carbon Fiber Reinforced Thermoplastics (CFRTP)”. In: *Innovative Composites Summit, JEC Europe, Paris, France* (2014), pp. 11–13.
- [9] Andreas Björnsson et al. “Getting to grips with automated prepreg handling”. In: *Production Engineering* 11.4 (Oct. 2017), pp. 445–453. ISSN: 1863-7353.
- [10] C Brecher et al. “Handling of preforms and prepregs for mass production of composites”. In: *19 th International Conference on Composite Materials*. 2013.
- [11] C Löchte et al. “Form-flexible handling technology for automated preforming”. In: *Proc. of 19th intern. Conf. on Comp. Mat. (ICCM19), Montreal, Canada*. 2013.
- [12] R Molfino et al. “Design of a Hyper-flexible cell for handling 3D Carbon fiber fabric”. In: *Recent advances in mechanical engineering and mechanics* 165 (2014).
- [13] J Brinker et al. “Automated Handling and Draping of Reinforcing Textiles — Challenges and Developments”. In: *New Advances in Mechanisms, Mechanical Transmissions and Robotics*. Springer, 2017, pp. 485–493.

- [14] Mona Eckardt, Andreas Buchheim and Tobias Gerngross. "Investigation of an automated dry fiber preforming process for an aircraft fuselage demonstrator using collaborating robots". In: *CEAS Aeronautical Journal* 7.3 (Sept. 2016), pp. 429–440. ISSN: 1869-5590.
- [15] Fredrik Martinsson. *Development of Robust Automated Handling of pre-impregnated Carbon Fibre (Master Thesis)*. 2018.
- [16] Tobias Gerngross and Dorothea Nieberl. "Automated manufacturing of large, three-dimensional CFRP parts from dry textiles". In: *CEAS Aeronautical Journal* 7.2 (June 2016), pp. 241–257. ISSN: 1869-5590.
- [17] Claudia Ehinger and Gunther Reinhart. "Robot-based automation system for the flexible preforming of single-layer cut-outs in composite industry". In: *Production Engineering* 8.5 (Oct. 2014), pp. 559–565. ISSN: 1863-7353.
- [18] H Apmann. "Automatic handling of dry carbon fabrics and prepregs". In: *17th International Conference of Composite Materials ICCM*. Vol. 17. 2009.
- [19] *High speed gantry*. <https://www.youtube.com/watch?v=g69xVXjScG4>. Accessed: 27-11-2022.

# 7

## CONCLUSIONS

**I**N this thesis a framework has been developed for the prediction and prevention of fiber angle deviations due to in-plane shear during handling of large-sized bi-axial NCFs. Three main steps were taken to reach the end result. First, setting tolerances for handling induced fiber angle deviations due to in-plane shear in bi-axial NCFs. Next, setting up and validating an RVE that is used for periodic RVE homogenisation to determine homogenised elastic properties for a bi-axial NCF. This was followed by the presentation of a model that can be used to predict in-plane shear induced fiber angle deviations for different pick-up point configurations. Finally, the work presented in this thesis is discussed and guidelines are given for industrial implementation.

It was found that even at low angles the application of in-plane shear on a bi-axial NCF will result in changes in the fabric. These changes were not reversed upon unloading of the reinforcement and build upon each other as the experiments continued and the fabric was further sheared. These observations were used to set tolerances for the fiber angle deviations and in-plane shear. The methodology as shown in the current work to set tolerances for in-plane shear induced fiber angle deviations can be repeated for any bi-axial NCF or other type of fabric.

Periodic RVE homogenisation was successfully used to determine homogenised elastic properties for the bi-axial NCF. The resulting homogenised elastic properties were validated using flexural rigidity tests and small displacement picture frame tests. The scripts have been set up in a way that allows for customization of the RVE. The methodology presented in the current work can be used with these scripts for any bi-axial NCF as long as the tow directions lay perpendicular to each other and the stitch pattern can be represented using four top and four bottom tows. If more tows are required the scripts are easily adapted to include additional tows. The presented framework opens up the possibility for rapid comparison of the elastic properties for different NCF architectures. This is valuable in NCF design, product design and design of handling processes. Predictions made using this method can be further improved through further research on

the mesoscopic fabric deformation mechanisms and how to capture these in an RVE.

Experimental work showed that bi-axial NCFs need to be treated as multiple layers when depending on the gripping mechanism of the pick-up points. Tows in unsupported layers will be free to slide leading to unexpected deformations. The gripping strategy used at pick-up points should be chosen to prevent this from happening. The best current available choice of gripping mechanism for handling multiple layers is needle grippers. This gripping mechanism is able to pick-up multiple layers without external fixing mechanisms, can be used at any desired location on the surface of the reinforcement, does not introduce undesired folds and will be able to almost fix the layers together. It is however expected that needle grippers cannot fully mitigate the undesired sliding behaviour. Future research on novel gripping techniques that can fully support all layers is recommended.

It was shown that it is possible to predict the suitability of a repeating pick-up point pattern for a specific reinforcement in terms of in-plane shear strains using a single quick simulation. Six possible different boundary conditions that can occur in a repeating pick-up point pattern were defined. The worst boundary condition case was determined through simulations. Then, the worst case in-plane shear strains can be predicted using a unit cell model. Reinforcements will experience both local and global in-plane shear strains. Local in-plane shear strains are defined as the region around pick-up points that is influenced by the shape of the pick-up point. Since the focus of the current set-up was on the location of the pick-up points and not the type of pick-up point only the global in-plane shear strains are taken into account. However, reinforcements will also experience these local in-plane shear strains that are highly dependent on the specific pick-up point. It is recommended that the effect of specific gripping strategies and pick-up point shapes on in-plane shear strains is studied in future work.

Guidelines were given for implementation of the current work in industry based on the research presented in chapter 3, chapter 4 and chapter 5. While the work presented in this thesis cannot be directly implemented as-is it does provide opportunities. Some parts are closer to industrial implementation than others but all provide a step in the right direction. The given recommendations will aid in fully preparing the framework presented in this research for industry.

# ACKNOWLEDGEMENTS

This dissertation presents the final product of several years of working as a PhD student. The corresponding PhD defense will be the end to a not always easy but important chapter of my life. A chapter that I would not have been able to complete this way without the support I have had along the way.

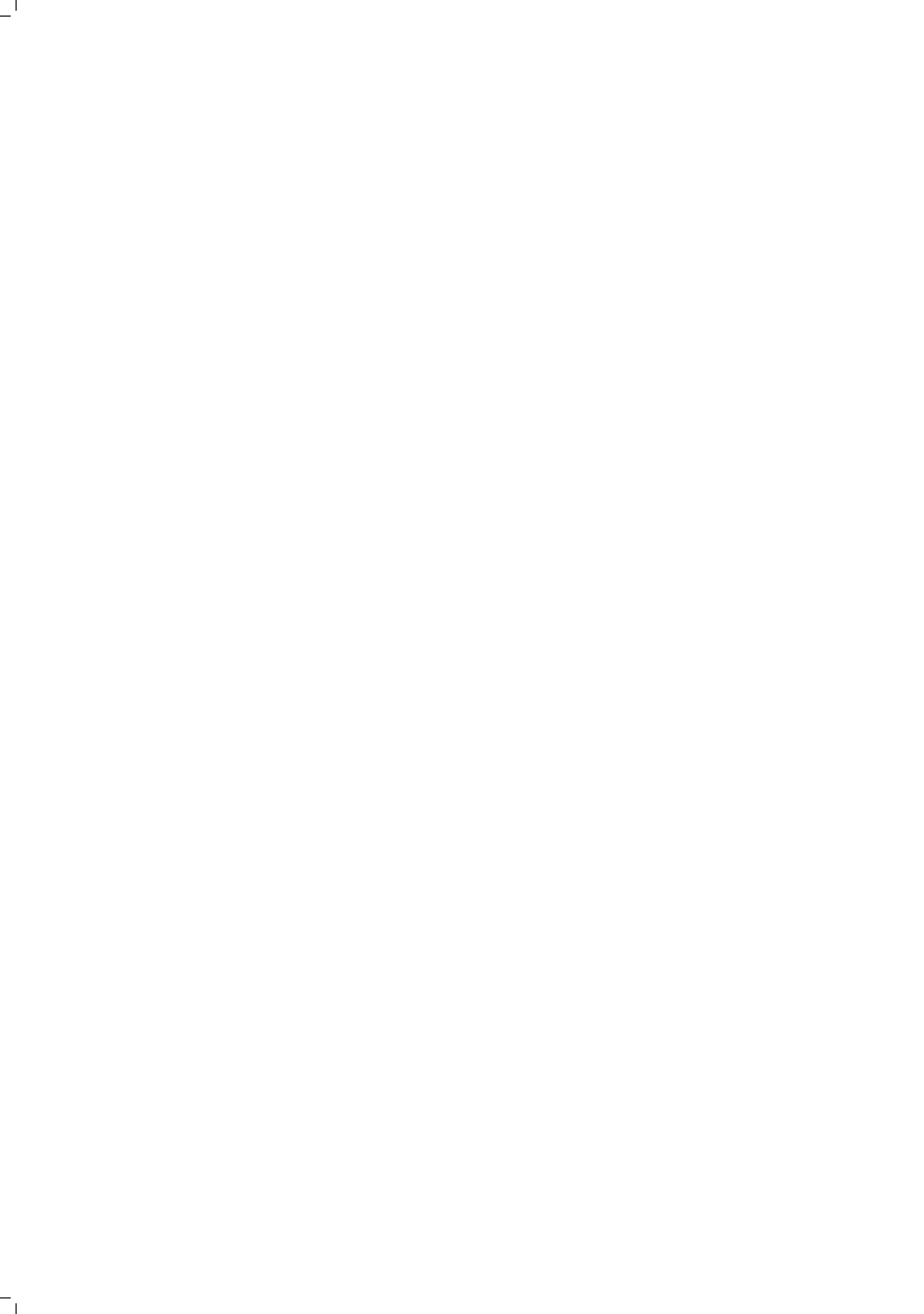
First of all I would like to thank my daily supervisors Daniël Peeters and Otto Bergsma. I could not have wished for better supervisors during these years. Great supervisors truly show their worth when a PhD student struggles. Thank you for your support and guidance. Thank you for the supervisor/PhD student relationship where it felt safe to share when things were not going well. Thank you for believing in me even when I couldn't.

The same goes for my promotor Rinze Benedictus. With two daily supervisors we did not have regular contact during my PhD. At our yearly meetings you were however always able to give valuable input. And despite the infrequent contact there was enough trust to share struggles with you.

Many thanks Dave Ruijtenbeek and Victor Horbowiec who supported me with part of the experimental work in this dissertation. And thank you to all other technicians, students and academic staff who were there during my PhD.

I could not have done this without my boyfriend Emiel Lorist, who has been there for better and for worse for over a decade. It is thanks to your suggestion that I started my Masters in Aerospace Engineering. It is only fitting that you will stand by me as a paronymph during the defense that will finish my academic education.

Thank you to all the friends who were interested in my research and who let me vent when that's what I needed. To everyone who kept being there even when I haven't been the most social in the past years. Finally, thank you to my parents for everything.



# A

## APPENDIX A

Source	Length [mm]	Width [mm]
[1]	1060 to 1500 300 to 430	200 to 800 155 to 250
[2]	150 to 700 500 to 1100	80 to 300 300 to 400
[3]	880	760
[4]	300	100
[5]	500	100 to 1800
[6]	100	100
[7]	100 to 1000	75
[8]	120 1989	120 1034
[9]	1034 268 to 318 933 to 958	706 to 784 139 to 184 139 to 184

Table A.1: Dimensions of plies as presented in literature

Source	Length [mm]	Width [mm]
[10]	300	210
[11]	2000	750
[12]	12000	1500
[13]	2250	1200
[9]	2000	210
[14]	2140 1450	1080 1450
[15]	1900 1780	1600 1350
[16]	100	60
[17]	1500	400
[18]	1725	1530
[8]	2500	1250

Table A.2: Dimensions of end-effectors as presented in literature



# B

## APPENDIX B

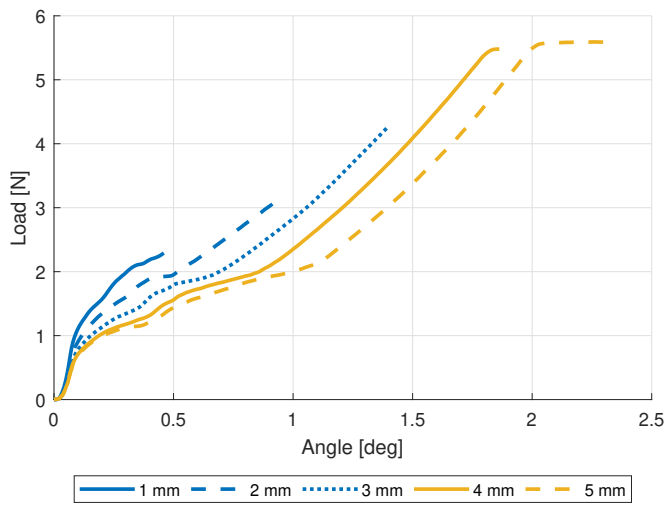


Figure B.1: Load displacement graphs for compression specimen 1 for displacement of 1 - 5 mm. After each displacement the specimen is fully unloaded.

B

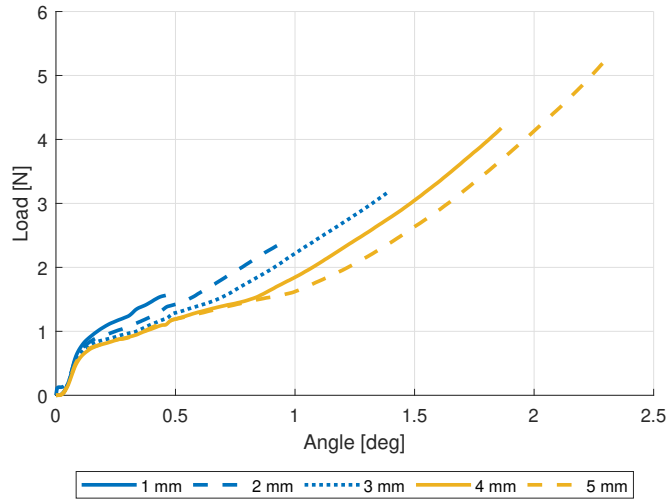


Figure B.2: Load displacement graphs for compression specimen 2 for displacement of 1 - 5 mm. After each displacement the specimen is fully unloaded.

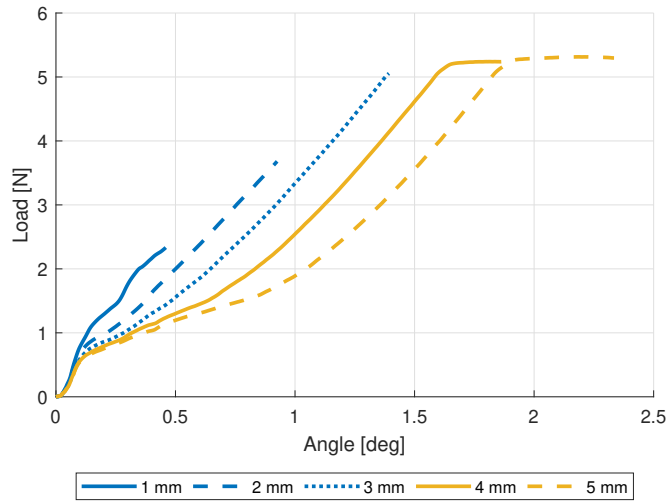


Figure B.3: Load displacement graphs for compression specimen 3 for displacement of 1 - 5 mm. After each displacement the specimen is fully unloaded.

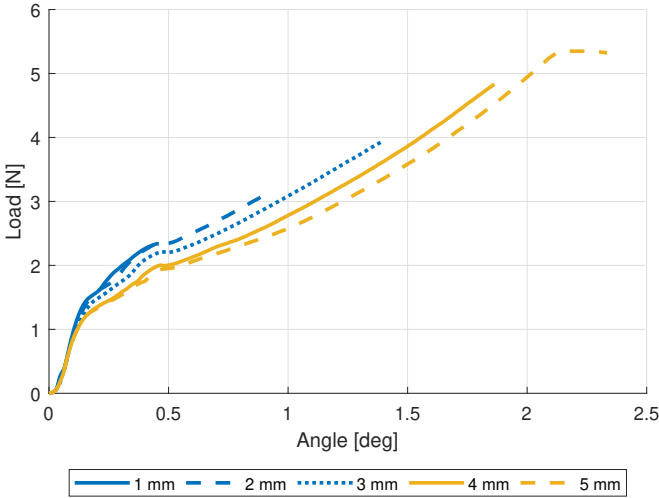


Figure B.4: Load displacement graphs for tension specimen 1 for displacement of 1 - 5 mm. After each displacement the specimen is fully unloaded.

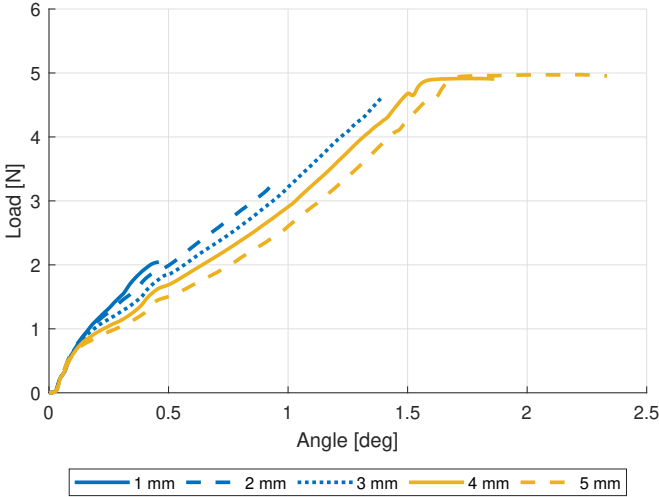


Figure B.5: Load displacement graphs for tension specimen 2 for displacement of 1 - 5 mm. After each displacement the specimen is fully unloaded.

B

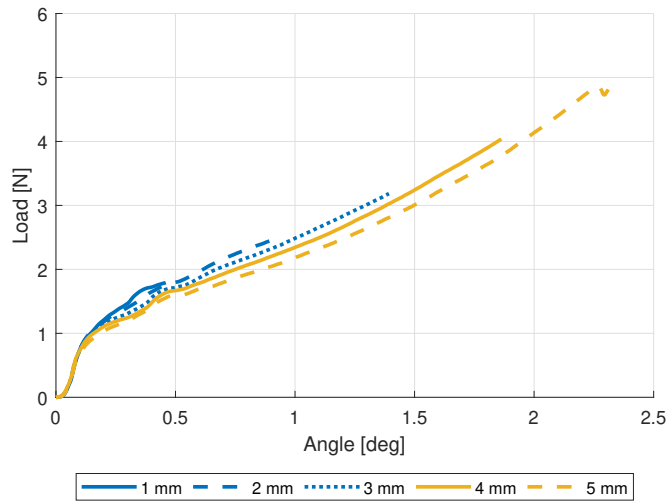


Figure B.6: Load displacement graphs for tension specimen 3 for displacement of 1 - 5 mm. After each displacement the specimen is fully unloaded.

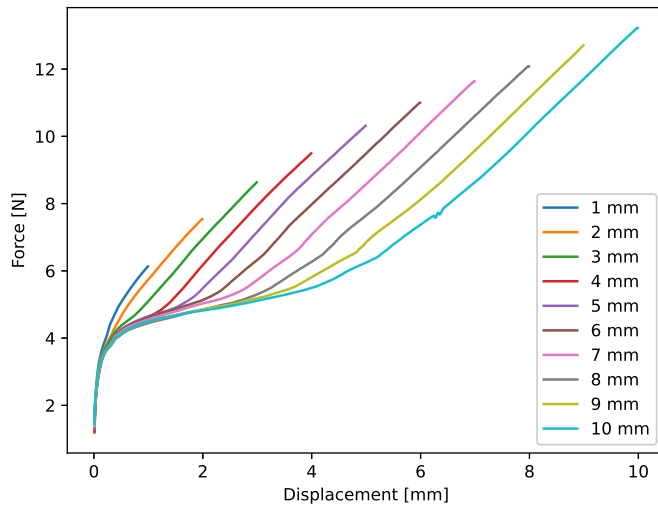


Figure B.7: Load displacement graphs for compression specimen for displacements of 1 - 10 mm recorded using 1 kN load cell. After each displacement the specimen is fully unloaded.

**B**

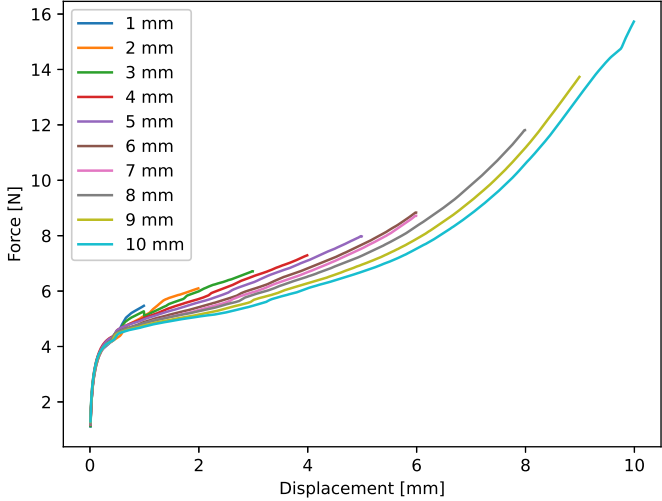


Figure B.8: Load displacement graphs for tension specimen for displacements of 1 - 10 mm recorded using 1 kN load cell. After each displacement the specimen is fully unloaded.



# C

## APPENDIX C

Table C.1: Abbreviations and descriptions for linear constraint equations. Based on Omairey *et al.* [1]

Abbreviation	Full description	Figure
TopS	Top surface	Figure C.1 red
BotS	Bottom surface	Figure C.1 -
FrontS	Front surface	Figure C.1 yellow
BackS	Back surface	Figure C.1 -
LeftS	Left surface	Figure C.1 blue
RightS	Right surface	Figure C.1 -
FT.edge	Front top edge	Figure C.2 red
B.T.edge	Back top edge	Figure C.2 blue
B.B.edge	Back bottom edge	Figure C.2 -
F.B.edge	Front bottom edge	Figure C.2 yellow
E.L.edge	Front left edge	Figure C.2 orange
B.L.edge	Back left edge	Figure C.2 green
B.R.edge	Back right edge	Figure C.2 -
E.R.edge	Front right edge	Figure C.2 purple
L.T.edge	Left top edge	Figure C.3 red
L.B.edge	Left bottom edge	Figure C.3 blue
R.B.edge	Right bottom edge	Figure C.3 -
R.T.edge	Right top edge	Figure C.3 yellow
C1, C2, C3, C4	Top corners	Figure C.4 red
C5, C6, C7, C8	Bottom corners	Figure C.4 blue

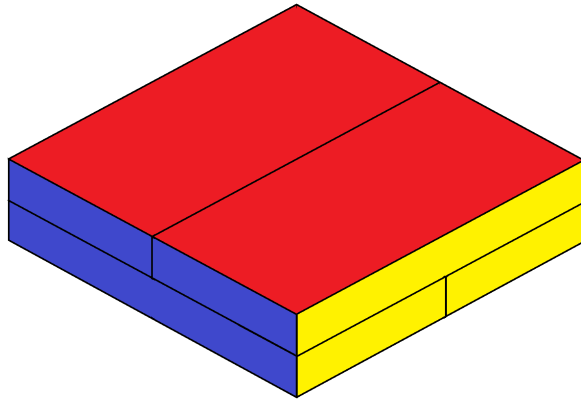
**C**

Figure C.1: Illustration of surface sets as described in Table C.1 and used for linear constraint equations

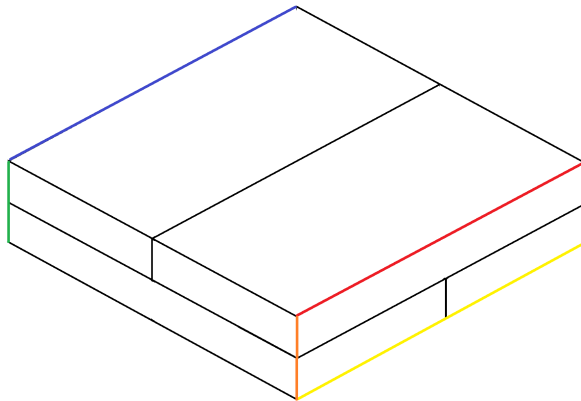


Figure C.2: Illustration of front and back edge sets as described in Table C.1 and used for linear constraint equations

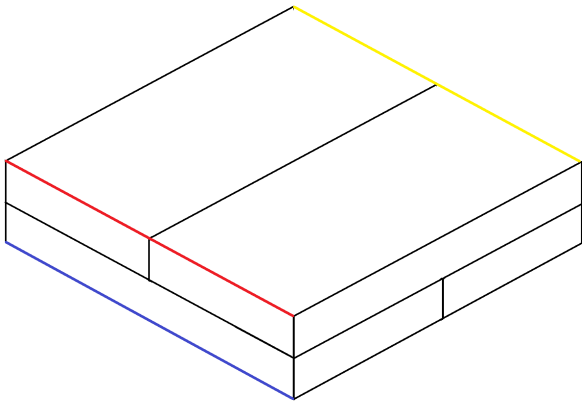


Figure C.3: Illustration of left and right edge sets as described in Table C.1 and used for linear constraint equations

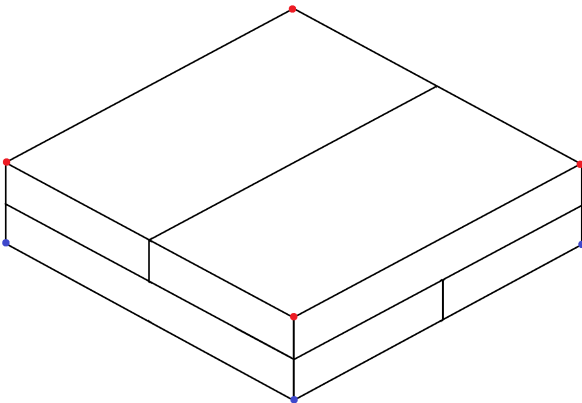


Figure C.4: Illustration of corner sets as described in Table C.1 and used for linear constraint equations

Table C.2: Linear constraint equations for Young's moduli  $E_{11}$ ,  $E_{22}$  and  $E_{33}$  with  $A \times U_{set1}^{DoF} + B \times U_{set2}^{DoF} + C \times U_{RP(i)}^{DoF} = 0$ . From: Omairey *et al.* [1]

Set 1	Set 2	DoF	A	B	C	RP(i)
TopS	BotS	1, 2, 3	1	-1	0, -1, 0	N/A,5, N/A
FrontS	BackS	1, 2, 3	1	-1	-1, 0, 0	4, N/A, N/A
LeftS	RightS	1, 2, 3	1	-1	0, 0, -1	N/A, N/A, 6
F.T.edge	B.T.edge	1, 2, 3	1	-1	-1, 0, 0	4, N/A, N/A
B.T.edge	B.B.edge	1, 2, 3	1	-1	0, -1, 0	N/A, 5, N/A
B.B.edge	F.B.edge	1, 2, 3	1	-1	1, 0, 0	4, N/A, N/A
F.L.edge	B.L.edge	1, 2, 3	1	-1	-1, 0, 0	4, N/A, N/A
B.L.edge	B.R.edge	1, 2, 3	1	-1	0, 0, -1	N/A, N/A, 6
B.R.edge	F.R.edge	1, 2, 3	1	-1	1, 0, 0	4, N/A, N/A
L.T.edge	L.B.edge	1, 2, 3	1	-1	0, -1, 0	N/A, 5, N/A
L.B.edge	R.B.edge	1, 2, 3	1	-1	0, 0, -1	N/A, N/A, 6
R.B.edge	R.T.edge	1, 2, 3	1	-1	0, 1, 0	N/A, 5, N/A
C6	C2	1, 2, 3	1	-1	0, 1, 0	N/A, 5, N/A
C2	C3	1, 2, 3	1	-1	0, 0, -1	N/A, N/A, 6
C3	C4	1, 2, 3	1	-1	1, 0, 0	4, N/A, N/A
C4	C8	1, 2, 3	1	-1	0, -1, 0	N/A, 5, N/A
C8	C5	1, 2, 3	1	-1	0, 0, 1	N/A, N/A, 6
C5	C1	1, 2, 3	1	-1	0, 1, 0	N/A, 5, N/A
C1	C7	1, 2, 3	1	-1	-1, -1, -1	4, 5, 6

Table C.3: Displacement boundary conditions for Young's moduli  $E_{11}$ ,  $E_{22}$  and  $E_{33}$ . From: Omairey *et al.* [1]

Elastic moduli	Set	Boundary condition value of		Disp DoF3	Rot DoF1	Rot DoF2	Rot DoF3
		Disp DoF1	Disp DoF2				
$E_{11}$	RP4	Assigned value	Unset	Unset	Unset	Unset	Unset
$E_{22}$	RP5	Unset	Assigned value	Unset	Unset	Unset	Unset
$E_{33}$	RP6	Unset	Unset	Assigned value	Unset	Unset	Unset

Table C.4: Linear constraint equations for Shear moduli  $G_{12}$ ,  $G_{13}$  and  $G_{23}$  with  $A \times U_{set1}^{DoF} + B \times U_{set2}^{DoF} + C \times U_{RP(i)}^{DoF} + D \times U_{RP(j)}^{DoF} + E \times U_{RP(k)}^{DoF} = 0$ . From: Omairey *et al.* [1]

Set 1	Set 2	DoF	A	B	C	RP(i)	D	RP(j)	E	RP(k)
TopB.C	BotB.C	1, 2, 3	1	-1	-1	4, 1, 6	0	N/A	0	N/A
LeftB.C	RightB.C	1, 2, 3	1	-1	-1	5, 6, 2	0	N/A	0	N/A
FrontB.C	BackB.C	1, 2, 3	1	-1	-1	3, 4, 5	0	N/A	0	N/A
F.T.edge	B.T.edge	1, 2, 3	1	-1	-1	3, 4, 5	0	N/A	0	N/A
B.T.edge	B.B.edge	1, 2, 3	1	-1	-1	4, 1, 6	0	N/A	0	N/A
B.B.edge	F.B.edge	1, 2, 3	1	-1	1	3, 4, 5	0	N/A	0	N/A
F.L.edge	B.L.edge	1, 2, 3	1	-1	-1	3, 4, 5	0	N/A	0	N/A
B.L.edge	B.R.edge	1, 2, 3	1	-1	-1	5, 6, 2	0	N/A	0	N/A
B.R.edge	F.R.edge	1, 2, 3	1	-1	1	3, 4, 5	0	N/A	0	N/A
L.T.edge	L.B.edge	1, 2, 3	1	-1	-1	3, 1, 6	0	N/A	0	N/A
L.B.edge	R.B.edge	1, 2, 3	1	-1	-1	5, 6, 2	0	N/A	0	N/A
R.B.edge	R.T.edge	1, 2, 3	1	-1	1	4, 1, 6	0	N/A	0	N/A
C6	C2	1, 2, 3	1	-1	1	4, 1, 6	0	N/A	0	N/A
C2	C3	1, 2, 3	1	-1	-1	5, 6, 2	0	N/A	0	N/A
C3	C4	1, 2, 3	1	-1	1	3, 4, 5	0	N/A	0	N/A
C4	C8	1, 2, 3	1	-1	-1	4, 1, 6	0	N/A	0	N/A
C8	C5	1, 2, 3	1	-1	1	5, 6, 2	0	N/A	0	N/A
C5	C1	1, 2, 3	1	-1	1	4, 1, 6	0	N/A	0	N/A
C1	C7	1, 2, 3	1	-1	-1	3, 1, 2	-1	4, 4, 5	-1	5, 6, 6

Table C.5: Displacement boundary conditions for Shear moduli  $G_{12}$ ,  $G_{13}$  and  $G_{23}$ . From: Omairey *et al.* [1]

		Disp DoF1	Disp DoF2	Disp DoF3	Rot DoF 1	Rot DoF 2	Rot DoF 3
$G_{12}$	RP4	Assigned value	unset	unset	unset	unset	unset
	RP5, RP6	0	0	0	unset	unset	unset
$G_{13}$	RP5	unset	Assigned value	unset	unset	unset	unset
	RP4, RP6	0	0	0	unset	unset	unset
$G_{23}$	RP6	unset	unset	Assigned value	unset	unset	unset
	RP4, RP5	0	0	0	unset	unset	unset

# CURRICULUM VITÆ

## Chantal Marina DE ZEEUW

Born 06-09-1992 in Purmerend, the Netherlands

Sep 2015 - Jan 2018

**MSC in Aerospace Engineering**, Delft University of Technology

Specialisation: Aerospace Structures and Materials

Title Master Thesis: *"The behaviour of steel bonded joints under creep and hygrothermal loadings"*

Sep 2012 - Aug 2015

**BSC CUM LAUDE in Marine Technology**, Delft University of Technology

Title Bachelor End Project: *"The influence of navigational errors on the total duration of the mine hunting process as performed by two Autonomous Unmanned Vehicles"*

Sep 2010 - Aug 2015

**BSC in Business Administration**, Vrije Universiteit Amsterdam

Title Bachelor Thesis: *"Overcapacity and the increasing size of ships in the inland shipping sector"*



# LIST OF PUBLICATIONS

1. Chantal M. de Zeeuw, Daniël M. J. Peeters, Otto K. Bergsma & Rinze Benedictus (2022) The effect of pick-up point location on fibre angle deviations in Non-Crimp Fabrics, Proceedings of the 20th European Conference on Composite Materials: Composites Meet Sustainability. Lausanne
2. Chantal M. de Zeeuw, Daniël M. J. Peeters, Otto K. Bergsma & Rinze Benedictus (2022) Setting bounds for in-plane shear induced fiber angle deviations in bi-axial non-crimp fabrics, Journal of Industrial Textile, 52, 1-23, DOI: 10.1177/15280837221113921
3. Chantal M. de Zeeuw, Daniël M. J. Peeters, Otto K. Bergsma & Rinze Benedictus (2020) Strategies for swift automated pick-and-place operations of multiple large-sized layers of reinforcement - a critical review, Advanced Manufacturing: Polymer & Composites Science, 6:2, 57-71, DOI: 10.1080/20550340.2020.1750329
4. Chantal de Zeeuw, Sofia Teixeira de Freitas, Dimitrios Zarouchas, Markus Schilling, Romina Lopes Fernandes, Pedro Dolabella Portella & Ute Niebergall (2019) Creep behaviour of steel bonded joints under hygrothermal conditions, International Journal of Adhesion and Adhesives, 91, 45-63, DOI: 10.1016/j.ijadhadh.2019.03.002